Drying of Softwood Kraft Lignin and Its Cationic Derivatives

Ameena Bacchus

B.Eng. Chemical Engineering, Lakehead University

Supervisor: Pedram Fatehi, PhD, P.Eng.

Thesis

Presented to the Faculty of Graduate Studies

Lakehead University

Thunder Bay, Ontario, Canada

in Partial Fulfillment of the Requirements for the Degree of Master of Science in Chemical Engineering

September 2024

Dedication

This work is dedicated to Armin Weiss, my love, my light…without you, none of it would be possible.

Acknowledgements

First, I would like to start by thanking my supervisor, Dr. Pedram Fatehi, for the opportunity to pursue my master's studies in this group. Your guidance and your encouragement during this time have been invaluable.

Thank you to our lab manager, Dr. Jane Gao. Without your tireless work ethic, testing my endless samples, this would not have been possible. As a lab manager, you are the glue that keeps our lab together, ensuring that it functions well at all times.

To Sutita Densakulsub (Jin) and Thanaporn Wetchakornpatiwong (Mind) of King Mongkut's University of Technology Thonburi, thank you for your assistance in the lab synthesizing polymer batches and drying. Your bright smiles and energy filled our lab with positivity and sheer joy.

To my dear friends Yichen and Shrikanta, thank you for always encouraging me and making me laugh.

To my dear friends Saba, Rozita and Fatemeh, thank you all for sharing your beautiful culture with me. Your presence made the work and these past years an absolute joy.

To my dear friends Banchi and Jonathan, your pragmatism was sobering. You both listened, always, and encouraged me constantly, patiently. You also blessed me with your knowledge and expertise, it was truly my honour to learn from you both.

To my beloved Armin, your steadfast support and love has been the light leading the way along this path. Words cannot sufficiently express the depth of my gratitude for you, my love, my light.

Table of Contents

List of Figures

List of Tables

Abstract

Our dependence on petroleum-based materials comes with significant environmental challenges such as environmental pollution, including oil spills and air pollution. Furthermore, the utilization of petroleum-based products leads to the emission of greenhouse gases, which contributes to climate change. Additionally, many petroleum-based products, such as plastics, are not biodegradable and accumulate in the environment, causing harm to wildlife and ecosystems. For these reasons, researchers continue to seek out sustainable alternatives to petroleum-based materials. Lignin is a promising starting material for producing sustainable and environmentally compatible chemistries. Lignin is an abundant and sustainable resource. Organic synthesis and polymerization reactions are utilized as effective methods for derivatizing lignin and tailoring it for application in various industries. After synthesis and purification, drying is a crucial final step. Generally drying conditions should be carefully selected to introduce minimal changes to the properties of the synthesized products. Furthermore, there have been reports of lignin's sensitivity to heat, stimulating condensation reactions which alter the properties of the sample. There are no comprehensive studies that investigate the topic of drying of lignin derivatives.

In this work, the objectives were to derivatize lignin in two ways via: 1) grafting reaction to create a low molecular weight cationic lignin derivative and 2) polymerization to create a high molecular weight cationic lignin derivative. Subsequently, unmodified kraft lignin and the derivatized lignin samples were freeze-dried and oven-dried. The samples were then characterized using advanced techniques, such as XPS, NMR, DSC, TGA and GPC.

It was found that the kraft lignin sample experienced condensation reactions during oven-drying. This resulted in condensed, etherified structures at temperatures as low as 80 and 105ºC. Meanwhile, at 130ºC it was found that degradation reactions predominated. Additionally, it was

found that molecular weight and glass transition temperature increased significantly after drying at 105ºC. This is thought to be a result of the condensation reactions occurring during the drying process.

The cationic grafted lignin derivative underwent degradation to produce secondary amine structures at 105 and 130ºC, but not at 80ºC. Furthermore, it was found that the samples undergo condensation as well, at 80 and 105ºC, which was seen to analogously affect the molecular weight and glass transition temperature.

For the cationic polymerized lignin derivative, it was found that drying at 55ºC resulted in more chain interactions due to electrostatic interactions amongst the cationic polymer chains with the electronegative atoms present in kraft lignin. At 80, 105 and 130ºC drying temperatures, it was found that hydrolysis reactions predominated, resulting in lower molecular weight. Meanwhile, at 105 and 130ºC, a quaternary ammonium group and an aldehyde group were detected.

Overall, this work showed that there is a complex relationship between chemical and physical phenomena occurring during the drying of lignin derivatizes. There are key considerations that should be taken into account, such as chain interactions, hydrolysis, and thermal degradation, when selecting the drying temperatures of lignin.

Chapter 1 – Introduction

1.1 Background

Drying is often a crucial step in recovering any polymer product after synthesis and purification [1]. During the drying step, the polymer is treated as two phases, solid and liquid, while the gas streams become less of a consideration [1]. Although drying is the oldest and most common unit operation in chemical engineering, it is still the most complex and least understood [1]. The selection of drying conditions for a polymer product depends on the synthesis step of the polymer under consideration [1]. Oven-drying is still the most convenient, cost-effective and facile method for drying polymers. However, it has been documented that biomass undergoes certain changes as a result of heating, even at moderately low temperatures [2-4]. Such changes have been shown to affect the properties of polymers, which may be undesirable for the intended final application.

In this work, inspiration was taken from the food industry, in which food quality and nutrient content are highly affected by the mode of drying [5, 6]. In the food industry, it is well understood that the functional properties of food components are affected by the drying process, which subsequently affects the food product quality [7]. Functional properties dictate the behaviour of the polymer during production and use [7]. During the drying process, there exists simultaneous heat and mass transfer, along with physicochemical transformations of polymers [7, 8]. Drying a biopolymer is a fine balance between process efficiency and conserving the quality of the final product [7]. Drying occurs in two distinct stages, the first is the constant rate drying and the second is the falling rate period [1, 7, 8]. During the first stage, water removal occurs, as internal moisture of the product is transported to the surface [1, 7, 8]. During the second stage, the phase change of the product occurs, and this may manifest in several rates occurring. Once the critical moisture

level is reached, drying occurs at a slower rate [1, 7, 8]. This critical moisture level is a unique property of the polymer product [1, 7, 8]. The scope of the present work revolves around the physical process of drying, which may induce chemical events as well, both of which are theorized to affect the final physical and chemical properties of lignin.

Lignin, a complex, polyphenolic biopolymer is the largest natural source of aromatic carbon, and as such it has continued to be extensively researched for its potential to replace chemicals and materials derived from petroleum sources, as countries around the world endeavour to mitigate climate change [9]. From wound dressings to pharmaceutical drugs, to battery applications to 3D printing, the potential applications for lignin-based products are numerous and diverse [10-14]. Derivatizing lignin with quaternary substituted nitrogen, possessing a positive charge, creating cationic lignin, is a promising lignin derivative with potential applications in wastewater treatment, ion exchange resins, and dye and textile manufacturing [15-18]. Yet another way to derivatize lignin is through sulfo-ethylation, which results in a charged anionic lignin derivative that can also be utilized as a dispersant [19-21]. Another promising application for sulfo-functionalized lignin is as a flame-retardant material [22, 23]. Despite its potential, the drying process of lignin has not been studied comprehensively.

Lignin is classified as a polyphenolic compound, which is pervasively found in the food industry as it lends the valuable antioxidant properties to certain berries and other citrus fruits [24, 25]. The effect of heat on the stability of polyphenolic compounds in food has been studied [24, 25]. It is well-accepted that freeze-drying has the least detrimental effect on the properties and quality of the final product [8, 24, 25]. However, due to the high cost of energy consumption required for freeze-drying on a large scale, it is not always the ideal approach [25]. For these two reasons, throughout this work, freeze-dried samples were compared to oven-dried samples, as a point of

reference, understanding that the ultimate goal is to find the ideal condition for drying of the samples.

Historically, lignin has been treated as a waste product, to be separated from valuable wood fibres of the pulp and paper industry and burned as a low-value fuel [9]. Due to the abrasive conditions during pulping, unstable intermediates are formed on the lignin backbone via the elimination of water molecules. It is theorized that these intermediates may be the source of solubility reduction post-heat treatment, even at lower drying temperatures [26-28]. In this thesis, the overall objective was to investigate the effect of drying temperature during the drying of kraft lignin and its derivatives.

1.2 Objectives

The objectives of this work were:

1. To study the effect of drying temperature on kraft lignin.
2. To study the effect of drying temperature on aminated and cationically polymerized kraft lignin.

1.3 Novelty

To the best of our knowledge, at the time of writing this thesis, the following aspects have not been previously reported in the existing literature:

1. Characterizing the effect of drying temperature on KL derivatives.
2. Proposing drying induced chemical structures.

The following chapters are presented in this thesis to address the targeted objectives and novelty of this work:

Chapter 1: In chapter one, the context for the work is provided, as well as a summary of each chapter.

Chapter 2: In chapter two, a literature review is provided on the background of lignin drying. Possible drying induced reactions for derivatized lignin are discussed, based on the functional group grafted to lignin.

Chapter 3: Chapter three presents the key findings of the drying study that was conducted on the lower molecular weight cationic kraft lignin samples synthesized in this work.

Chapter 4: Chapter four presents the key findings of the drying study on the higher molecular weight kraft lignin cationic polymer synthesized in this work.

Chapter 5: Chapter five discusses the overall conclusions of the work.

1.4 References

[1] B. Bhandari, "Handbook of Industrial Drying, Fourth EditionEdited by A. S. Mujumdar: CRC Press: Boca Raton, FL; 2015. ISBN: 978-1-4665-9665-8," *Drying technology,* vol. 33, no. 1, pp. 128-129, 2015, doi: 10.1080/07373937.2014.983704.

[2] O. Gordobil, R. Herrera, F. Poohphajai, J. Sandak, and A. Sandak, "Impact of drying process on kraft lignin: lignin-water interaction mechanism study by 2D NIR correlation spectroscopy," *Journal of Materials Research and Technology,* vol. 12, pp. 159-169, 2021/05/01/ 2021, doi: https://doi.org/10.1016/j.jmrt.2021.02.080.

[3] H. Zhang, S. Fu, and Y. Chen, "Basic understanding of the color distinction of lignin and the proper selection of lignin in color-depended utilizations," *International Journal of Biological Macromolecules,* vol. 147, pp. 607-615, 2020/03/15/ 2020, doi: https://doi.org/10.1016/j.ijbiomac.2020.01.105.

[4] C. Cui, H. Sadeghifar, S. Sen, and D. Argyropoulos, "Toward Thermoplastic Lignin Polymers; Part II: Thermal & Polymer Characteristics of Kraft Lignin & Derivatives," *Bioresources,* vol. 8 (1), pp. 864-886, 11/05 2013, doi: 10.15376/biores.8.1.864-886.

[5] N. Chhabra, M. Arora, D. Garg, and M. K. Samota, "Spray freeze drying - A synergistic drying technology and its applications in the food industry to preserve bioactive compounds," *Food Control,* vol. 155, p. 110099, 2024/01/01/ 2024, doi: https://doi.org/10.1016/j.foodcont.2023.110099.

[6] A. Menon, V. Stojceska, and S. A. Tassou, "A systematic review on the recent advances of the energy efficiency improvements in non-conventional food drying technologies," *Trends in Food Science & Technology,* vol. 100, pp. 67-76, 2020/06/01/ 2020, doi: https://doi.org/10.1016/j.tifs.2020.03.014.

[7] D. Dehnad, S. M. Jafari, and M. Afrasiabi, "Influence of drying on functional properties of food biopolymers: From traditional to novel dehydration techniques," *Trends in Food Science & Technology,* vol. 57, pp. 116-131, 2016, doi: 10.1016/j.tifs.2016.09.002.

[8] S. M. Jafari, V. Ghanbari, M. Ganje, and D. Dehnad, "Modeling the Drying Kinetics of Green Bell Pepper in a Heat Pump Assisted Fluidized Bed Dryer," *Journal of Food Quality,* vol. 39, no. 2, pp. 98-108, 2016/04/01 2016, doi: https://doi.org/10.1111/jfq.12180.

[9] V. N. Novikov and E. A. Rössler, "Correlation between glass transition temperature and molecular mass in non-polymeric and polymer glass formers," *Polymer,* vol. 54, no. 26, pp. 6987-6991, 2013/12/13/ 2013, doi: https://doi.org/10.1016/j.polymer.2013.11.002.

[10] W. Zhang *et al.*, "Lignin derived carbon materials: current status and future trends," *Carbon Research,* vol. 1, no. 1, p. 14, 2022/07/29 2022, doi: 10.1007/s44246-022-00009-1.

[11] A. Beaucamp *et al.*, "Lignin for energy applications – state of the art, life cycle, technoeconomic analysis and future trends," *Green Chemistry,* 10.1039/D2GC02724K vol. 24, no. 21, pp. 8193-8226, 2022, doi: 10.1039/D2GC02724K.

[12] E. A. Agustiany *et al.*, "Recent developments in lignin modification and its application in lignin-based green composites: A review," *Polymer Composites,* vol. 43, no. 8, pp. 4848-4865, 2022/08/01 2022, doi: https://doi.org/10.1002/pc.26824.

[13] P. D. H. Vu, A. Rodklongtan, and P. Chitprasert, "Whey protein isolate-lignin complexes as encapsulating agents for enhanced survival during spray drying, storage, and in vitro gastrointestinal passage of Lactobacillus reuteri KUB-AC5," (in English), *Lwt-Food Sci Technol,* vol. 148, Aug 2021, doi: ARTN 111725
10.1016/j.lwt.2021.111725.

[14] D. Sun *et al.*, "Ultrafast fabrication of organohydrogels with UV-blocking, anti-freezing, anti-drying, and skin epidermal sensing properties using lignin-Cu^{2+} plant catechol chemistry," (in English), *J Mater Chem A,* vol. 9, no. 25, pp. 14381-14391, Jul 7 2021, doi: 10.1039/d1ta02139g.

[15] J.-m. Yin *et al.*, "Cationic modified lignin: Regulation of synthetic microspheres for achieving anti-photolysis and sustained release of the abscisic acid," *Industrial Crops and Products,* vol. 177, p. 114573, 2022/03/01/ 2022, doi: https://doi.org/10.1016/j.indcrop.2022.114573.

[16] A. Eraghi Kazzaz and P. Fatehi, "Technical lignin and its potential modification routes: A mini-review," *Industrial Crops and Products,* vol. 154, p. 112732, 2020/10/15/ 2020, doi: https://doi.org/10.1016/j.indcrop.2020.112732.

[17] Y. Guo, W. Gao, F. Kong, and P. Fatehi, "One-pot preparation of zwitterion-type lignin polymers," *International Journal of Biological Macromolecules,* vol. 140, pp. 429-440, 2019/11/01/ 2019. [Online]. Available: https://www.sciencedirect.com/science/article/pii/S0141813019335780.

[18] F. Kong, K. Parhiala, S. Wang, and P. Fatehi, "Preparation of cationic softwood kraft lignin and its application in dye removal," vol. 67, p. 345, 2015.

[19] N. Ghavidel and P. Fatehi, "Pickering/Non-Pickering Emulsions of Nanostructured Sulfonated Lignin Derivatives," *ChemSusChem,* vol. 13, no. 17, pp. 4567-4578, 2020/09/07 2020, doi: https://doi.org/10.1002/cssc.202000965.

[20] A. Eraghi Kazzaz, Z. Hosseinpour Feizi, and P. Fatehi, "Grafting strategies for hydroxy groups of lignin for producing materials," *Green Chemistry,* 10.1039/C9GC02598G vol. 21, no. 21, pp. 5714-5752, 2019, doi: 10.1039/C9GC02598G.

[21] M. K. R. Konduri and P. Fatehi, "Designing anionic lignin based dispersant for kaolin suspensions," *Colloids and Surfaces A: Physicochemical and Engineering Aspects,* vol. 538, pp. 639-650, 2018/02/05/ 2018, doi: https://doi.org/10.1016/j.colsurfa.2017.11.011.

[22] J. Ruwoldt, F. H. Blindheim, and G. Chinga-Carrasco, "Functional surfaces, films, and coatings with lignin – a critical review," *RSC Advances,* 10.1039/D2RA08179B vol. 13, no. 18, pp. 12529-12553, 2023, doi: 10.1039/D2RA08179B.

[23] C. Zheng, D. Li, and M. Ek, "Improving fire retardancy of cellulosic thermal insulating materials by coating with bio-based fire retardants," vol. 34, no. 1, pp. 96-106, 2019, doi: doi:10.1515/npprj-2018-0031.

[24] D. de Beer, T. Beelders, C. Human, and E. Joubert, "Assessment of the stability of compounds belonging to neglected phenolic classes and flavonoid sub-classes using reaction kinetic modeling," *Critical Reviews in Food Science and Nutrition,* pp. 1-28, 2022, doi: 10.1080/10408398.2022.2096561.

[25] W. Li *et al.*, "Effect of hot air drying on the polyphenol profile of Hongjv (Citrus reticulata Blanco, CV. Hongjv) peel: A multivariate analysis," *Journal of Food Biochemistry,* vol. 44, no. 5, p. e13174, 2020/05/01 2020, doi: https://doi.org/10.1111/jfbc.13174.

[26] J. D. Zwilling *et al.*, "Understanding lignin micro- and nanoparticle nucleation and growth in aqueous suspensions by solvent fractionation," *Green Chemistry,* 10.1039/D0GC03632C vol. 23, no. 2, pp. 1001-1012, 2021, doi: 10.1039/D0GC03632C.

[27] M. Ma, L. Dai, J. Xu, Z. Liu, and Y. Ni, "A simple and effective approach to fabricate lignin nanoparticles with tunable sizes based on lignin fractionation," *Green Chemistry,* 10.1039/D0GC00377H vol. 22, no. 6, pp. 2011-2017, 2020, doi: 10.1039/D0GC00377H.

[28] S. Bertella and J. S. Luterbacher, "Lignin Functionalization for the Production of Novel Materials," *Trends in Chemistry,* vol. 2, no. 5, pp. 440-453, 2020/05/01/ 2020, doi: https://doi.org/10.1016/j.trechm.2020.03.001.

Chapter 2 – Literature Review

2.1 Introduction

Kraft pulping conditions are known to affect the resultant lignin and the properties conferred by this pulping process [1]. Lignin is a by-product of the pulp and paper process, which has the target of isolating the valuable cellulosic components for further processing to ultimately make paper products. As such, the pulp and paper industry is the dominant producer of lignin [1]. The kraft process facilitates the separation of lignin from the cellulosic components through the use of highly alkaline solutions, along with high temperatures and high pressures, which invariably results in a highly condensed and chemically modified lignin biopolymer [2]. Due to these abrasive cooking conditions, unstable intermediates are formed on the lignin backbone via the elimination of water molecules. As a result, these intermediates undergo condensation reactions through intra or intermolecular reactions with other lignin oligomers, producing new, highly stable carbon-carbon linkages on the lignin structure [2]. These intermediates can also react with other species that may be present in the reaction medium [3]. As stated by Bertella et al., these side reactions may limit the formation of functional lignin polymers and ultimately their industrial uses [3]. Perhaps it is this very view that exemplifies the necessity of further investigation into controlling these side reactions as they may also hamper the successful industrial-scale modification of lignin.

During the kraft process, lignin is broken down into oligomers that differ completely from their original structure, natively found in its biomass of origin. These resulting oligomers are then soluble at pH values greater than 11 because of the deprotonation of the phenolic hydroxyl groups [4]. While the pulp comes out in a slurry, the solubilized lignin (along with other components such as hemicellulose, soaps, and inorganic compounds) exits the process as black liquor. This black

liquor is then dried through the use of a series of evaporators and then the lignin is typically combusted in a recovery boiler of the plant to recover inorganic salts, while simultaneously utilizing the liberated thermal energy to fulfill the heat demand of the pulp mill.

Interestingly, as long as pulping continues, there will be production of lignin, yet the challenge of utilizing such a non-uniform material (i.e., kraft lignin) remains. When compared to other feedstock chemicals, kraft lignin is non-uniform due to the nature of the kraft pulping process conditions, wood species type, and growing conditions. Because of its functionality, lignin tends to depolymerize and re-polymerize with itself under different conditions [5, 6]. This leads to a higher concentration of carbon-carbon linkages, which are very stable and serve to decrease the linear structural components of the oligomers and increase the overall molecular weight of lignin, which may also cause a reduction in the aqueous solubility of lignin [7]. As a result, the increase in newly formed carbon-carbon linkages may increase the risk of losing the ability to further functionalize lignin for value-added applications [8]. In the same vein, these newly formed carbon-carbon linkages are very difficult to break and the oligomers tend to form various inter and intra-molecular noncovalent interactions, such as hydrogen bonds, carbon-hydrogen-pi bonds, and pi-pi stacking, to name a few [9]. These non-covalent interactions are thought to impede the solubility of lignin with many common solvents and polymers [10].

On the other hand, functionalization of lignin to overcome the heterogeneity of lignin via facile and effective chemical modification pathways has been studied comprehensively. Yet a topic that has not been fully addressed in the literature is how this phenomenon of lignin re-polymerizing and depolymerization may or may not play a role during the drying process of lignin. It seems a valid concern that if kraft lignin tends to undergo condensation or other reactions, the presence of

other functional groups on lignin's structure may affect the reactions during drying as well, which has not been studied fully.

Derivatizing lignin through chemical modification is one of the techniques used to confer functional properties for its application in various industries to replace conventional petroleum-based products that are commonly used in wastewater treatment, cosmetics, plastics, electronics, biomedical applications, energy storage and building materials, to name a few [11, 12]. Of particular interest are quaternary ammonium, sulfo-alkyl and carboxy alkyl functionalized lignin derivatives as these reactions are exceptionally promising in terms of their performance and facile preparation [13-15]. Aminated lignin was found to be efficient in the removal of textile dyes from wastewater [13]. One of the gaps in the current literature on lignin derivatization is the lack of information on the effect of drying temperature on derivatized lignin. As drying can significantly affect the properties of lignin [16, 17], it may affect the characteristics of derivatized lignin as well. The present chapter reviews the thermal stability of kraft lignin and derivatized lignin as well as the thermal stability of the reagents used in the modification reactions.

Figure 2-1 depicts the molecular structures of lignin derivatives studied in this thesis work. In assessing the thermal stability of these derivatives, it is important to note the unique chemical modification environments that are present during reactions and how they may contribute to any drying of the lignin products.

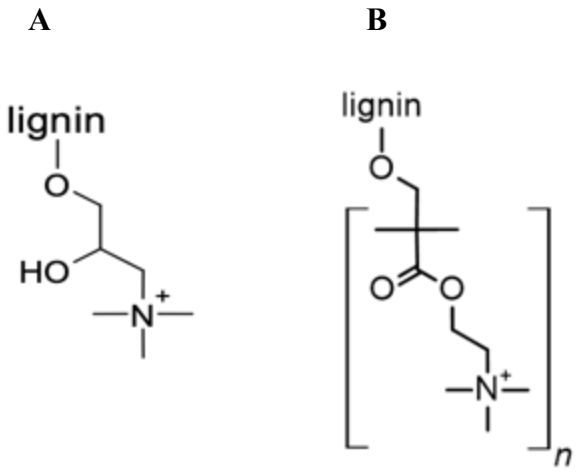

Figure 2-1: Molecular structures of lignin derivatives: amination (A) and high molecular weight cationic lignin polymer (B).

Table 2-1 summarizes the key properties that enable each derivative to be used for the stated target application. Properties, such as water solubility, charge density and molecular weight, are a few of the key parameters that should be conserved after the drying process. It can be seen in Table 2-1 that kraft lignin is not soluble in water, however, after derivatization lignin becomes water-soluble due to the highly electronegative functional groups that may be grafted to the lignin core structure [15, 18]. Additionally, kraft lignin does not bear a significant charge, but after derivatization, it can be made to possess a charge.

Table 2-1: Properties of kraft lignin and some select derivatives such as cationic kraft lignin (CKL), and radically polymerized kraft lignin-METAC (KLM).

Property	KL	CKL	KLM	Reference
Application	-	Flocculant	Flocculant	[19], [20], [14], [21]
Water Solubility (g/L)	1.8	9.0	9.3	[20],[14], [19], [21]
Charge Density (meq/g)	-	+1.0	+2.5	[13], [14], [21]
Mw (g/mol)	1,500 -25,000	9,980	824,000	[17], [10], [11], [21]

2.1.1 Impact of drying temperature on biomass properties

Biomass drying has been shown to cause property changes [22]. Specifically, this phenomenon has been documented to occur in biomass, such as cellulose, in which the formation of cross-linked structures happens during drying [22]. Such structures reduce the water-holding capacity of the material [22]. Cellulose has been reported to undergo changes to its water-holding capacity due to drying, which in turn becomes one of the main bottlenecks for industrial processing of this material [23, 24]. Moreover, polyphenolic compounds such as those found in fruits and vegetables are known to undergo a process of, autooxidation, in the presence of oxygen [25, 26]. This process involves the phenolic hydroxyl groups reacting with oxygen, forming peroxides and carbonyl groups [25, 26]. Hydroxyl groups are directly involved in autooxidation so the higher the concentration of -OH groups, the higher the instability they exhibit [25, 26]. After the process of autooxidation has occurred, the concentration of polyphenols is lower and oxidative

polymerization, or degradation sets in [25, 26]. It has been reported that exposure to temperatures as low as 70ºC for 30 minutes, can decrease the total phenolic content within a polyphenol by as much as 20% [26]. Analogously, similar changes may occur in lignin and lignin derivatives during drying. It has been reported that drying is an important consideration for lignin production [27-29]. Gordobil, et al. [27] reported that drying at lower temperatures (i.e., 25ºC instead of 55ºC) would preserve the colour and structure of lignin more effectively [7]. Another study compared freeze-drying, oven-drying and vacuum-drying of lignin and reported that freeze-drying resulted in significantly less agglomeration of surface particles of lignin while oven-drying and vacuum-drying at a low temperature (40ºC) resulted in large clumps forming at the surface of lignin as well as a darker colour [28]. A more recent study also investigated oven-drying, freeze-drying and vacuum-drying and found that freeze-drying resulted in the highest and most stable hydroxyl content [30]. Furthermore they found that oven-drying at 105ºC resulted in a reduction of hydroxyl content by over 50%, as compared to freeze-drying [30].

2.1.2 Kraft Lignin properties

Kraft lignin has an increased concentration of phenolics, as a result of the cleavage of the β-aryl bonds and the condensed C-C bonds during pulping [9, 31]. Additionally, it is insoluble in water at neutral pH; polydisperse in its molecular weight; amorphous in its structure and a rich polyphenol [32]. In terms of decomposition, under an air atmosphere, lignin decomposes to carbon dioxide and water, and under a nitrogen atmosphere, it decomposes to carbon dioxide, water and compounds containing ethers, ketones and methine groups [32]. Regarding thermal properties, lignin can be considered both as a thermoplastic due to its structure and the presence of hydrogen-bonding, and a thermoset due to the formation of cross-linked structures at raised temperatures [27]. It has been reported that kraft lignin begins to decompose at temperatures as low as 120 and

125ºC [27, 28]. Other studies have reported that lignin decomposes slowly over a broad temperature range of 100 to 180ºC [29]. It was also reported that at elevated temperatures, softwood kraft lignin participates in radical initiated "self-polymerization," resulting in a large increase in its molecular weight [28]. This phenomenon was also reported when lignin was heated under a nitrogen atmosphere at 153ºC, for 20 minutes [29]. The researchers attributed this phenomenon to the creation of three-dimensional cross-linked structures that formed during heating. In another study, the thermal heating of lignin from 60 to 200ºC increased its glass transition temperature due to a loss of chain flexibility, which was in turn caused by cross-linking under heating [27].

2.1.3 Reactivity of polyphenolic compounds

Lignin is known to be composed primarily of phenylpropane units linked together by α-O-4 and β-O-4 linkages. During the pulping process, the α-O-4 linkages in the phenolic units are the most reactive, while the aliphatic units are the most stable [33]. Polyphenolic compounds exhibit high reactivity towards oxygen [28]. This reactivity is ameliorated under alkaline conditions, as alkaline pH levels are electrochemically favourable for electron-shuttling characteristics of polyphenolic compounds [28].

An additional consideration in the reactivity of lignin during the drying process is the impact of the solvent, in this context, water. Water is known to have an important catalytic effect as it behaves both as a proton donor and a proton acceptor and thus plays a key role in mediating proton transfer during reactions [33]. It has been shown that water, as a solvent, has a unique catalytic role in aromatic carbon-hydrogen activation, at neutral pH and low ambient temperatures for small phenolic compounds like catechin, resorcinol and phloroglucinol [29].

2.2 Known Hydrothermal Reactions

In this section, the chemical modifications of lignin in the presence of water and heating will be discussed. This will help to predict the behavior of modified lignin under various drying temperatures when it is suspended in high concentrations of water for drying purposes.

2.2.1 Kraft Lignin Self-Condensation

The phenomenon of kraft lignin self-condensing has been well documented in the literature [34, 35]. It typically occurs during the delignification process [34, 36]. In delignification, various types of condensation reactions can occur, including aldol condensation, dehydrogenative coupling and quinone methide formation. Aldol condensation occurs when two lignin units react to form a β-aryl ether bond. Dehydrogenative coupling is a reaction where two lignin units are linked together by a C-C bond. Quinone methide formation is the reaction between a lignin unit and a nucleophile [34, 36]. This leads to the formation of an ether bond. It has also been described in the literature that the thermal treatment of lignin results in condensation [34, 36].

Previous literature has shown that high temperatures induce condensation of lignin structures [37]. It is worth mentioning that, as kraft lignin tends to self-condense, there have been some attempts to control or minimize this phenomenon by modifying lignin with certain aldehyde compounds, such as formaldehyde [34, 37]. One such study investigated the acid-catalyzed condensation of lignin and reported the stabilizing effects of formaldehyde as a means of preventing condensation reactions from occurring [35]. It has been shown that it may be possible to block the reactive benzylic positions, with a "protecting" agent, such as formaldehyde [37-39]. However, this solution may not be ideal due to the toxic nature of formaldehyde. Yet it is a topic that has drawn a considerable amount of attention. Mu et al., have shown that it is possible to swap out formaldehyde for other types of aldehyde compounds [37]. The authors showed that when

compared to aromatic aldehydes, aliphatic aldehydes are much better at protecting against the undesired lignin condensation process [38]. The explanation as to why aldehydes can be used for this purpose is that they stimulate the formation of an intermediate structure that readily breaks down, facilitating further depolymerization of lignin [37].

It was also reported that lignin condensation reactions occur as a result of the harsh reaction conditions during biomass pre-treatment, i.e., a common first step for lignin depolymerization processes [33]. This condensation poses a problem for such processes because the end goal is to break apart the very linkages that lend lignin its recalcitrant nature. However, the process conditions seem to induce more condensation, hindering the depolymerization process. Possible products that can be formed during condensation reactions under acidic conditions were proposed by Shimada et al. [28]. They have reported that, under acidic conditions, the benzylic carbons on the side chains and the electron-rich carbons on the aromatic nuclei are mainly involved in condensation reactions. In this reaction either a guaiacyl unit or a syringyl unit may be the cationic site and the electron-rich aromatic carbon site facilitates the condensation linkage formation [35]. Additionally, they found that the guaiacol compounds showed higher reactivity for condensation linkages due to the carbonium ions [5]. They also found that particular factors, such as reaction time and acidity of the reaction media, can affect the condensation reaction [36]. Interestingly, they report that although both guaiacyl and syringyl units may take part in condensation reactions, the resulting product of the guaiacyl condensation is much more stable and resistant to heat treatment and acidic conditions [39]. More recent studies have also been conducted on the topic of condensation.

The tendency of kraft lignin to condense with itself may not always be undesirable. Lv, et al. [37] found a pattern of temperature affecting the linkages of lignin during various treatments of

hydrothermal treatments. They investigated hydrothermal treatment of lignin between 40-190ºC. In their work, they assert that during hydrothermal treatment demethylation, dealkylation and cleavage of β-O-4 ether linkages progressively increased. While the aromatic skeleton was preserved [37]. Specifically, increasing the temperature from 70 to 190ºC increased the demethylation of lignin [37]. The authors found that there was a reduction in the methoxy group content as temperature increased. Additionally, they found an initial rise in concentration of carboxyl and or carbonyl groups as temperature increased from 70 to 160ºC. This was followed by a decrease in carboxyl and or carbonyl groups as temperature was increased beyond 160ºC [40]. The authors assert that there is competition between the cleavage of bonds and the self-condensation of free radicals during the heating process [41]. They go on to explain that at lower temperatures (below 160ºC) the bonds possess a lower bond dissociation energy. As such, methoxy and β-O-4 ether linkages predominate over other hydrothermal reactions [20]. Then, at high temperatures (above 160ºC), free monomers like alkanes and monomeric phenolic structures are concurrently produced [16]. They also showed that as the temperature increased to 160ºC the methyl and β-O-4 bond concentration incrementally decreased from 59 atom % to 44 atom % and 14 atom % to 11 atom % respectively. They explain this as a result of dehydration reactions. These reactions eliminate the functional groups that contain carbon and increase the oxygen content [35]. Furthermore, as the temperature increased up to 190ºC the carboxyl content was reduced as a result of the formation of a three-dimensional network structure of covalently cross-linked lignin structures due to self-condensation.

Lv et al. utilized lignin self-condensing to their advantage to minimize the amount of crosslinker required for the process of generating lignin hydrogels [36]. Lv et al. produced 100% lignin hydrogels at various reaction temperatures between 40 to 190ºC by making use of the hydrothermal

treatment method. They found that conducting hydrothermal treatment at lower temperatures, between 40 to 100ºC, before the hydrogel synthesis, caused the methoxy and β-O-4 ether bonds, which have lower dissociation energy interactions, mainly, to break down [15]. This process produces monomeric phenolic subunits and alkanes from lignin [15]. However, at elevated temperatures, like 160ºC, they found that the self-condensation was accompanied by splitting of low bond dissociation energy interactions [15]. The authors confirmed a significant increase in the concentration of C-OH and C=O linkages when they compared the samples that reacted at 40ºC to the samples that reacted at 160ºC. They attributed this change to the dehydration reaction of hydroxyl groups [42]. Upon increasing the temperature to 190ºC, they noticed that the carboxyl content decreased with the formation of self-crosslinked structures of lignin [43]. The authors explain that the process of self-condensation results in the elimination of a certain amount of oxygen groups, which in turn results in an increase of the carbon content and a reduction in oxygen content [44]. Furthermore, they concluded that conducting hydrothermal treatment at high temperatures, causes β-O-4 ether, C_{α}-C_{β} and other low energy linkages to be broken, which generates free radicals and chemical cross-linking via covalent bonds such as α-5, β-5, β-β' linkages [45]. They explained that these new cross-linked structures actually would work to ameliorate the mechanical properties of their lignin-based hydrogels [22].

2.2.2 Thermal stability of Quaternary Ammonium derivatives of lignin

Generally, quaternary ammonium compounds are known for their thermal and chemical stability, as well as their low price. As such, they are commonly utilized in various industries, such as biomedical applications, wastewater treatment, papermaking, textile dyeing and solar cell technology [27-29]. They can also be used in high-temperature applications as coatings for electronics [28]. Modifying lignin with trimethylammonium-carrying epoxide reagents, as is

commonly conducted, imparts a permanent cationic charge to the lignin structure [29]. This strategy is particularly beneficial when compared to other types of modifications, such as amine or carboxyl groups, which are either charged or neutral, depending on the pH of the solution [32]. The resulting quaternary amine structure is not subject to changes in pH. Furthermore, quaternary ammonium compounds are also known as zwitterion molecules, which are a class of molecules that are conferred with particular stability in the realm of thermomechanical properties and moisture stability as compared to primary ammonium compounds [32]. Within the context of interlayer material fabrication for the protection of solar cells to increase their lifetime, Hou et al. investigated how introducing an aryl quaternary ammonium group would be affected by environmental factors, like corrosion and moisture [32]. The authors synthesized the aryl quaternary ammonium compound and used it to create a film that was deposited on the surface of perovskite film via spin coating [32]. They found that, with the addition of the aryl quaternary compound to the perovskite layer, it successfully protected against corrosion and other environmental factors, like humidity, oxygen, and greatly reduced the degradation of the perovskite [32].

A recent study investigated the thermal stability of a quaternary ammonium compounds, in ionic liquids [46]. The compounds contained an aliphatic hydroxyl group but with different types of alkyl chains attached to the cationic nitrogen atom [32]. It was found that the compounds were stable only up to 80ºC, but began to degrade rapidly between 80 to 180ºC [32]. The authors propose that the thermal degradation takes place in two stages. In the first stage, the cationic nitrogen atom is cleaved from the alkyl group. Then, in the second stage, one of two reaction pathways may occur, either a β-E_2-elimination or a nucleophilic substitution at the cationic nitrogen. The elimination pathway is affected by factors like the steric environment of the ammonium ion and

temperature. This pathway for thermal decomposition of quaternary ammonium salts with alkyl groups proceeds through the E_2 bimolecular mechanism and is accompanied by the formation of an alkene (given that there is at least one carbon in the β-position to the electrophilic centre), along with a tertiary amine and a hydrogen halide [32]. Alternatively, the inductive effects of the cationic nitrogen group increase the ability of the β-position hydrogen atoms to protonation and stimulate the formation of terminal alkenes [47].

2.2.3 Thermal Stability of Cationically Radically Polymerized Kraft Lignin

The strategy of radical polymerization to synthesize polymer products is a common method used in polymer chemistry via successive addition of free radicals [48]. This process occurs in three main steps, namely, initiation, propagation and termination [48].

The initiation phase marks the commencement of the polymerization process. In this stage, an active center is formed, which serves as the starting point for the generation of a polymer chain [49]. The initiator molecules undergo heating until a bond is homolytically cleaved, leading to the production of two radicals. Then during propagation, the polymer expands its chain length [49]. The active species for polymerization is a carbon-centred radical known as the propagating radical, which is produced by the additions of an initiating radical during initiation and of the propagating radical during propagation to the monomer [49]. Finally, radical reactions undergo termination, where two radicals combine in such a way that neither remains radical. The most straightforward scenario for this to occur is when two growing chains meet head-to-head, with two benzylic radicals connecting to form a bond [49]. There are certain advantages conferred on the final product via the use of this technique such as high molecular weight, regioselectivity and chain growth [49]. When this method of synthesis is compared to the simpler reactions discussed previously in this chapter, the advantage of radical polymerization is that the resultant product will

carry a higher charger density due to the repeating chains of charged groups. This in turn could improve the performance of the polymer product in its intended application.

Quaternary ammonium compounds (QAC) have long been utilized for their disinfectant properties, serving as the active ingredient in over 200 disinfectants currently recommended by the American EPA, for their effective deactivation of the COVID-19 virus [50]. QACs began to be researched as early as 1915 [51, 52], shortly after that, by 1935, QACs started to see broader use as a disinfectant [50]. Presently, QACs are some of the most widely used classes of cleaners in various industries [50]. From this, it can be seen that this compound is a well-researched candidate for hybridizing with lignin.

Synthesizing such a polymer, whereby two materials are combined, a completely organic component, with a component that is inorganic and hybridizing them in this way via radical polymerization enables the product to have several applications such as biological engineering [53, 54], sustainable battery design [53, 55] and wastewater treatment products [56, 57]. Lignin-based polymers are currently being studied for their application in wastewater treatment as a more environmentally friendly and sustainable option to conventionally used chemicals [58]. Currently, this industry relies on commercial flocculants that are composed mostly of non-biodegradable synthetic polymers [58]. The suitability of polymers for this application depends on their molecular weight and charge density [56]. As such the radical polymerization of lignin with cationic functionality is desired for this application [58].

Drying conditions of such compounds should be carefully considered since they have a high reactivity as a result of having unpaired electrons in the radical species, which itself may participate in further chemical reactions [49]. Additionally, during the drying process of cationic polymers,

certain molecular interactions can occur like electrostatic interactions, hydrogen bonding, Van der Waals interactions and hydrophobic interactions [49].

2.3 Conclusions

Based on the literature reviewed, it is clear that oven-drying may induce certain reactions that have been documented to occur at fairly mild conditions. Furthermore, due to the tendency of lignin to condense with itself, the drying temperature of derivatized lignin should be carefully considered to take into account the kinetics of the potential reactions that may occur during drying and whether they will cause any particular issues for the final desired product. Currently, there are no comprehensive studies available on this particular topic. There is a clear need for future experimental studies to be conducted on this topic.

2.4 References

[1] J. M. Anderson, R. L. Johnson, K. Schmidt-Rohr, and B. H. Shanks, "Hydrothermal degradation of model sulfonic acid compounds: Probing the relative sulfur–carbon bond strength in water," *Catalysis communications,* vol. 51, pp. 33-36, 2014, doi: 10.1016/j.catcom.2014.03.021.

[2] S. S. Zumdahl and S. A. Zumdahl, *Chemistry*. Cengage Learning, 2013.

[3] F. Jin *et al.*, "Oxidation of unsaturated carboxylic acids under hydrothermal conditions," *Bioresource Technology,* vol. 101, no. 19, pp. 7624-7634, 2010/10/01/ 2010, doi: https://doi.org/10.1016/j.biortech.2010.04.056.

[4] W. J. Chen, C. X. Zhao, B. Q. Li, T. Q. Yuan, and Q. Zhang, "Lignin-derived materials and their applications in rechargeable batteries," *Green Chemistry,* vol. 24, no. 2, pp. 565-584, Jan 2022, doi: 10.1039/d1gc02872c.

[5] T. Komatsu and T. Yokoyama, "Revisiting the condensation reaction of lignin in alkaline pulping with quantitativity part I: the simplest condensation between vanillyl alcohol and creosol under soda cooking conditions," *Journal of Wood Science,* vol. 67, no. 1, p. 45, 2021/06/09 2021, doi: 10.1186/s10086-021-01978-4.

[6] M. Nuopponen, H. Wikberg, T. Vuorinen, S. L. Maunu, S. Jämsä, and P. Viitaniemi, "Heat-treated softwood exposed to weathering," *J Appl Polym Sci,* https://doi.org/10.1002/app.13351 vol. 91, no. 4, pp. 2128-2134, 2004/02/15 2004, doi: https://doi.org/10.1002/app.13351.

[7] M. R. Roger, P. Roger, and A. T. Mandla, "Cell Wall Chemistry," in *Handbook of Wood Chemistry and Wood Composites*: CRC Press, 2012, ch. Cell Wall Chemistry.

[8] F. Asgari and D. Argyropoulos, "Fundamentals of o×ygen delignification. Part II. Functional group formation/elimination in residual kraft lignin," *Canadian Journal of Chemistry-revue Canadienne De Chimie - CAN J CHEM,* vol. 76, 11/01 1998, doi: 10.1139/cjc-76-11-1606.

[9] X. Mu, Z. Han, C. Liu, and D. Zhang, "Mechanistic Insights into Formaldehyde-Blocked Lignin Condensation: A DFT Study," *The Journal of Physical Chemistry C,* vol. 123, no. 14, pp. 8640-8648, 2019/04/11 2019, doi: 10.1021/acs.jpcc.9b00247.

[10] L. Shuai *et al.*, "Formaldehyde stabilization facilitates lignin monomer production during biomass depolymerization," *Science,* vol. 354, no. 6310, pp. 329-333, 2016/10/21 2016, doi: 10.1126/science.aaf7810.

[11] K. Shimada, S. Hosoya, and T. Ikeda, "Condensation reactions of softwood and hardwood lignin model compounds under organic acid cooking conditions," *Journal of wood chemistry and technology,* vol. 17, no. 1/2, pp. 57-72, 1997, doi: 10.1080/02773819708003118.

[12] G. Smook, *Handbook for Pulp & Paper Technologists (The Smook Book)*. TAPPI Press, 2016.

[13] F. Kong, K. Parhiala, S. Wang, and P. Fatehi, "Preparation of cationic softwood kraft lignin and its application in dye removal," vol. 67, p. 345, 2015.

[14] N. Ghavidel and P. Fatehi, "Pickering/Non-Pickering Emulsions of Nanostructured Sulfonated Lignin Derivatives," *ChemSusChem,* vol. 13, no. 17, pp. 4567-4578, 2020/09/07 2020, doi: https://doi.org/10.1002/cssc.202000965.

[15] A. Eraghi Kazzaz, Z. Hosseinpour Feizi, and P. Fatehi, "Grafting strategies for hydroxy groups of lignin for producing materials," *Green Chemistry,* 10.1039/C9GC02598G vol. 21, no. 21, pp. 5714-5752, 2019, doi: 10.1039/C9GC02598G.

[16] S. Bertella and J. S. Luterbacher, "Lignin Functionalization for the Production of Novel Materials," *Trends in Chemistry,* vol. 2, no. 5, pp. 440-453, 2020/05/01/ 2020, doi: https://doi.org/10.1016/j.trechm.2020.03.001.

[17] M. Y. Balakshin *et al.*, "Cover Feature: New Opportunities in the Valorization of Technical Lignins (ChemSusChem 4/2021)," *ChemSusChem,* https://doi.org/10.1002/cssc.202100110 vol. 14, no. 4, pp. 992-992, 2021/02/18 2021, doi: https://doi.org/10.1002/cssc.202100110.

[18] A. Eraghi Kazzaz and P. Fatehi, "Technical lignin and its potential modification routes: A mini-review," *Industrial Crops and Products,* vol. 154, p. 112732, 2020/10/15/ 2020, doi: https://doi.org/10.1016/j.indcrop.2020.112732.

[19] T. Aro and P. Fatehi, "Production and Application of Lignosulfonates and Sulfonated Lignin," *ChemSusChem,* https://doi.org/10.1002/cssc.201700082 vol. 10, no. 9, pp. 1861-1877, 2017/05/09 2017, doi: https://doi.org/10.1002/cssc.201700082.

[20] M. Aldajani, N. Alipoormazandarani, F. Kong, and P. Fatehi, "Acid hydrolysis of kraft lignin-acrylamide polymer to improve its flocculation affinity," *Sep Purif Technol,* vol. 258, p. 117964, 2021/03/01/ 2021, doi: https://doi.org/10.1016/j.seppur.2020.117964.

[21] S. Sabaghi and P. Fatehi, "Phenomenological Changes in Lignin Following Polymerization and Its Effects on Flocculating Clay Particles," *Biomacromolecules,* vol. 20, no. 10, pp. 3940-3951, 2019/10/14 2019, doi: 10.1021/acs.biomac.9b01016.

[22] W. Mo, K. Chen, X. Yang, F. Kong, J. Liu, and B. Li, "Elucidating the hornification mechanism of cellulosic fibers during the process of thermal drying," *Carbohydrate Polymers,* vol. 289, p. 119434, 2022/08/01/ 2022, doi: https://doi.org/10.1016/j.carbpol.2022.119434.

[23] Z. J. Xie, J. J. Guan, L. Chen, Z. Y. Jin, and Y. Q. Tian, "Effect of Drying Processes on the Fine Structure of A-, B-, and C-Type Starches," (in English), *STARCH-STARKE,* vol. 70, no. 3-4, MAR 2018, Art no. 1700218, doi: 10.1002/star.201700218.

[24] M. Beaumont, J. König, M. Opietnik, A. Potthast, and T. Rosenau, "Drying of a cellulose II gel: effect of physical modification and redispersibility in water," *Cellulose,* vol. 24, no. 3, pp. 1199-1209, 2017/03/01 2017, doi: 10.1007/s10570-016-1166-9.

[25] H. Zhang, M. Wang, and J. Xiao, "Chapter One - Stability of polyphenols in food processing," in *Advances in Food and Nutrition Research*, vol. 102, F. Toldrá Ed.: Academic Press, 2022, pp. 1-45.

[26] J. Deng, H. Yang, E. Capanoglu, H. Cao, and J. Xiao, "9 - Technological aspects and stability of polyphenols," in *Polyphenols: Properties, Recovery, and Applications*, C. M. Galanakis Ed.: Woodhead Publishing, 2018, pp. 295-323.

[27] O. Gordobil, R. Herrera, F. Poohphajai, J. Sandak, and A. Sandak, "Impact of drying process on kraft lignin: lignin-water interaction mechanism study by 2D NIR correlation spectroscopy," *Journal of Materials Research and Technology,* vol. 12, pp. 159-169, 2021/05/01/ 2021, doi: https://doi.org/10.1016/j.jmrt.2021.02.080.

[28] H. Zhang, S. Fu, and Y. Chen, "Basic understanding of the color distinction of lignin and the proper selection of lignin in color-depended utilizations," *International Journal of*

Biological Macromolecules, vol. 147, pp. 607-615, 2020/03/15/ 2020, doi: https://doi.org/10.1016/j.ijbiomac.2020.01.105.

[29] C. Cui, H. Sadeghifar, S. Sen, and D. Argyropoulos, "Toward Thermoplastic Lignin Polymers; Part II: Thermal & Polymer Characteristics of Kraft Lignin & Derivatives," *Bioresources,* vol. 8 (1), pp. 864-886, 11/05 2013, doi: 10.15376/biores.8.1.864-886.

[30] A. Mazar and M. Paleologou, "Comparison of the effects of three drying methods on lignin properties," *International Journal of Biological Macromolecules,* vol. 258, p. 128974, 2024/02/01/ 2024, doi: https://doi.org/10.1016/j.ijbiomac.2023.128974.

[31] O. Yu and K. H. Kim, "Lignin to Materials: A Focused Review on Recent Novel Lignin Applications," *Applied Sciences,* vol. 10, no. 13, 2020, doi: 10.3390/app10134626.

[32] H. Wang *et al.*, "Preparation and Formation Mechanism of Covalent–Noncovalent Forces Stabilizing Lignin Nanospheres and Their Application in Superhydrophobic and Carbon Materials," *ACS Sustainable Chemistry & Engineering,* vol. 9, no. 10, pp. 3811-3820, 2021/03/15 2021, doi: 10.1021/acssuschemeng.0c08780.

[33] B. Bhandari, "Handbook of Industrial Drying, Fourth EditionEdited by A. S. Mujumdar: CRC Press: Boca Raton, FL; 2015. ISBN: 978-1-4665-9665-8," *Drying technology,* vol. 33, no. 1, pp. 128-129, 2015, doi: 10.1080/07373937.2014.983704.

[34] D. Dehnad, S. M. Jafari, and M. Afrasiabi, "Influence of drying on functional properties of food biopolymers: From traditional to novel dehydration techniques," *Trends in Food Science & Technology,* vol. 57, pp. 116-131, 2016, doi: 10.1016/j.tifs.2016.09.002.

[35] N. Chhabra, M. Arora, D. Garg, and M. K. Samota, "Spray freeze drying - A synergistic drying technology and its applications in the food industry to preserve bioactive

compounds," *Food Control,* vol. 155, p. 110099, 2024/01/01/ 2024, doi: https://doi.org/10.1016/j.foodcont.2023.110099.

[36] A. Menon, V. Stojceska, and S. A. Tassou, "A systematic review on the recent advances of the energy efficiency improvements in non-conventional food drying technologies," *Trends in Food Science & Technology,* vol. 100, pp. 67-76, 2020/06/01/ 2020, doi: https://doi.org/10.1016/j.tifs.2020.03.014.

[37] Z. Lv *et al.*, "Hydrothermal method-assisted synthesis of self-crosslinked all-lignin-based hydrogels," *International Journal of Biological Macromolecules,* vol. 216, pp. 670-675, 2022/09/01/ 2022, doi: https://doi.org/10.1016/j.ijbiomac.2022.07.003.

[38] D. de Beer, T. Beelders, C. Human, and E. Joubert, "Assessment of the stability of compounds belonging to neglected phenolic classes and flavonoid sub-classes using reaction kinetic modeling," *Critical Reviews in Food Science and Nutrition,* pp. 1-28, 2022, doi: 10.1080/10408398.2022.2096561.

[39] W. Li *et al.*, "Effect of hot air drying on the polyphenol profile of Hongjv (Citrus reticulata Blanco, CV. Hongjv) peel: A multivariate analysis," *Journal of Food Biochemistry,* vol. 44, no. 5, p. e13174, 2020/05/01 2020, doi: https://doi.org/10.1111/jfbc.13174.

[40] S. Sen, S. Patil, and D. S. Argyropoulos, "Thermal properties of lignin in copolymers, blends, and composites: a review," *Green Chemistry,* 10.1039/C5GC01066G vol. 17, no. 11, pp. 4862-4887, 2015, doi: 10.1039/C5GC01066G.

[41] M. Ma, L. Dai, J. Xu, Z. Liu, and Y. Ni, "A simple and effective approach to fabricate lignin nanoparticles with tunable sizes based on lignin fractionation," *Green Chemistry,* 10.1039/D0GC00377H vol. 22, no. 6, pp. 2011-2017, 2020, doi: 10.1039/D0GC00377H.

[42] W. Zhang *et al.*, "Lignin derived carbon materials: current status and future trends," *Carbon Research,* vol. 1, no. 1, p. 14, 2022/07/29 2022, doi: 10.1007/s44246-022-00009-1.

[43] A. Beaucamp *et al.*, "Lignin for energy applications – state of the art, life cycle, technoeconomic analysis and future trends," *Green Chemistry,* 10.1039/D2GC02724K vol. 24, no. 21, pp. 8193-8226, 2022, doi: 10.1039/D2GC02724K.

[44] U. Ejaz and M. Sohail, "Lignin: A Renewable Chemical Feedstock," in *Handbook of Smart Materials, Technologies, and Devices: Applications of Industry 4.0*, C. M. Hussain and P. Di Sia Eds. Cham: Springer International Publishing, 2020, pp. 1-15.

[45] X. Chen, K. Zhang, L.-P. Xiao, R.-C. Sun, and G. Song, "Total utilization of lignin and carbohydrates in Eucalyptus grandis: an integrated biorefinery strategy towards phenolics, levulinic acid, and furfural," *Biotechnology for Biofuels,* vol. 13, no. 1, p. 2, 2020/01/06 2020, doi: 10.1186/s13068-019-1644-z.

[46] E. I. Evstigneyev and S. M. Shevchenko, "Structure, chemical reactivity and solubility of lignin: a fresh look," *Wood Science and Technology,* vol. 53, no. 1, pp. 7-47, 2019/01/01 2019, doi: 10.1007/s00226-018-1059-1.

[47] R. Wahlström, A. Kalliola, J. Heikkinen, H. Kyllönen, and T. Tamminen, "Lignin cationization with glycidyltrimethylammonium chloride aiming at water purification applications," *Industrial Crops and Products,* vol. 104, pp. 188-194, 2017/10/01/ 2017, doi: https://doi.org/10.1016/j.indcrop.2017.04.026.

[48] G. B. Smith and G. T. Russell, "The Cutthroat Competition Between Termination and Transfer to Shape the Kinetics of Radical Polymerization," in *Radical Polymerization*, 2007, pp. 1-11.

[49] C. E. Carraher, *Carraher's polymer chemistry*, Ninth edition. ed. (Polymer chemistry). Boca Raton: CRC Press/Taylor & Francis Group, 2014.

[50] P. I. Hora, S. G. Pati, P. J. McNamara, and W. A. Arnold, "Increased Use of Quaternary Ammonium Compounds during the SARS-CoV-2 Pandemic and Beyond: Consideration of Environmental Implications," *Environmental Science & Technology Letters,* vol. 7, no. 9, pp. 622-631, 2020/09/08 2020, doi: 10.1021/acs.estlett.0c00437.

[51] W. A. Jacobs, M. Heidelberger, and H. L. Amoss, "The Bactericidal Properties of The Quaternary Salts of Hexamethylenetetramine : Ii. The Relation Between Constitution And Bactericidal Action In The Substituted Benzylhexamethylenetetraminium Salts," *Journal of Experimental Medicine,* vol. 23, no. 5, pp. 569-576, 1916, doi: 10.1084/jem.23.5.569.

[52] W. A. Jacobs and M. Heidelberger, "On a New Group of Bactericidal Substances Obtained from Hexamethylenetetramine," *Proceedings of the National Academy of Sciences,* vol. 1, no. 4, pp. 226-228, 1915/04/01 1915, doi: 10.1073/pnas.1.4.226.

[53] R. Kouser, A. Vashist, M. Zafaryab, M. A. Rizvi, and S. Ahmad, "Na-Montmorillonite-Dispersed Sustainable Polymer Nanocomposite Hydrogel Films for Anticancer Drug Delivery," *ACS Omega,* vol. 3, no. 11, pp. 15809-15820, 2018/11/30 2018, doi: 10.1021/acsomega.8b01691.

[54] R. Kouser, A. Vashist, M. Zafaryab, M. A. Rizvi, and S. Ahmad, "pH-Responsive Biocompatible Nanocomposite Hydrogels for Therapeutic Drug Delivery," *ACS Applied Bio Materials,* vol. 1, no. 6, pp. 1810-1822, 2018/12/17 2018, doi: 10.1021/acsabm.8b00260.

[55] Y. Wang, X. Huang, T. Li, L. Li, X. Guo, and P. Jiang, "Polymer-Based Gate Dielectrics for Organic Field-Effect Transistors," *Chemistry of Materials,* vol. 31, no. 7, pp. 2212-2240, 2019/04/09 2019, doi: 10.1021/acs.chemmater.8b03904.

[56] J. A. Diaz-Baca, A. Salaghi, and P. Fatehi, "Generation of Sulfonated Lignin-Starch Polymer and Its Use As a Flocculant," *Biomacromolecules,* vol. 24, no. 3, pp. 1400-1416, 2023/03/13 2023, doi: 10.1021/acs.biomac.2c01437.

[57] S. Sabaghi, N. Alipoormazandarani, and P. Fatehi, "Production and Application of Triblock Hydrolysis Lignin-Based Anionic Copolymers in Aqueous Systems," *ACS Omega,* vol. 6, no. 9, pp. 6393-6403, 2021/03/09 2021, doi: 10.1021/acsomega.0c06344.

[58] A. Salaghi, J. A. Diaz-Baca, and P. Fatehi, "Enhanced flocculation of aluminum oxide particles by lignin-based flocculants in dual polymer systems," *Journal of Environmental Management,* vol. 328, p. 116999, 2023/02/15/ 2023, doi: https://doi.org/10.1016/j.jenvman.2022.116999.

Chapter 3 – Structural changes of cationic grafted lignin at different drying temperatures

3.1 Abstract

The reaction of glycidyl-trimethylammonium chloride (GTMAC) with lignin is promising since it generates a cationic lignin derivative with potential applications in various fields, such as wastewater treatment, ion exchange resins, dye, and textile manufacturing. Drying is an important step of polymer fabrication. This work investigates the effect of drying temperatures (-55, 80, 105, and 130ºC) on the properties of kraft lignin (KL) and cationic kraft lignin (CKL). For KL, condensation products were detected after oven-drying, along with an increase in molecular weight and glass transition temperature at 105ºC. Meanwhile, nitrogen-containing groups were degraded in addition to condensation for CKL. Additionally, the molecular weight of the CKL samples was more temperature-sensitive than KL. The CKL samples exhibited lower glass transition temperatures than KL after drying. This work demonstrates that the drying temperature of cationically grafted lignin is an important consideration in conserving the desired properties of the material.

3.2 Introduction

Lignin is the most abundant source of aromatic carbon on Earth. As such, it has great potential to be utilized for the sustainable production of green products [1-6]. The pulp and paper industry generates a substantial amount of lignin, of which only a fraction is sold as technical lignin [2, 3, 7]. Meanwhile, the majority of lignin is combusted for energy generation [2, 3, 7]. Kraft lignin is still the most pervasive type of lignin on the market [8]. Generally, kraft lignin is known for its

insolubility in water [9]. To widen its application, it is important to modify or chemically derivatize kraft lignin in order to confer the desired properties [10, 11]. Derivatizing lignin is particularly important as a strategy to tune lignin's solubility [12, 13]. Currently, cationic lignin is a promising lignin derivative with potential applications in wastewater treatment, ion exchange resin, as well as dye and textile manufacturing [10-12, 14]. Despite progress in its reaction chemistry, the process of producing this material has not been fully developed, and drying is an important step, towards this.

Drying of biomass is known to affect its physicochemical characteristics [15]. For example, cellulose has been reported to change its water-holding capacity due to drying, which in turn becomes one of the main bottlenecks for the industrial processing of this material [16, 17]. Moreover, polyphenolic compounds, such as those found in fruits and vegetables, are known to undergo a process of autooxidation in the presence of oxygen [5, 18]. This process involves the phenolic hydroxyl groups reacting with oxygen, forming peroxides and carbonyl groups [5, 18]. Hydroxyl groups are directly involved in autooxidation in air, and the higher the concentration of -OH groups, the higher the instability they exhibit [5, 18]. In this regard, exposure to temperatures as low as 70ºC could decrease the total phenolic content by as much as 20% [18]. This is important because the phenolic content of the biomass may be an important feature of the product. Such observations can be important in the consideration of lignin, as it is rife with polyphenolic structures.

It has been shown that drying conditions should be carefully considered, as they affect the final properties of this biopolymeric substance [19-21]. It has been previously documented that drying of KL causes both optical and chemical structural changes as a result of the depolymerization and re-polymerization [19, 21-23]. Gordobil, et al. [19] showed that drying at 55ºC could better

preserve the colour and structure of lignin. In a different study, researchers compared freeze-drying, oven-drying, and vacuum-drying of lignin. They reported that freeze-drying caused less agglomeration of lignin particles while oven-drying and vacuum-drying at 40ºC resulted in large clumps of lignin particles as well as a darker colouration of lignin [20]. Recent work by Mazar and Paleologou [24] has shown that drying condition plays an important role in the hydroxyl content of KL. It was found that the total hydroxyl content of KL decreased by over 50% after oven-drying at 105ºC when compared to freeze-drying [24]. It was also found that freeze-drying provided the highest and most stable hydroxyl content, as compared to oven-drying, vacuum-drying, and freeze-drying [24]. However, no information is available on how chemically modifying lignin with an altered hydroxyl group would respond to drying temperature. Additionally, no comprehensive chemical characterization, utilizing XPS and HSQC NMR, was conducted in the literature on KL after drying to understand the details of structural changes of KL in drying.

The focus of this work was to understand the influence of drying temperature on the properties of cationic kraft lignin (CKL). CKL was synthesized using a facile water-based technique. This technique utilizes nucleophilic substitution of the phenolic group of lignin under alkaline conditions to graft a cationic nitrogen group to the lignin structure [10, 11, 13]. Samples of lignin derivatives were dried under various temperatures. Afterward, the properties of the polymers were investigated, and they were related to drying temperature. The results of this work provide valuable information about the influence of drying temperature on the properties of cationic lignin products.

3.3 Materials and Methods

3.3.1 Materials

Softwood kraft lignin (KL) was sourced from a mill located in Hinton, Alberta. Glycidyl-trimethylammonium chloride (GTMAC), sodium hydroxide (NaOH), sulfuric acid (H_2SO_4), deuterated dimethyl sulfoxide (DMSO-d_6), 3-2-chloro-4,4,5,5-tetramethyl-1,3,2-dioxaphospholane (CDP), (trimethylsilyl)propionic-2,2,3,3-d4 acid sodium salt tetramethylsilane (TSP), cyclohexanol (99%), and chromium (III) acetylacetonate were all obtained from Sigma, Oakville, Canada. Potassium polyvinyl sulfate (PVSK) was obtained from Wako Pure Chem. Ltd., Osaka, Japan. Dialysis membranes (1,000 g/mol cut off) were obtained from Spectrum Labs.

3.3.2 CKL Synthesis and drying

A 500 mL 3-neck round bottom flask was pre-heated in a 70ºC water bath. A 20 wt.% solution of KL in water was prepared and adjusted to pH 11.5 using 5 M NaOH. Then, the KL solution was transferred to the 3-neck flask. The temperature was allowed to equilibrate, then the GTMAC was added, and the reaction was allowed to proceed for 1 hour. Subsequently, the flask was submerged in a cold-water bath for 15 minutes. Then, the product was neutralized using 1.5 mol/L sulfuric acid. Finally, it was dialyzed for 48 hours, and the product was denoted as cationic kraft lignin (CKL). A quantity of the purified product was freeze-dried, and the remaining was oven-dried at 80, 105, and 130ºC for 48 hours. The KL control sample was prepared by following the same steps listed above in the absence of GTMAC.

3.3.3 Water Solubility and Charge Density

The water solubility and charge density of the samples were measured, as described by Konduri et al. [25]. The samples were prepared by making a 1% concentration of the lignin derivative sample in water, and then it was shaken for one hour at 30ºC in a shaker bath. After that, a portion was

taken for water solubility [25]. The other portion was titrated against PVSK (for cationic samples) and PDADMAC (for anionic samples) to determine the charge density using a PCD-04+Titrator from Mütek, Germany, charge titrator.

3.3.4 Differential scanning calorimetry (DSC)

The glass transition temperature, T_g, of the samples, was determined by a DSC. 10-15 mg samples were placed in hermetic Tzero aluminum pans and ran in a DSC Q2000, TA instrument, DE, USA. The tests were run under a nitrogen atmosphere. A heating and cooling cycle was employed at a rate of 5ºC/min in the range of 20 to 230ºC. Another heating cycle from 20 to 230ºC at a rate of 10ºC/min was then applied to determine the T_g.

3.3.5 Gel permeation chromatography (GPC)

The molecular weight of the samples was determined through GPC. The preparation of each sample involved dissolving 5 mg of the samples in 10 mL of a solution containing 5 wt.% acetic acid (for cationic samples) and sodium nitrate (for anionic samples), which acted as the mobile phase. These samples were stirred at a speed of 300 rpm at room temperature throughout the night and subsequently filtered through a nylon filter with a pore size of 0.2 μm. Then, the analysis of molecular weight was conducted by injecting the solution into a gel permeation chromatography instrument. The Malvern GPCmax VE2001 Module and Viscotek TDA305 with multidetectors (UV, RI, viscometer, low angle, and right angle laser detectors) were used. The mobile phase had a flow rate of 0.50 mL/min. For the CKL samples, the mobile phase was acetic acid, and the laser detector was used. For the KL samples, the mobile phase was sodium nitrate, and the UV detector was used.

3.3.6 ^{1}H and HSQC nuclear magnetic resonance spectroscopy (NMR)

The chemical compositions of the samples were examined using hydrogen proton nuclear magnetic resonance (^{1}H NMR) and two-dimensional heteronuclear single quantum coherence (HSQC NMR). For each test, a sample of 70-75 mg and an internal standard of 6-10 mg of TSP were dissolved in 1 mL of DMSO-d_6. These samples were stirred at room temperature overnight before the analysis. The spectra were collected using a nuclear magnetic resonance spectroscopy with a Bruker AVANCE NEO 500 MHz instrument, Switzerland, at a temperature of 25ºC. The ^{1}H NMR spectra acquisition settings included 64 scans, a relaxation delay of 2 seconds, an acquisition time of 3.28 seconds, and a pulse of 30º. The HSQC spectra were acquired using the Bruker pulse program hsqcetgpsisp, with a spectra width of 13 ppm in the F2 (^{1}H) dimension with 2048 data points (155 microseconds acquisition time), a spectra width of 165 ppm in the F1 (^{13}C) dimension with 256 data points (6.2 microseconds acquisition time), a pulse delay of 2 seconds, and 16 scans. The NMR spectra were processed using TopSpin 4.1.9 software.

3.3.7 ^{31}P NMR

The hydroxyl concentration of the different types of hydroxyl groups was quantified using the ^{31}P NMR method as described in the past [13]. The solvent workup consisted of a 1:1.6 v/v solution of chloroform-d ($CDCL_3$) and pyridine. 70-75 mg of each sample was dissolved in 1 mL of the solvent. 2.5 mg/mL of chromium (III) acetylacetonate was added as a relaxation agent. The sample was allowed to be stirred overnight. Then, it was reacted with 200 µL of phosphitylating reagent, CDP. The ^{31}P NMR spectra were acquired using the AVANCE NEO 500 MHz, Bruker instrument, at 25ºC. Also, 256 scans, a 0.6-second acquisition time, a 90º pulse, and a 5-second relaxation delay were adjusted for each sample. The spectra were processed using TopSpin 4.1.9 from Bruker.

3.3.8 X-Ray Photoelectron Spectroscopy (XPS)

Samples were characterized using an XPS instrument from Kratos AXIS Supra, Shimadzu Group Company, Japan, which was equipped with a dual anode Al/Ag monochromatic X-ray source (1486.7 eV). The settings were 15kV in fixed analyzer transmission mode, with a pass energy of 40eV for the region of interest and 80eV for the survey region. The XPS spectra were processed and quantified using CASAXPS software by Casa Software Ltd., UK.

3.3.9 Organic Element Analysis

The organic elements of the samples, carbon, hydrogen, nitrogen, and sulfur were determined by combusting 2 mg of each sample at 1200ºC. The elemental analyzer from Vario EL cube, (Elementar Analyse Systeme GmbH, Germany) was used in this experiment. The oxygen content was found by mass balance.

3.4 Results & Discussion

3.4.1 Water solubility, charge density, and elemental composition

Table 3-1 shows the water solubility, charge density, and elemental compositions of KL-0 and CKL-0. It can be seen that the control sample, KL-0, has a charge density of -1.0 meq/g and a water solubility of 90.5 wt.%. The organic elemental content of the KL-0 sample was found to be 62.5% carbon, 7.2% hydrogen, 30.3% oxygen and no nitrogen nor sulfur. The CKL-0 sample possessed a charge density of +1.5 meq/g and was completely water-soluble.

Table 3-1: Water solubility, charge density, and elemental composition of freeze-dried kraft lignin (KL-0) and freeze-dried cationic kraft lignin (CKL-0).

Sample	KL-0	CKL-0
Water solubility (%)	90.5	100
Charge density (meq/g)	-1.0	+1.5
C (%)	62.5	60.6
H (%)	7.2	9.9
N (%)	0.0	2.2
S (%)	0.0	0.0
O (%)	30.3	27.3

By comparing the elemental composition of KL-0 and CKL-0, it can be seen that the reaction of KL with GTMAC increased the nitrogen content of the sample to 2.2%. The increase in nitrogen content, along with the improved water solubility, indicates the success of the reaction. These results were further confirmed by NMR and XPS (Figures 3-1, 3-2, and 3-3), which will be discussed later.

3.4.2 ^{1}H NMR analysis

Figure 3-1 shows the ^{1}H NMR of KL-0 and CKL-0. It can be seen that there are four distinct regions for the KL-0 spectra. The region between 6 and 7.8 ppm was assigned to the protons in the aromatic rings of lignin [26-28]. The region between 4.2 and 5.6 ppm was assigned to the oxygenated aliphatic protons groups [26-28]. The region between 3 and 4 ppm was assigned to the methoxy groups [26-28]. Finally, the region between 0.5 and 2.3 ppm was assigned to the aliphatic

protons of the β-1 linkages of lignin [26-28]. The peak at 2.5 ppm was assigned to the solvent, DMSO-d_6. For the CKL-0 sample, the same regions as KL-0 were present, but with the addition of a distinct and new peak between 3.2-3.6 ppm, which corresponds to the protons of the methyl groups attached to the cationic nitrogen atom [1].

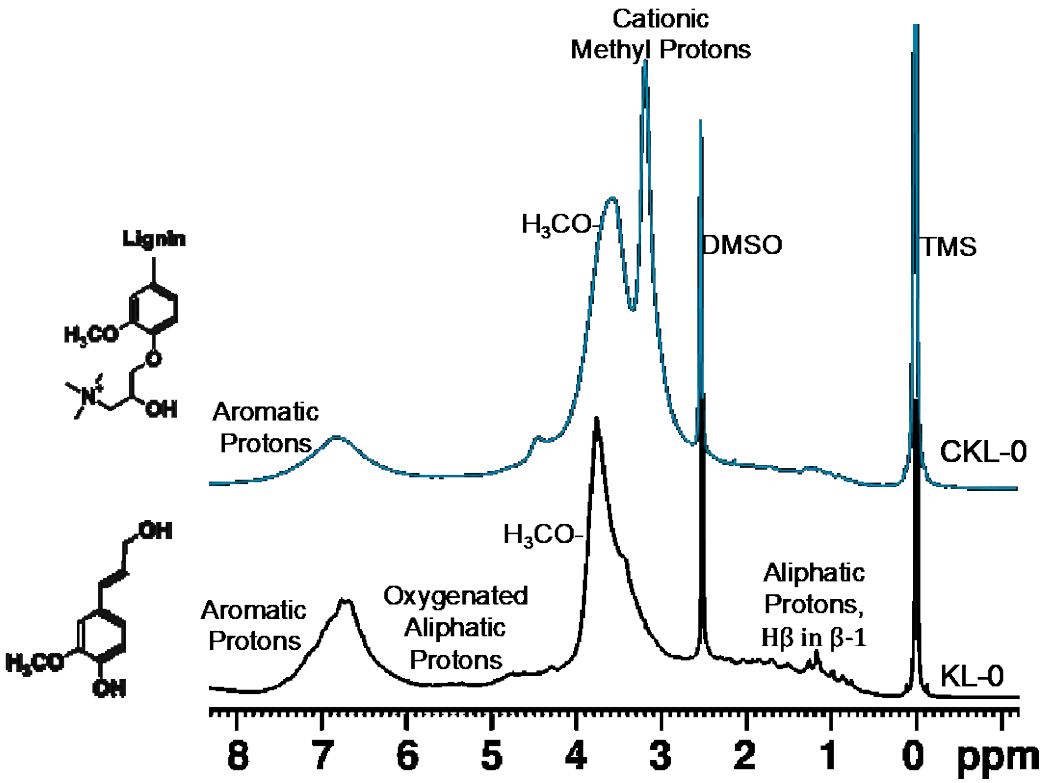

Figure 3-1: ^{1}H NMR spectra of the freeze-dried kraft lignin control sample (KL-0) along with the freeze-dried cationic kraft lignin (CKL-0).

3.4.3 HSQC NMR analysis

Due to the broad, overlapping signals in the proton NMR spectra, HSQC was utilized to derive further chemical structural information for the CKL-0 sample. Figure 3-2 shows the HSQC spectra of the aliphatic and oxygenated aliphatic regions of KL-0 (A) and CKL-0 (B). For the HSQC of

KL-0, the gamma-carbon, denoted as Cγ in the figure, which is adjacent to the β-O-4 linkages, was assigned to the signal appearing at H_δ/C_δ = 3.6/61 ppm [8]. Another characteristic functional group of KL-0 is the methoxy group, whose signal was attributed to the contour occurring at H_δ/C_δ = 3.2-4/57-60 ppm [8]. Other smaller signals in the aliphatic region were attributed to the protons and carbons involved in the aliphatic chains of KL [8].

For CKL-0, along with methoxy and aliphatic signals, new signals appeared and were attributed to the reaction of GTMAC with KL. The signal Ca at H_δ/C_δ = 4.1/72 ppm was attributed to the -CH_2- group adjacent to the formerly phenolic oxygen atom of KL [10, 11]. The signal Cb at H_δ/C_δ = 4.5/64 ppm was attributed to the -OH group of the GTMAC [10, 11]. The signal Cc at H_δ/C_δ = 3.5/60 ppm was attributed to the -CH_2- group adjacent to the cationic nitrogen atom of GTMAC [10, 11]. The signal C_d was attributed to the -CH_3 groups bound to the cationic nitrogen atom of GTMAC [10, 11].

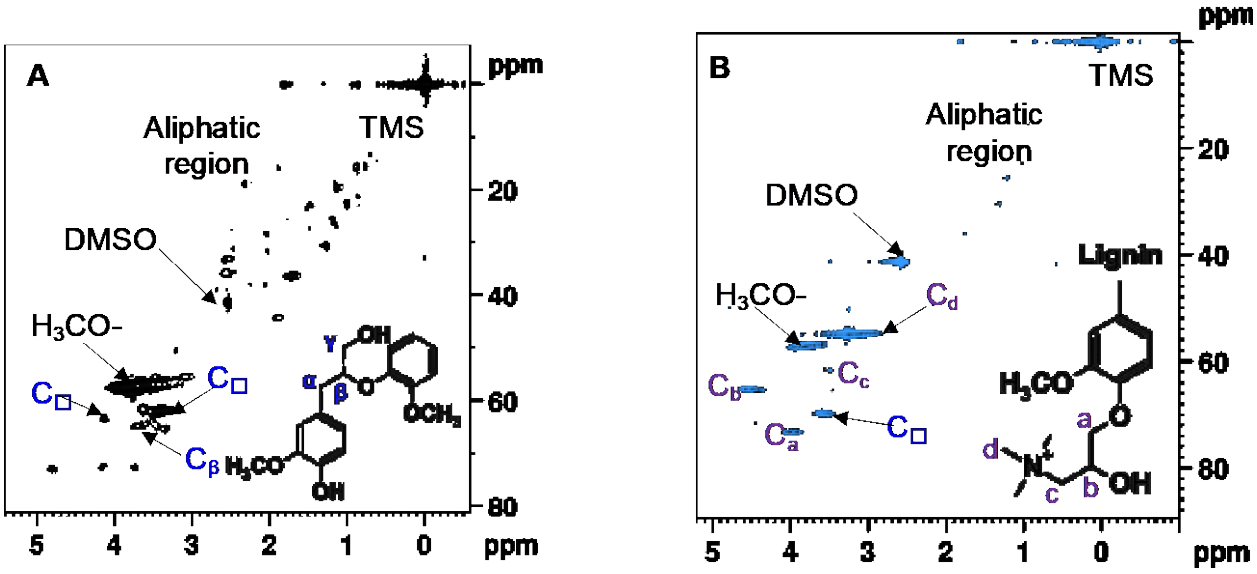

Figure 3-2: HSQC NMR characteristic signals KL-0 (A) and CKL-0 (B).

3.4.4 XPS analysis

XPS was used to study the elemental and chemical bonds of the samples as a result of the reaction. Figure 3-3 shows the XPS survey spectra (A), along with the C1s (B) and O1s (C) scans of KL-0 and CKL-0, along with the N1s scan of the CKL-0 sample (D). In the survey spectra of CKL-0, the smaller peak at 400 eV was attributed to N1s and the absence of this peak in the KL-0 spectra was interpreted as the confirmation of the reaction of GTMAC with KL. Deconvolution of the C1s spectra for KL-0 resulted in two major peaks. These peaks were attributed to the aliphatic C-C/C-H (284.5 eV) and C-OH (286 eV). For the CKL-0 C1s spectra, two peaks were found. These were attributed to C-C/C-H/ (284.5 eV) and C-OH (286 eV) [29, 30]. Deconvolution of the O1s spectra for KL-0 resulted in two peaks. These peaks were attributed to C=O (532 eV), and C-O-C / phenolic-OH (533 eV) [31, 32].

For the CKL-0 samples, the same peaks were found. In the N1s scans, two major peaks were found. These peaks were attributed to the cationic nitrogen C-N+ (402 eV) and then a smaller peak was attributed to C-N (399 eV) [33, 34]. The presence of the second smaller peak indicates that a side reaction may have occurred during the synthesis reaction of CKL. There is existing literature that points to the susceptibility of quaternary ammonium groups breaking down to form tertiary amide groups as a result of being exposed to higher temperatures (i.e., 70ºC) and alkaline conditions (i.e., pH 11) [35].

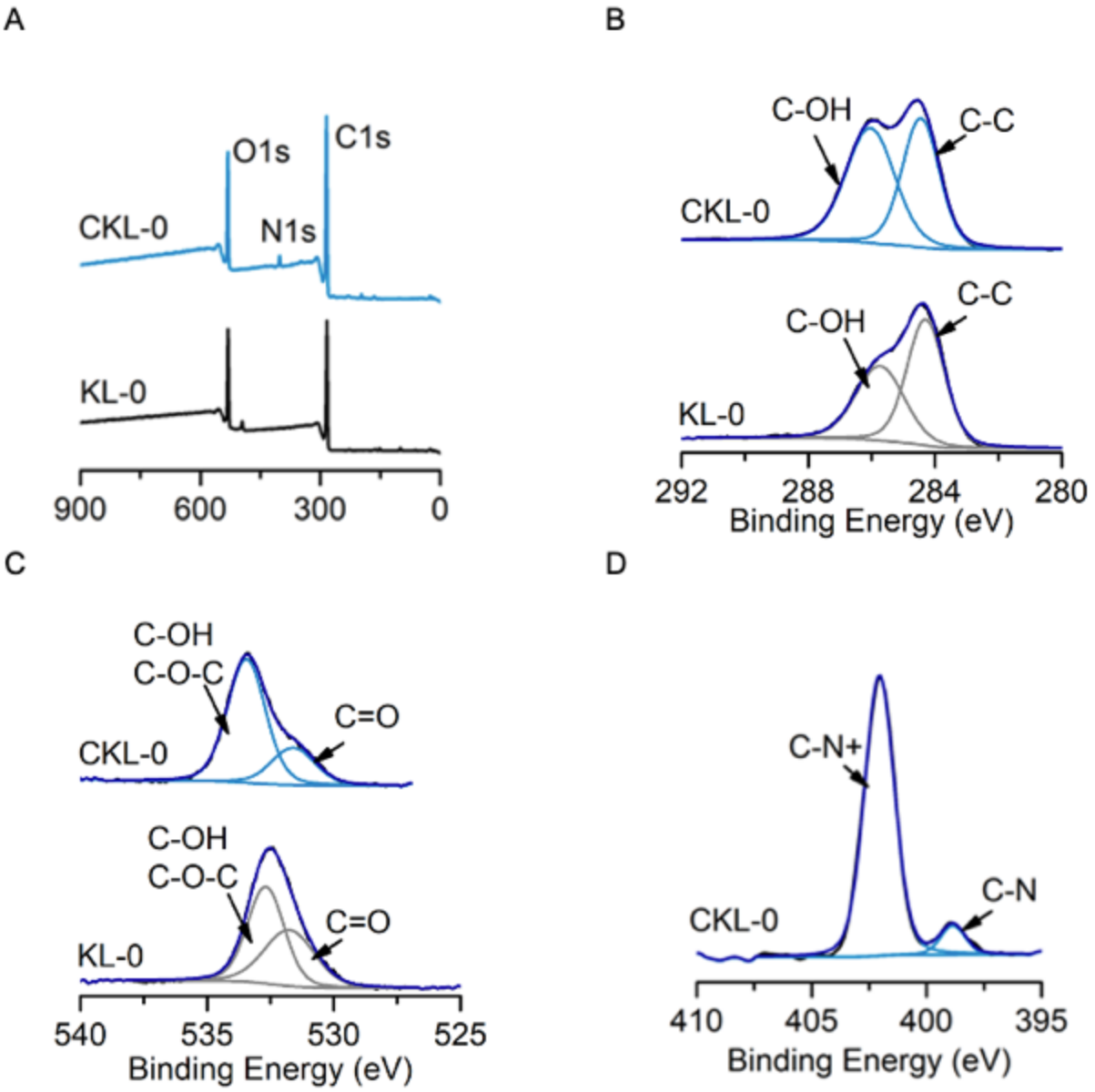

Figure 3-3: XPS spectra for KL-0 and CKL-0 samples. Survey spectra (A), C1s scan (B), O1s scan (C) and N1s scan (D).

3.4.5 Quantitative ^{31}P NMR analysis

The concentration of the hydroxyl groups in KL-0 and CKL-0 was measured quantitatively using ^{31}P NMR. Figure 3-4A shows the ^{31}P NMR spectra, where it can be seen that the total phenolic hydroxyl content of CKL-0 was relatively lower than KL-0. Figure 3-4B shows the quantification

values of hydroxyl groups in the samples. The aliphatic hydroxyl content of CKL-0 was higher than that of KL-0 due to the presence of the extra -OH group on the GTMAC. The total phenolic hydroxyl content of CKL-0 was significantly lower than KL-0, indicating that the reaction with GTMAC was selective for the phenolic position of KL. For carboxylic acid hydroxyl content, KL-0 possessed almost three times as much as that of CKL-0. This may be explained by an esterification reaction that could occur during the reaction process whereby an aliphatic hydroxyl group would react with carboxylic acid to create esters [24]. This can be seen from the reduction in carboxylic acid groups shown in Figure 3-4B, while the relative increase in C-O-C structures in the CKL-0 sample of Figure 3-3C. This shows that as carboxylic acid is being consumed, C-O-C structures may be produced.

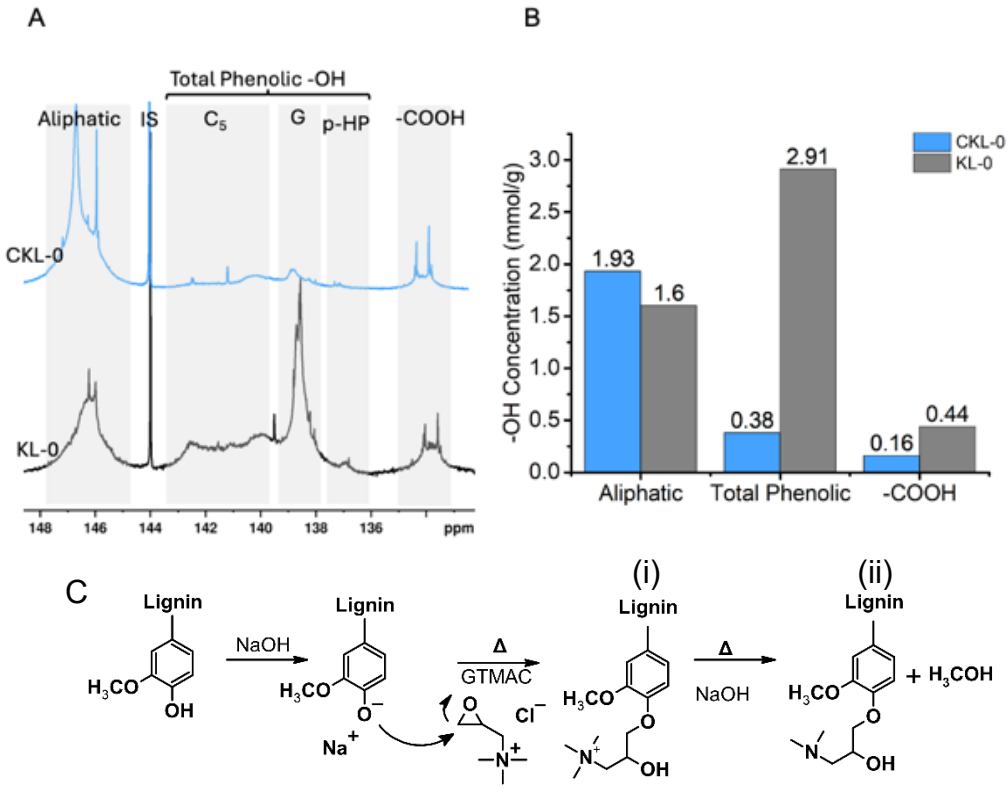

Figure 3-4: Quantitative ^{31}P NMR spectra of CKL-0 and KL-0 (A) and the quantification values for each sample in mmol/g (B). Reaction scheme (C), showing the target (i) and side (ii) product.

3.4.6 Drying Effect

The effect of drying temperature on the KL samples was investigated using XPS and ^{1}H NMR. Figure 3-5 shows the XPS C1s scans (A) and the O1s scans (B). The KL-130 sample showed a peak for C=O structures in the C1s scan that was absent in the other samples dried at lower temperatures. This peak can be explained by oxidation reactions, which can cause the cleavage of lignin side chains, thereby producing aldehydes and carboxylic acids [36, 37]. This observation was also further supported by the O1s scan, which shows a relatively larger C=O peak for the KL-130 sample, as compared to the other samples. It is known that at higher temperatures, the oxidation reaction can be accelerated [36, 37]. This may be the reason, why the C=O structures were more prevalent in KL-130 and KL-105.

A broadening of the C=O peak also occurs, showing that oxidation reactions may take place at all drying temperatures [36, 37]. After the oxidation reaction, there are more C=O structures which may cause the broadening of the overall signal. It can also be seen that C-O groups are present across all drying temperatures, indicating the presence of ether structures.

2D HSQC was conducted to investigate the changes in the chemical structure of the samples as a result of drying. Figure 3-6 shows the proton NMR spectra for KL (A), the oxygenated aliphatic regions of the HSQC spectra for the oven-dried samples of the freeze-dried sample, KL-0 (B), the oven-dried samples, KL-80 (C), KL-105 (D), KL-130 (E) and possible condensation products that formed after drying (F). ^{1}H NMR corroborated the presence of ether structures with a new peak at 3.3 ppm in all of the oven-dried samples. The HSQC spectra showed that KL-80 and KL-105 have benzodioxane structures, which was attributed to the cross peak at H_{δ}/C_{δ} = 4.8/71 ppm [22, 23, 38]. Previous studies have shown that such structures represent uncondensed groups [22, 23, 38].

KL-80 and KL-105 also show the appearance of new cross peaks at H_δ/C_δ = 3.3/50 ppm (highlighted in yellow). KL-80 shows a cross peak, which was attributed to the condensation product, CP-I, which is a diphenylmethane-type structure [22, 23, 38]. KL-80 also shows a pair of cross peaks occurring at H_δ/C_δ = 3.7/70 ppm and 4.2/70 ppm, which was attributed to CP-II and is a phenyldihydrobenzofuran type structure [22, 23, 38]. These same cross-peaks were also present in KL-105. Notably, only the signal for CP-I remains in KL-130. This may be explained by the CP-I structure having relatively more stability than CP-II. The benzodioxane signal was also completely absent from the KL-130 spectra. This temperature seems to impart a higher degree of condensation due to the complete absence of the uncondensed, benzodioxane signal.

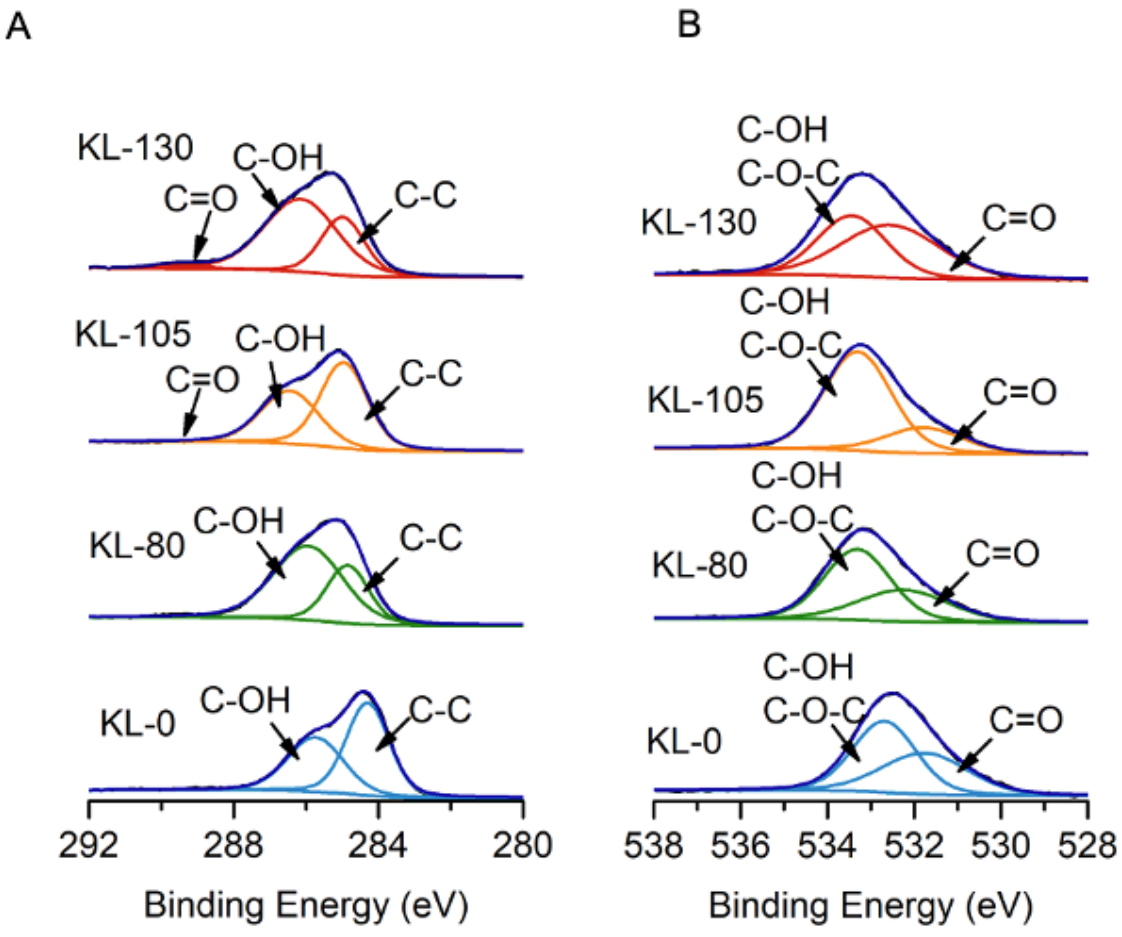

Figure 3-5: High-resolution XPS scans for C1s (A) and O1s (B)

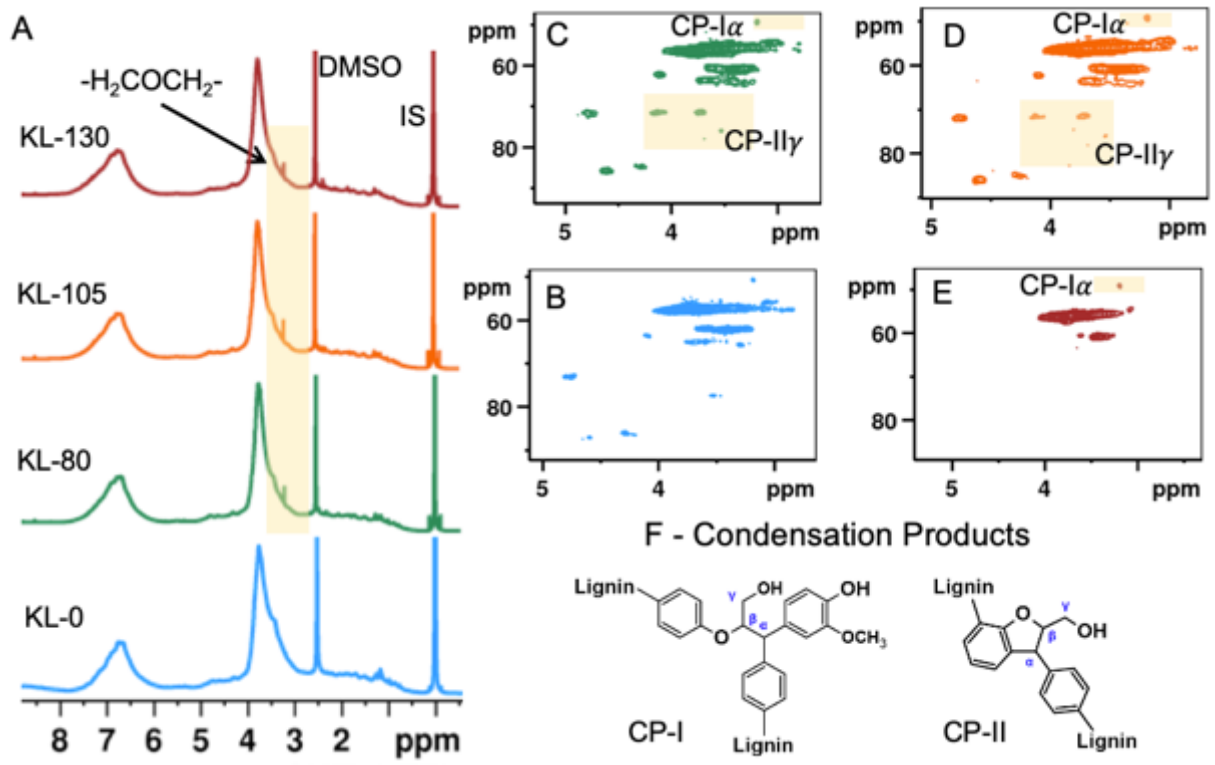

Figure 3-6: Proton NMR spectra for KL (A), the oxygenated aliphatic regions of the HSQC spectra for the oven-dried samples of the freeze-dried sample, KL-0 (B), the oven-dried samples, KL-80 (C), KL-105 (D), KL-130 (E) and possible condensation products that formed after drying (F).

Figure 3-7 shows the XPS scans of CKL, C1s (A), O1s (B) and N1s (C). The CKL-105 sample showed a strong peak for C=O, which was not present in the other samples. This may indicate a higher degree of oxidation reactions occurring during the drying process at 105ºC. When examining the O1s scans, it appears that there is a presence of C=O in all samples. As for the N1s scans, it seems that both the cationic quaternary ammonium, as well as the tertiary amide group, remain at all drying conditions.

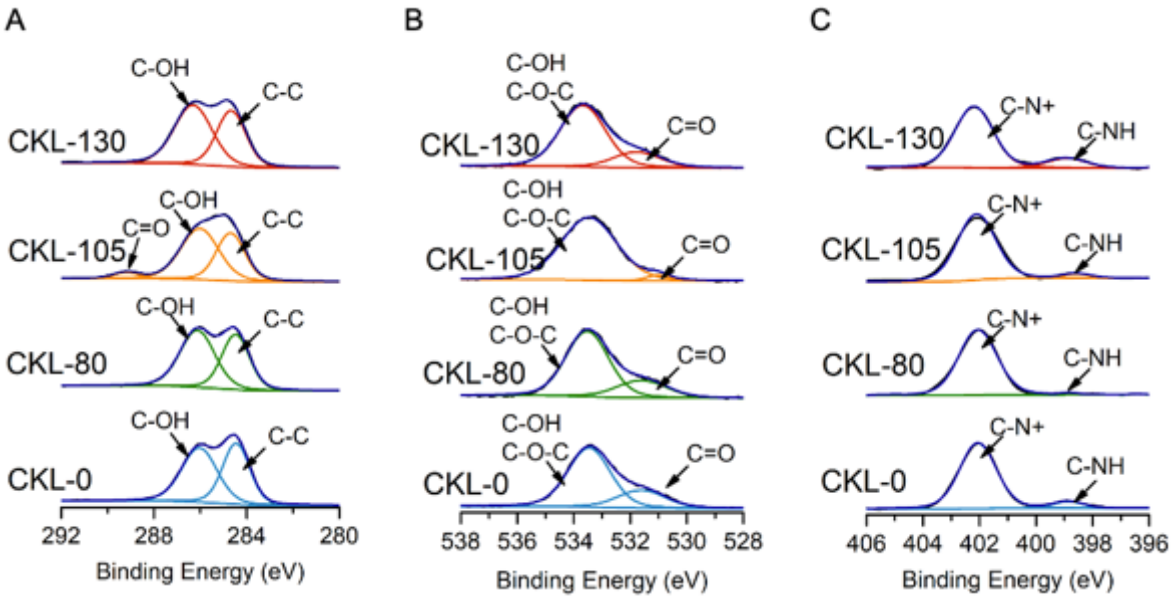

Figure 3-7: High-resolution XPS scans for C1s (A), O1s (B) and N1s (C) of CKL samples.

To investigate the chemical changes during the drying of CKL, ^{1}H NMR and HSQC NMR of CKL samples were conducted. Figure 3-8 shows the ^{1}H NMR spectra (A) for CKL after drying, along with the HSQC of CKL-0 (B), CKL-80 (C), CKL-105 (D) and CKL-130 (E). Expanded spectral regions showing changes in the nitrogen group of CKL-0 (F), CKL-80 (G), CKL-105 (H), CKL-130 (I) and proposed nitrogen structures (J). No new signals could be observed in the proton spectra, except CKL-130. It showed a new signal at 3.5 ppm. This peak was attributed to degradation products from the cationic nitrogen degradation as a result of drying at 130ºC. Additionally, when examining the HSQC spectra, it can be seen that there are changes in the KL-105 and KL-130 spectra. Upon expanding the regions showing the cationic nitrogen group signal (Figures 3-8F to 3-8I), it becomes apparent that CKL-105 and CKL-130 experienced changes to the nitrogen-containing group. As stated previously, the cationic nitrogen group of CKL is inferred by the appearance of the strong signal occurring at H_{δ}/C_{δ} = 3.3/55 ppm. This chemical structure is

denoted as N-I in Figure 3-8. The second structure shown is that of N-II, which is the tertiary amide, as a result of a side reaction during synthesis (Figure 3-3D). Figures 3-8H and 3-8I show that CKL-105 and CKL-130 have new chemical structures (highlighted in purple) that are not shown in the other samples. These signals were attributed to the formation of secondary amine groups [39], as shown by structure N-III. Additionally, all CKL samples had the cross peak at H_{δ}/C_{δ} = 3.3/50 ppm, which was also present in KL samples after drying, attributing to CP-I structures.

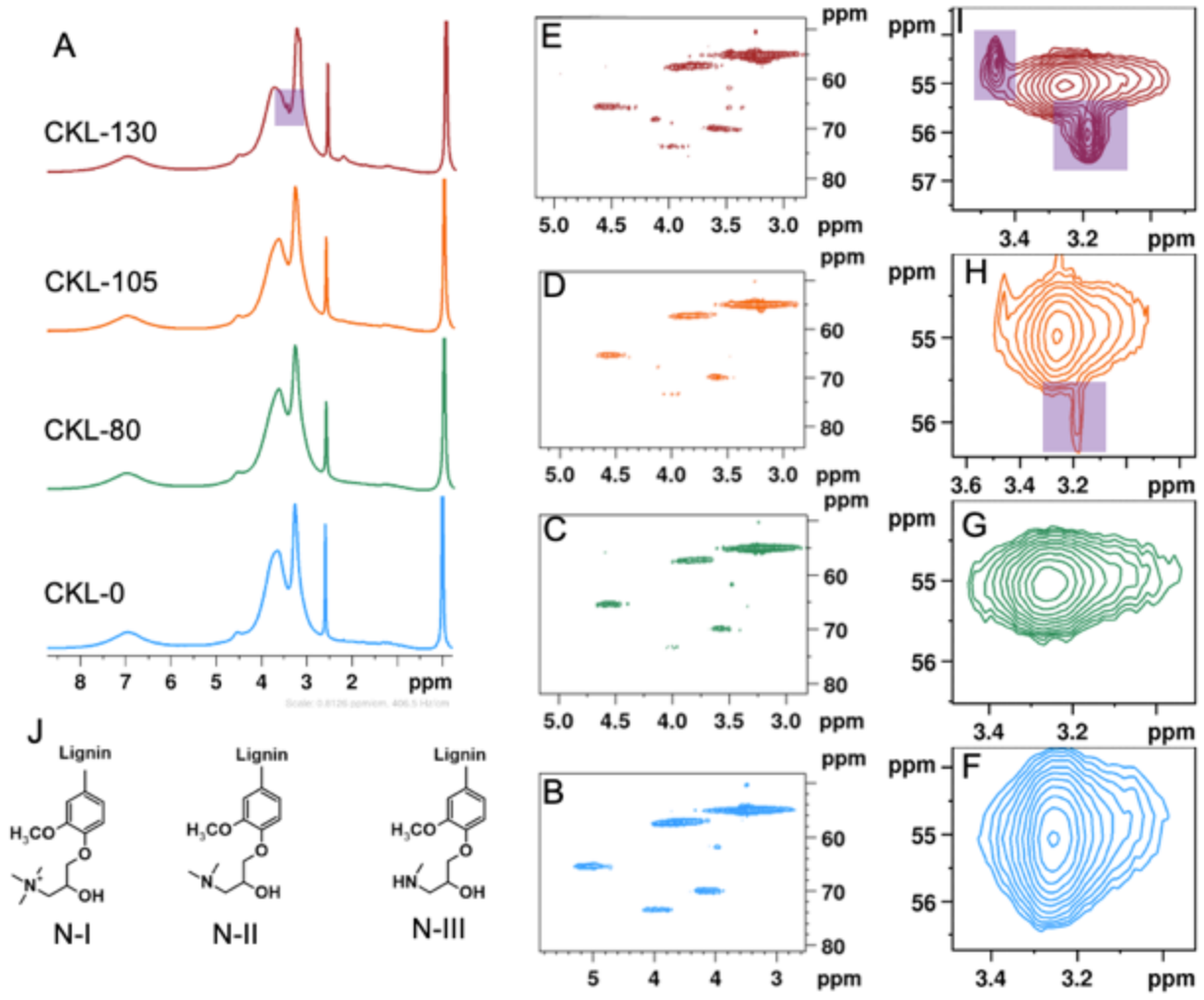

Figure 3-8: ^{1}H NMR (A) HSQC NMR for CKL-0 (B), CKL-80 (C), CKL-105 (D), CKL-130 (E). Expanded spectral regions showing changes in nitrogen group of CKL-0 (F), CKL-80 (G), CKL-105 (H), CKL-130 (I) and proposed nitrogen structures (J).

3.4.7 Impact on hydroxyl groups of lignin derivatives

To understand the impact of drying on the hydroxyl group of lignin derivatives, quantitative ^{31}P NMR was conducted for both CKL and KL samples. Figure 3-9 shows the quantification of hydroxyl groups for KL (A) and CKL (B) samples after freeze-drying and oven-drying. KL-0 showed the highest overall hydroxyl content, while the oven-dried samples showed relatively lower hydroxyl concentrations. This reduction in overall hydroxyl content is in line with the

observation of ether structures shown in XPS and NMR spectra (Figures 3-6 and 3-7) that condensation reactions occur during the oven-drying process. As the hydroxyl groups are consumed by the condensation reaction, ether structures are produced. C5 hydroxyl groups remained approximately the same across all the oven-drying temperatures, but overall, their content was less than that in KL-0. This may indicate that C5 structures are more susceptible to condensation reactions during the oven-drying process. Guaiacyl (G) type hydroxyl structures seemed to be relatively constant across all drying temperatures.

CKL samples showed an apparent reduction in overall hydroxyl content as the drying temperature increased. The majority of the hydroxyl content in all CKL samples was attributed to aliphatic hydroxyl structures, which is related to the introduction of the aliphatic -OH group on the GTMAC structure. The depletion of these aliphatic hydroxyl groups may be attributed to the aforementioned condensation reaction.

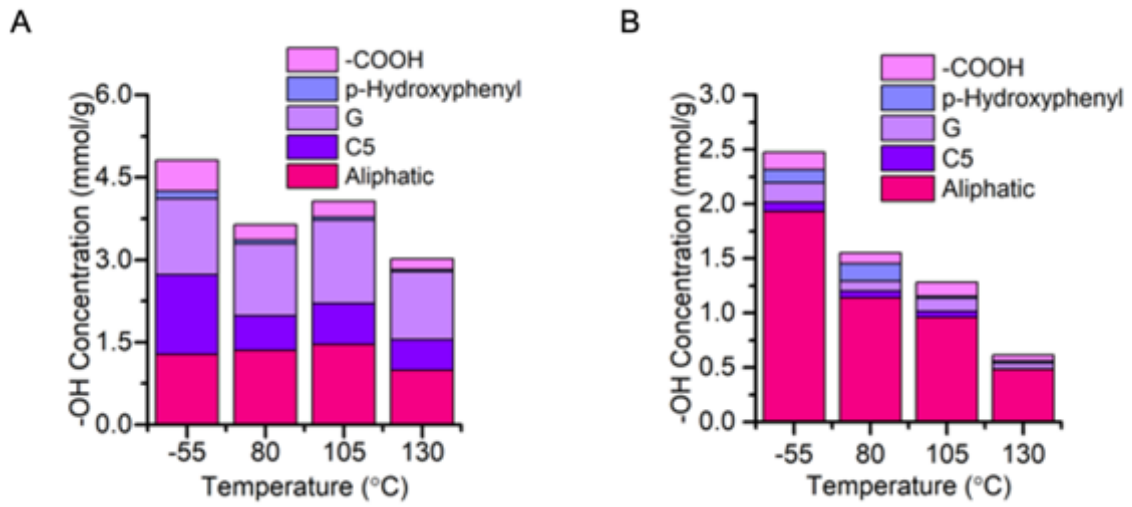

Figure 3-9: Hydroxyl group concentration of KL (A) and CKL (B)

3.4.8 Impact on molecular weight

Figure 3-10 shows the effect of temperature on the molecular weight, both weight-average and number-average (M_W and Mn) of KL (A) and CKL (B). It should be noted that there is an obvious difference in the molecular weight, M_W, values of the two samples, and the results cannot be compared. This large discrepancy between the two samples is due to the different detectors utilized for GPC analysis [10]. For cationic samples, the IR detector of the GPC is typically used, while for anionic samples, the UV detector is used [10]. Currently, no GPC system can be utilized to measure the molecular weight of cationic and anionic lignin samples following the same procedure, and research on this topic is ongoing internationally. However, the current GPC analysis can provide a comparative assessment of the drying temperature of each sample independently.

For KL samples, the KL-105 showed the highest MW. The MW trends, along with the concurrence of ether signals observed in the HSQC spectra of KL-105 (Figure 3-6D) seem to indicate that condensation reactions are more prevalent at 105ºC. KL-130 exhibited the lowest MW. This finding was expected, as the degradation of KL has been reported to start as low as 120ºC [21, 27]. For CKL, it appears that as drying temperature increased, the MW increased as well, with the exception of the CKL-130 sample which showed the lowest MW. This seems to indicate that derivatizing KL with GTMAC may change the MW behaviour in response to drying.

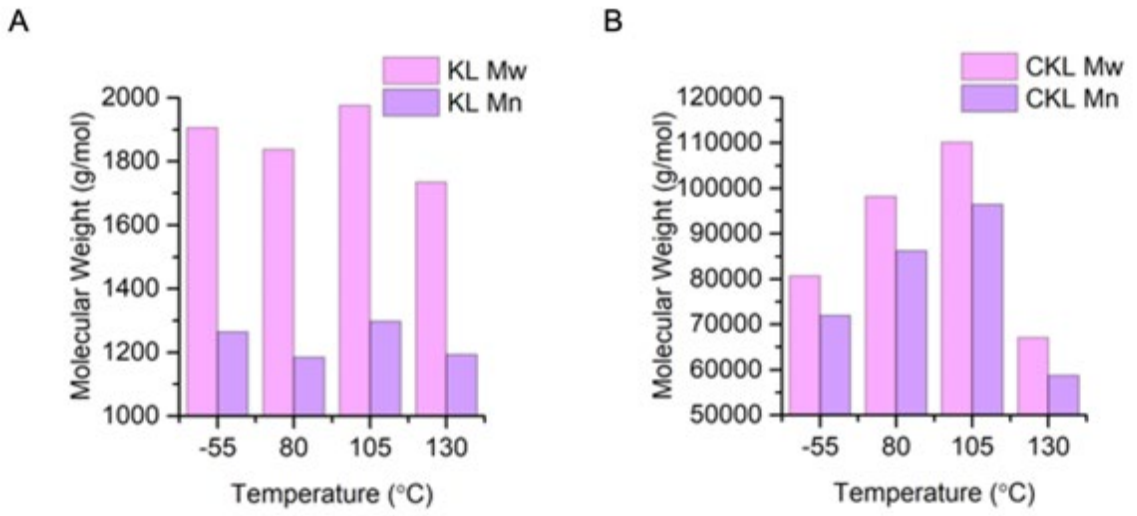

Figure 3-10: Weight average and number average molecular weights of KL (A) and CKL (B) dried at -55, 80, 105, and 130ºC.

3.4.9 Impact on T_g

Figure 3-11 shows the effect of drying temperature on the glass transition temperature, T_g, of the samples. For KL, T_g increased directly with drying temperature, except KL-130. It has been reported that a higher T_g is associated with a higher degree of condensed structures within the sample [27, 40]. This is also in line with the ether structures seen in the HSQC spectra of KL-105 (Figure 3-6D) and also the Mw change of this sample (Figure 3-10A). Together these observations may indicate that drying of KL at 105ºC may be conducive to a higher occurrence of condensation. For CKL samples, the trend is very similar to KL. CKL-105 showed the highest relative T_g of the CKL samples, which was also in line with the Mw result (Figure 3-10B). However, the KL samples exhibited higher T_g than CKL samples. This result may be due to the overall less available phenolic -OH groups to partake in the condensation reactions, as they were already occupied by the nitrogen-containing structures; therefore they could not participate in as many condensation reactions to create ether structures which would allow it to have higher T_g values. Another explanation could be that the introduction of the aliphatic chain on GTMAC could play a role.

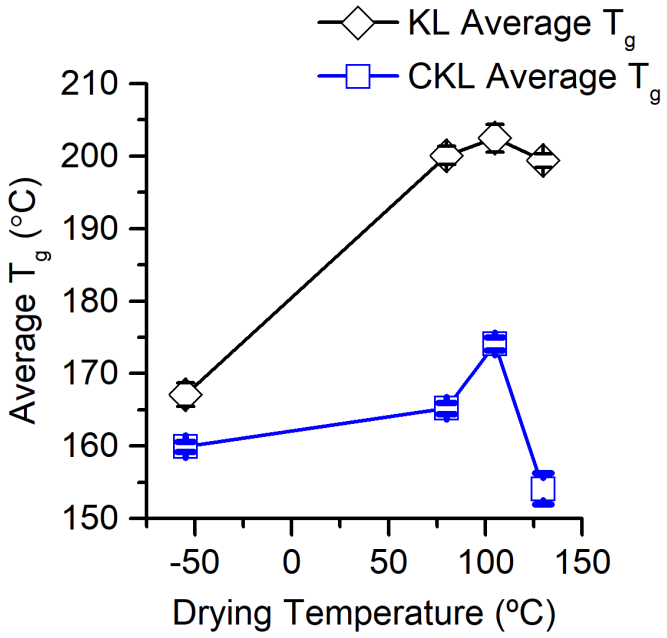

Figure 3-11: Glass transition temperature, Tg, for KL and CKL samples dried -55, 80, 105 and 130ºC.

It has been reported that branching on the main chain of cationic nitrogen groups lowers the glass transition temperature significantly [41]. Branching, like that of the methyl groups attached to the cationic nitrogen atom, presents a barrier to the internal rotation that is necessary for the molecular movement or flexion needed for higher glass transition temperatures [41].

3.4.10 Proposed drying induced reactions

Based on the results obtained in this work, there were three main drying induced events proposed, as shown in Figure 3-12. For KL, there were two main condensation products, as seen from NMR (Figure 3-6). Drying at all temperatures (80, 105 and 130ºC) seemed to result in the formation of a diphenylmethane-type condensation structure (CP-I). While drying at 80 and 105ºC, resulted in phenyldihydrobenzofuran type condensation structure (CP-II), in addition to CP-I.

For CKL, in addition to the formation of CP-I structures, the degradation of the nitrogen groups occurred at 105 and 130ºC. The quaternary substituted nitrogen groups seem to be prone to degeneration to tertiary nitrogen groups (as seen from the increase in C-NH bonds in Figure 3-8D) along with degeneration of those tertiary nitrogen groups to secondary amines (as seen from the new signals found in the HSQC in Figure 3-8H and 3-8I).

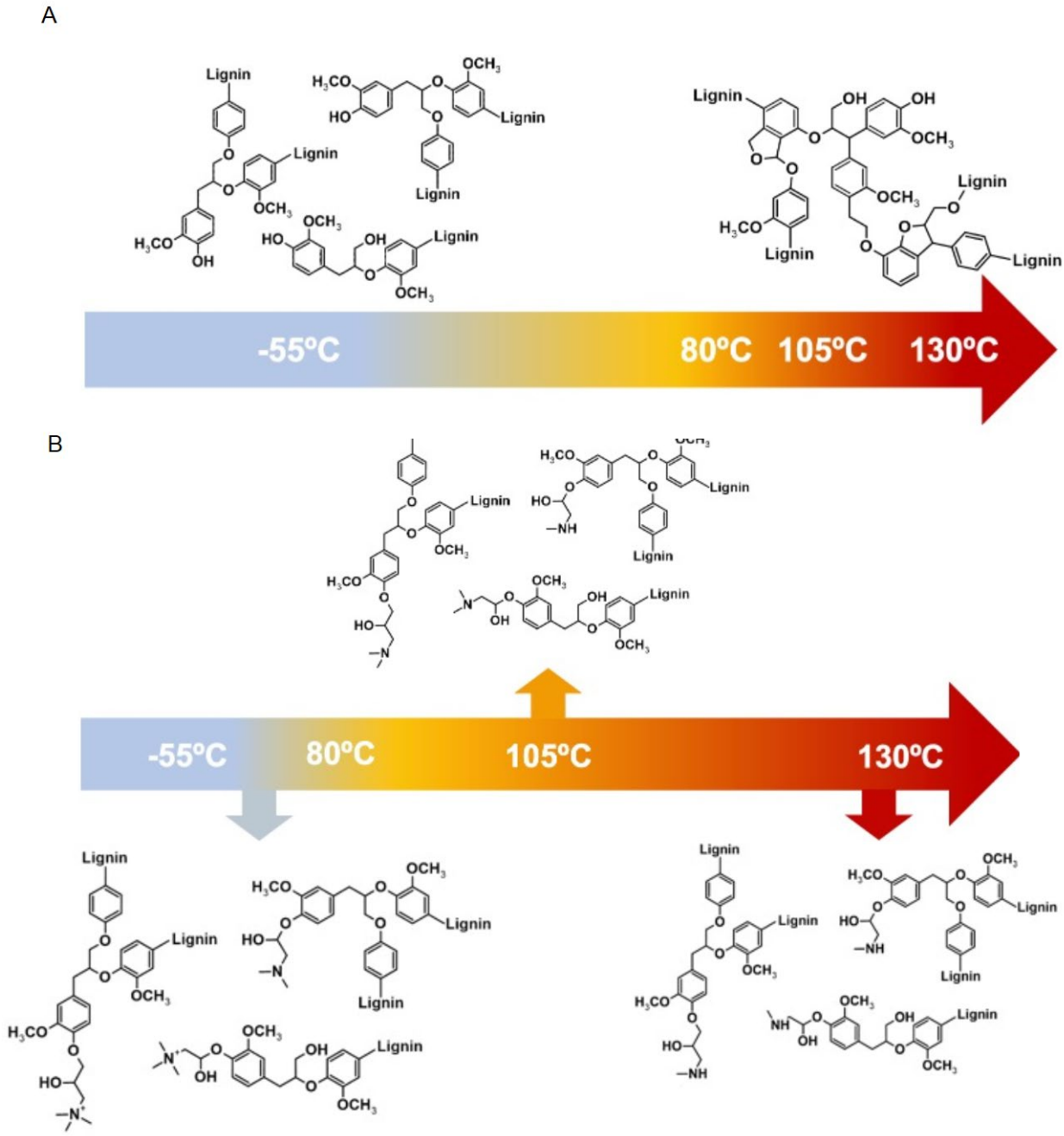

Figure 3-12: Proposed drying induced condensation for KL (A) and CKL (B) occurring at 80, 105, and 130ºC.

3.5 Conclusions

XPS and NMR results revealed that the KL experienced condensation during oven-drying, resulting in condensed, etherified structures, namely diphenylmethane and phenyldihydrobenzofuran structures. In particular, the diphenylmethane structure was identified at all oven-drying temperatures, while the phenyldihydrobenzofuran was only present at lower temperatures (80 and 105ºC). At 130ºC, it seems that degradation reactions were more prevalent than condensation reactions. This, combined with the results for M_w and T_g shows that drying KL at 105ºC, yields increased M_w and increased T_g, likely due to the increase in ether structures.

As for CKL, XPS and HSQC NMR revealed that one or both of the products of the cationic synthesis reaction undergo degradation to produce secondary amine structures at 105 and 130ºC. The quaternary substituted nitrogen groups seem to be prone to degeneration to tertiary nitrogen groups along with degeneration of those tertiary nitrogen groups to secondary amines. Furthermore, it was found that the CKL samples undergo condensation, analogously affecting the M_w and T_g. Specifically, it was found that CKL was more susceptible to reductions in -OH groups, which were directly proportional to increasing drying temperature. This was also found to concurrently result in higher molecular weight values. These higher molecular weight values were attributed to the presence of ether structures, observed from XPS and NMR, as a result of -OH groups condensing during drying. Yet the T_g values were overall lower for CKL than KL. This is thought to occur for two reasons. First, the KL phenolic groups that would normally condense more readily are taken up by the GTMAC cationic groups. Second, the introduction of more branched groups such as the three methyl groups attached to the cationic nitrogen atom, reduces the molecular mobility of the structure in response to heating. This makes the structure more rigid in response to heating, causing the T_g values to be lower.

The results of this work demonstrate that cationically modifying KL with GTMAC, not only confers cationic charge to KL but also effectively changes the response of KL to drying conditions. This work provides previously unknown insights into drying conditions for cationically derivatized KL.

3.6 References

[1] W. Zhang *et al.*, "Lignin derived carbon materials: current status and future trends," *Carbon Research,* vol. 1, no. 1, p. 14, 2022/07/29 2022, doi: 10.1007/s44246-022-00009-1.

[2] A. Beaucamp *et al.*, "Lignin for energy applications – state of the art, life cycle, technoeconomic analysis and future trends," *Green Chemistry,* 10.1039/D2GC02724K vol. 24, no. 21, pp. 8193-8226, 2022, doi: 10.1039/D2GC02724K.

[3] U. Ejaz and M. Sohail, "Lignin: A Renewable Chemical Feedstock," in *Handbook of Smart Materials, Technologies, and Devices: Applications of Industry 4.0*, C. M. Hussain and P. Di Sia Eds. Cham: Springer International Publishing, 2020, pp. 1-15.

[4] X. Chen, K. Zhang, L.-P. Xiao, R.-C. Sun, and G. Song, "Total utilization of lignin and carbohydrates in Eucalyptus grandis: an integrated biorefinery strategy towards phenolics, levulinic acid, and furfural," *Biotechnology for Biofuels,* vol. 13, no. 1, p. 2, 2020/01/06 2020, doi: 10.1186/s13068-019-1644-z.

[5] H. Zhang, M. Wang, and J. Xiao, "Chapter One - Stability of polyphenols in food processing," in *Advances in Food and Nutrition Research*, vol. 102, F. Toldrá Ed.: Academic Press, 2022, pp. 1-45.

[6] D. S. Bajwa, G. Pourhashem, A. H. Ullah, and S. G. Bajwa, "A concise review of current lignin production, applications, products and their environmental impact," *Industrial Crops and Products,* vol. 139, p. 111526, 2019/11/01/ 2019, doi: https://doi.org/10.1016/j.indcrop.2019.111526.

[7] C. Y. Wan, Y. Zhang, and Y. X. Zhang, "Effect of alkyl quaternary ammonium on processing discoloration of melt-intercalated PVC-montmorillonite composites,"

POLYMER TESTING, vol. 23, no. 3, pp. 299-306, MAY 2004, doi: 10.1016/j.polymertesting.2003.08.001.

[8] C. S. Lancefield, Hans L. J. Wienk, R. Boelens, B. M. Weckhuysen, and P. C. A. Bruijnincx, "Identification of a diagnostic structural motif reveals a new reaction intermediate and condensation pathway in kraft lignin formation," *Chemical Science,* 10.1039/C8SC02000K vol. 9, no. 30, pp. 6348-6360, 2018, doi: 10.1039/C8SC02000K.

[9] M. Y. Balakshin *et al.*, "Cover Feature: New Opportunities in the Valorization of Technical Lignins (ChemSusChem 4/2021)," *ChemSusChem,* https://doi.org/10.1002/cssc.202100110 vol. 14, no. 4, pp. 992-992, 2021/02/18 2021, doi: https://doi.org/10.1002/cssc.202100110.

[10] Y. Guo, W. Gao, F. Kong, and P. Fatehi, "One-pot preparation of zwitterion-type lignin polymers," *International Journal of Biological Macromolecules,* vol. 140, pp. 429-440, 2019/11/01/ 2019. [Online]. Available: https://www.sciencedirect.com/science/article/pii/S0141813019335780.

[11] F. Kong, K. Parhiala, S. Wang, and P. Fatehi, "Preparation of cationic softwood kraft lignin and its application in dye removal," vol. 67, p. 345, 2015.

[12] A. Eraghi Kazzaz and P. Fatehi, "Technical lignin and its potential modification routes: A mini-review," *Industrial Crops and Products,* vol. 154, p. 112732, 2020/10/15/ 2020, doi: https://doi.org/10.1016/j.indcrop.2020.112732.

[13] R. Wahlström, A. Kalliola, J. Heikkinen, H. Kyllönen, and T. Tamminen, "Lignin cationization with glycidyltrimethylammonium chloride aiming at water purification applications," *Industrial Crops and Products,* vol. 104, pp. 188-194, 2017/10/01/ 2017, doi: https://doi.org/10.1016/j.indcrop.2017.04.026.

[14] J.-m. Yin *et al.*, "Cationic modified lignin: Regulation of synthetic microspheres for achieving anti-photolysis and sustained release of the abscisic acid," *Industrial Crops and Products,* vol. 177, p. 114573, 2022/03/01/ 2022, doi: https://doi.org/10.1016/j.indcrop.2022.114573.

[15] W. Mo, K. Chen, X. Yang, F. Kong, J. Liu, and B. Li, "Elucidating the hornification mechanism of cellulosic fibers during the process of thermal drying," *Carbohydrate Polymers,* vol. 289, p. 119434, 2022/08/01/ 2022, doi: https://doi.org/10.1016/j.carbpol.2022.119434.

[16] Z. J. Xie, J. J. Guan, L. Chen, Z. Y. Jin, and Y. Q. Tian, "Effect of Drying Processes on the Fine Structure of A-, B-, and C-Type Starches," (in English), *STARCH-STARKE,* vol. 70, no. 3-4, MAR 2018, Art no. 1700218, doi: 10.1002/star.201700218.

[17] M. Beaumont, J. König, M. Opietnik, A. Potthast, and T. Rosenau, "Drying of a cellulose II gel: effect of physical modification and redispersibility in water," *Cellulose,* vol. 24, no. 3, pp. 1199-1209, 2017/03/01 2017, doi: 10.1007/s10570-016-1166-9.

[18] J. Deng, H. Yang, E. Capanoglu, H. Cao, and J. Xiao, "9 - Technological aspects and stability of polyphenols," in *Polyphenols: Properties, Recovery, and Applications*, C. M. Galanakis Ed.: Woodhead Publishing, 2018, pp. 295-323.

[19] O. Gordobil, R. Herrera, F. Poohphajai, J. Sandak, and A. Sandak, "Impact of drying process on kraft lignin: lignin-water interaction mechanism study by 2D NIR correlation spectroscopy," *Journal of Materials Research and Technology,* vol. 12, pp. 159-169, 2021/05/01/ 2021, doi: https://doi.org/10.1016/j.jmrt.2021.02.080.

[20] H. Zhang, S. Fu, and Y. Chen, "Basic understanding of the color distinction of lignin and the proper selection of lignin in color-depended utilizations," *International Journal of*

Biological Macromolecules, vol. 147, pp. 607-615, 2020/03/15/ 2020, doi: https://doi.org/10.1016/j.ijbiomac.2020.01.105.

[21] C. Cui, H. Sadeghifar, S. Sen, and D. Argyropoulos, "Toward Thermoplastic Lignin Polymers; Part II: Thermal & Polymer Characteristics of Kraft Lignin & Derivatives," *Bioresources,* vol. 8 (1), pp. 864-886, 11/05 2013, doi: 10.15376/biores.8.1.864-886.

[22] T. Komatsu and T. Yokoyama, "Revisiting the condensation reaction of lignin in alkaline pulping with quantitativity part I: the simplest condensation between vanillyl alcohol and creosol under soda cooking conditions," *Journal of Wood Science,* vol. 67, no. 1, p. 45, 2021/06/09 2021, doi: 10.1186/s10086-021-01978-4.

[23] N. Li *et al.*, "An uncondensed lignin depolymerized in the solid state and isolated from lignocellulosic biomass: a mechanistic study," *Green Chemistry,* 10.1039/C8GC00953H vol. 20, no. 18, pp. 4224-4235, 2018, doi: 10.1039/C8GC00953H.

[24] A. Mazar and M. Paleologou, "Comparison of the effects of three drying methods on lignin properties," *International Journal of Biological Macromolecules,* vol. 258, p. 128974, 2024/02/01/ 2024, doi: https://doi.org/10.1016/j.ijbiomac.2023.128974.

[25] M. Konduri and P. Fatehi, "Production of Water-Soluble Hardwood Kraft Lignin via Sulfomethylation Using Formaldehyde and Sodium Sulfite," *ACS Sustainable Chemistry & Engineering,* vol. 3, p. 150508121241009, 05/08 2015, doi: 10.1021/acssuschemeng.5b00098.

[26] K. Bahrpaima and P. Fatehi, "Synthesis and Characterization of Carboxyethylated Lignosulfonate," *ChemSusChem,* https://doi.org/10.1002/cssc.201800994 vol. 11, no. 17, pp. 2967-2980, 2018/09/11 2018, doi: https://doi.org/10.1002/cssc.201800994.

[27] S. Sen, S. Patil, and D. S. Argyropoulos, "Thermal properties of lignin in copolymers, blends, and composites: a review," *Green Chemistry,* 10.1039/C5GC01066G vol. 17, no. 11, pp. 4862-4887, 2015, doi: 10.1039/C5GC01066G.

[28] C. Heitner, D. Dimmel, and J. A. Schmidt, *Lignin and lignans : advances in chemistry*. Boca Raton, FL: Taylor & Francis, 2010.

[29] S. D. K. Seera and C. W. Pester, "Surface-Initiated PET-RAFT via the Z-Group Approach," *ACS Polymers Au,* vol. 3, no. 6, pp. 428-436, 2023/12/13 2023, doi: 10.1021/acspolymersau.3c00028.

[30] D. Son, S. Cho, J. Nam, H. Lee, and M. Kim, "X-ray-Based Spectroscopic Techniques for Characterization of Polymer Nanocomposite Materials at a Molecular Level," *Polymers*, vol. 12, no. 5*,* doi: 10.3390/polym12051053.

[31] S. Sutradhar, W. Gao, and P. Fatehi, "A Green Cement Plasticizer from Softwood Kraft Lignin," *Industrial & Engineering Chemistry Research,* vol. 62, no. 3, pp. 1676-1687, 2023/01/25 2023, doi: 10.1021/acs.iecr.2c03970.

[32] Z. Lv *et al.*, "Hydrothermal method-assisted synthesis of self-crosslinked all-lignin-based hydrogels," *International Journal of Biological Macromolecules,* vol. 216, pp. 670-675, 2022/09/01/ 2022, doi: https://doi.org/10.1016/j.ijbiomac.2022.07.003.

[33] M. S. Mohammed, H. Targhan, and K. Bahrami, "Design and introduction of quaternary ammonium hydroxide-functionalized graphene oxide quantum dots as a pseudo-homogeneous catalyst for epoxidation of α,β-unsaturated ketones," *Scientific Reports,* vol. 13, no. 1, p. 8140, 2023/05/19 2023, doi: 10.1038/s41598-023-34635-5.

[34] D. Kim *et al.*, "Quaternary ammonium salt grafted nanoporous covalent organic polymer for atmospheric CO2 fixation and cyclic carbonate formation," *Catalysis Today,* vol. 356, pp. 527-534, 2020/10/01/ 2020, doi: https://doi.org/10.1016/j.cattod.2020.03.050.

[35] M. G. Marino and K. D. Kreuer, "Alkaline Stability of Quaternary Ammonium Cations for Alkaline Fuel Cell Membranes and Ionic Liquids," *ChemSusChem,* vol. 8, no. 3, pp. 513-523, 2015, doi: 10.1002/cssc.201403022.

[36] A. Antony and M. Farid, "Effect of Temperatures on Polyphenols during Extraction," *Applied Sciences*, vol. 12, no. 4*,* doi: 10.3390/app12042107.

[37] Z. Diaconeasa, "Time-Dependent Degradation of Polyphenols from Thermally-Processed Berries and Their In Vitro Antiproliferative Effects against Melanoma," (in eng), *Molecules,* vol. 23, no. 10, Oct 4 2018, doi: 10.3390/molecules23102534.

[38] X. Mu, Z. Han, C. Liu, and D. Zhang, "Mechanistic Insights into Formaldehyde-Blocked Lignin Condensation: A DFT Study," *The Journal of Physical Chemistry C,* vol. 123, no. 14, pp. 8640-8648, 2019/04/11 2019, doi: 10.1021/acs.jpcc.9b00247.

[39] X. Meng *et al.*, "Synthesis, Characterization, and Utilization of a Lignin-Based Adsorbent for Effective Removal of Azo Dye from Aqueous Solution," *ACS Omega,* vol. 5, no. 6, pp. 2865-2877, 2020/02/18 2020, doi: 10.1021/acsomega.9b03717.

[40] Z. Börcsök and Z. Pásztory, "The role of lignin in wood working processes using elevated temperatures: an abbreviated literature survey," *European Journal of Wood and Wood Products,* vol. 79, no. 3, pp. 511-526, 2021/05/01 2021, doi: 10.1007/s00107-020-01637-3.

[41] T. Tsutsui, T. Sato, and T. Tanaka, "Glass Transition in Aliphatic Ionenes," *Polymer Journal,* vol. 5, no. 3, pp. 332-334, 1974/01/01 1974, doi: 10.1295/polymj.5.332.

Chapter 4 – Drying of Cationic polymerized Lignin

4.1 Abstract

In the development of polymers, drying is a crucial step after synthesis. Generally, drying conditions should be carefully selected to introduce minimal undesired changes to the characteristics of synthesized products. The cationic polymer resulting from radically polymerizing softwood kraft lignin (KL) with [2-(methacryloyloxy)ethyl] trimethylammonium chloride (METAC) is a promising new material that has been researched for its potential as a sustainable, competitive alternative to petroleum-based products. In this work, the effects of drying temperature (55 to 130ºC) on the properties of kraft lignin polymerized with METAC (KLM) was investigated. It was found that KLM exhibited a 3-fold drop in charge density, which was also accompanied by a 10% reduction in water-solubility when dried at 55ºC for 48 hours. These changes were found to be associated with both chemical and physical changes determined by NMR and XPS analyses. At 55ºC chain interactions were predominant due to electrostatic interactions amongst the pMETAC chains with the electronegative atoms present in KL. At 80, 105 and 130ºC drying temperatures, it was found that hydrolysis reactions predominated. Additionally, the thermal degradation resistance was measured after drying, and it was found that KL exhibited more robust resistance to thermal degradation than KLM polymer. TGA and DSC revealed that drying temperature may also affect the thermal behaviour of KL and KLM samples. TGA showed that drying KL at low temperatures (55 and 80ºC) did not have a significant effect on thermal degradation resistance. However, drying KL at 105ºC significantly increased the resistance to thermal degradation, as seen from the 50% degradation temperature, $T_{50\%}$, rising to 727ºC. Meanwhile, the $T_{50\%}$ of all other dried samples ranged between 504 to 638ºC. The KLM polymer

possessed, comparatively, a lesser resistance to thermal degradation than KL post drying and the KLM polymer had a more uniform thermal degradation behaviour, across the drying conditions. Glass transition temperature, T_g, was shown to be comparable for KL post drying across the various drying temperatures. KLM, however, showed an increasing trend as drying temperature increased, up to 130ºC, at which point T_g dropped due to KL degradation. This work investigates the effect of drying condition on the properties of both kraft lignin and cationically polymerized kraft lignin, showing that drying condition must be carefully considered in order to conserve the properties of such polymers.

4.2 Introduction

As the most abundant source of aromatic carbon in the world, lignin has great potential to be a raw material for the sustainable production of green chemicals and value-added products [1-4]. Presently, the pulping industry predominantly utilizes the kraft process to produce pulp [5]. However, lignin extracted in this process is burned and thus under-utilized. As of 2018, the kraft process accounted for 98% of all pulping operations in the world [5]. Thus, the availability and sustainability of utilizing kraft lignin make it an attractive resource in the endeavour to produce green products on a larger scale.

Drying of biomass has shown to result in material property alternations [6]. Specifically, this phenomenon has been documented to occur in biomass, such as cellulose, in which the formation of cross-linked structures happens during drying [6]. Such structures reduce the water-holding capacity of cellulose [6]. Analogously, similar changes may occur in lignin and lignin derivatives during drying. It has been reported that drying is an important consideration for lignin production [7-9]. Gordobil, et al. [7] reported that drying at lower temperature (i.e., 25 instead of 55ºC) would preserve the color and structure of lignin more effectively [7]. Another study compared freeze-

drying, oven-drying and vacuum-drying of lignin and reported that freeze-drying resulted in significantly less agglomeration of surface particles of lignin, while oven-drying and vacuum-drying at a low temperature (40ºC) resulted in large clumps forming at the surface of lignin as well as a darker colour [8].

Previous studies have shown both chemical and physical changes occurring within kraft lignin as a result of heat treatment [7-11]. In another study, heating kraft lignin for 30 minutes at temperatures of 130 and 140ºC resulted in 16-fold and 44-fold increases in its molecular weight, respectively, as compared to pristine kraft lignin [9]. This increase in molecular weight was correlated with the increase in the concentration of 5-5' carbon-carbon structures and 4-O-5 ether linkages [9]. Similarly, Duong, et al. [11] found that heating lignin above 100ºC resulted in cross-linked structures, which would cause a significant reduction in solubility of kraft lignin.

The aforementioned research work suggests that lignin may undergo chemical changes, i.e., condensation resulting in more carbon-carbon structures, during drying [12]. These changes are known to impact the thermal, acidic and alkaline stability of lignin [12]. Carbon-carbon linkages have a tendency to form various inter and intra molecular noncovalent interactions, such as hydrogen bonds, carbon-hydrogen-π bonds and π-π stacking [13]. These interactions are thought to impede the solubility of lignin with many common solvents and polymers [14]. This, in turn, would increase the overall molecular weight of lignin, which may also impair its water solubility [15].

Currently, the wastewater treatment industry relies on flocculants composed mostly of synthetic non-biodegradable polymers [23]. Lignin-based polymers are currently studied for their application in wastewater treatment as a competitive option to conventionally used chemicals [16-18]. Wang, et al. [19] demonstrated that kraft lignin polymerized with METAC (KLM) could

outperform pMETAC, on its own, in its ability to flocculate clay particles from wastewater. Sabaghi and Fatehi [17] compared the polymerization of KL with METAC and [2-(acryloyloxy)ethyl]trimethylammonium chloride (ATAC). They found that lignin-METAC outperformed lignin-ATAC polymers in flocculating clay particles in wastewater due to the extra methyl group on the METAC structure. Salaghi, et al. [16] further showed that combining cationic lignin with anionic lignin polymeric flocculants could improve their flocculating performance. Despite the extensive progress on the production of cationic lignin polymers, the drying process of such materials has not been studied. As drying may have a great impact on the properties of the generated material, one objective of this work was to understand the drying performance of cationic lignin polymers.

Radical polymerization has been used as a means of producing lignin polymers [20, 21], as it was proven to be a simple and scalable process. As a promising cationic agent with many uses in wastewater treatment [16, 17], anti-microbial resin-based sealants [22], and drug delivery [23], METAC was selected for conferring a cationic character to the lignin polymer in this work. The primary focus of this work was on the understanding of the impact of drying temperature on the characteristics of cationic kraft lignin-METAC polymer (KLM). KLM polymer was synthesized following the free radical polymerization technique, and the produced lignin derivatives were then dried under various temperatures. Afterwards, the properties of the polymers were studied comprehensively and related to drying conditions. The outcomes of this work provided insights into the drying process of cationic lignin polymers.

4.3 Materials and methods

4.3.1 Materials

The lignin used in this work was sourced from a Canadian mill located in Alberta, Canada, where softwood kraft lignin (KL) was produced using LignoForce technology. Acrylic acid (AA), [2-(methacryloyloxy) ethyl] trimethyl ammonium chloride solution (METAC) (80 wt.% in H_2O), sodium persulfate ($Na_2S_2O_8$), poly (diallyldimethylammonium chloride) (PDADMAC, 100–200 kg/mol), sodium hydroxide (NaOH, 97%), sulfuric acid (H_2SO_4, 98%), sodium trimethylsilyl-[2,2,3,3-2H4]-propionate (TSP), glacial acetic acid, deuterated dimethyl sulfoxide (DMSO-d_6) and deuterium oxide (D_2O) were all obtained from Sigma-Aldrich Company. Ethanol (95 vol.%) was supplied by Fisher Scientific. Potassium polyvinyl sulfate (PVSK, 100,000–200,000 g/mol, 97.7 wt.% esterified) was procured from Wako Pure Chem. Ltd., Osaka, Japan. Spectrum Labs provided a dialysis membrane with a cut-off of 1000 g/mol.

4.3.2 Kraft lignin-METAC (KLM) synthesis and drying method

The polymerization was carried out in a semidry manner (40 wt.% water content) [19, 24-28]. A hot water bath was pre-heated to 80ºC. A pre-determined amount of kraft lignin, METAC and deionized water were added to a heat-resistant plastic bag. The reaction medium was pre-heated in the bath to allow proper mixing of the reagents. Periodically, the bag was removed from the bath to adjust the pH to 3 using a 0.1 mol/L NaOH solution. Once the pH was stable at 3, the reaction medium was deoxygenated using nitrogen gas for 20 minutes. Next, a certain volume of 5 wt.% potassium persulphate solution was added to the medium to ensure a ratio of 0.015 g/g initiator to lignin. The reaction was allowed to proceed for 3 hours, periodically removing the bag to mix by hand. Subsequently, the reaction medium was washed with 80 vol.% ethanol to precipitate the cationic lignin, KLM, from any unreacted components. Finally, it was neutralized

and then dialyzed for 48 hours. A quantity of the purified product was freeze-dried, and the remaining was oven-dried at various temperatures and time intervals in a conventional oven. Throughout this work, the freeze-dried sample was considered as an ideal drying condition that would not induce any detrimental effects on the properties of the KLM polymer as this drying method is known to conserve the properties of biomaterials while removing water [29-31]. It should be noted that the KL used as the control underwent the same reaction conditions, pH adjustments, heating conditions and dialysis as the KLM. The freeze-dried kraft lignin control is defined as KL-0. The KL dried at 55ºC, 80ºC, 105ºC, and 130ºC for 48 hours are referred to as KL-55, KL-80, KL-105, and KL-130, respectively. Similarly, the KLM that was freeze-dried, is denoted as KLM-0. The KLM dried at 55ºC, 80ºC, 105ºC, and 130ºC for 48 hours are referred to as KLM-55, KLM-80, KLM-105 and KLM-130, respectively.

4.3.3 ^{1}H and HSQC nuclear magnetic resonance spectroscopy

The chemical structures of KL and KLM samples dried under different conditions were analyzed using hydrogen proton nuclear magnetic resonance (^{1}H NMR) and two-dimensional heteronuclear single quantum coherence (HSQC NMR). For each analysis, 70-75 mg of the sample and 6-10 mg of TSP, as an internal standard, were dissolved in 1 mL of DMSO-d_6 for KL and D_2O for KLM, respectively. The samples were stirred overnight at room temperature before analysis. The spectra were obtained using a nuclear magnetic resonance spectroscopy with an AVANCE NEO 1.2 GHz machine from Bruker at a temperature of 25ºC. The acquisition settings for the ^{1}H NMR spectra included 64 scans, a relaxation delay of 2 seconds, an acquisition time of 3.28 seconds, and a pulse of 30º. The Bruker pulse program hsqcetgpsisp was used for the acquisition of the HSQC spectra, with a spectra width of 13 ppm in the F2 (^{1}H) dimension with 2048 data points (155 microseconds acquisition time), a spectra width of 165 ppm in the F1 (^{13}C) dimension with 256 data points (6.2

microseconds acquisition time), a pulse delay of 2 seconds, and 16 scans. The NMR spectra were processed using TopSpin 4.1.9 software.

4.3.4 Gel permeation chromatography

The molecular weight distribution of KLM samples was measured using a gel permeation chromatography. Each sample was prepared by dissolving 5 mg of the sample in 10 mL of a 5 wt.% acetic acid solution, which served as the mobile phase. The samples were stirred at 300 rpm overnight at room temperature and then passed through a nylon filter with a pore size of 0.2 μm. The molecular weight analysis was performed on each sample using a Malvern GPCmax VE2001 Module + Viscotek system equipped with viscometer and RI detectors. PolyAnalytic columns were used at a temperature of 35°C for this analysis.

4.3.5 Differential scanning calorimetry & thermal gravimetric analysis

The glass transition temperature (T_g) of KLM samples was determined using a differential scanning calorimetry (DSC). Samples weighing between 10 and 15 mg were placed in a hermetic Tzero aluminum pan and placed in the chamber of a DSC Q2000, TA instrument, DE, USA. The measurements were taken under a nitrogen atmosphere with a heating and cooling rate of 5ºC/min. The analysis involved several heating/cooling cycles. The chamber was first heated from 20 to 230ºC to erase the thermal history of the sample. It was then cooled from 230 to 20ºC at a rate of 5ºC/min. A second heating cycle from 20 to 230ºC at a rate of 10ºC/min was then applied to determine the T_g of the samples. Each sample was tested in duplicate, and the average and standard deviation were calculated.

The thermal stability of KLM samples was characterized using thermogravimetric analysis (TGA) with a TGA analyzer, i1000, Instrument Specialist. In this experiment, the temperature was

increased from room temperature to 800ºC at a rate of 10ºC/min and with a heat flow rate of 10ºC/min and a nitrogen flow rate of 100 mL/min.

4.3.6 Water solubility and charge density

The water solubility and particle charge density of the KLM samples were measured using a PCD-04+Titrator from Mütek, Germany, following the method described by Konduri et al. [32]. The samples were prepared by dissolving them to a concentration of 1% in water and then shaken for one hour in a shaker bath at 30ºC. After the samples were completely suspended in water, a portion was taken for solubility analysis and another portion was titrated against PVSK (0.005 mol/g) to determine the charge density of the samples.

4.4 Results and Discussion

4.4.1 Water solubility, charge density and elemental composition

Table 4-1 shows the water solubility, charge density and elemental compositions of KL and KLM. As seen, KL-0 has a charge of -1.1 meq/g and water solubility of 87.5 wt.%. The organic element content of the KL-0 sample was found to be 59.4% carbon, 7.4% hydrogen, 0.0% nitrogen, 1.6% sulphur, and 31.6% oxygen. The KL-0 sample served as the control for this study. Also, KLM-0 possessed a charge density of 4.8 meq/g and was completely water-soluble.

Table 4-1: Water solubility, charge density and elemental composition of freeze-dried kraft lignin (KL-0) and freeze-dried kraft lignin-METAC (KLM-0).

Sample	KL-0	KLM-0
Solubility (%)	87.5	100
Charge Density (meq/g)	-1.1	4.8
C (%)	59.4	42.0

H (%)	7.4	7.5
N (%)	0.0	5.0
S (%)	1.6	0.3
O (%)	31.6	45.2

By comparing the elemental composition of KL-0 and KLM-0, it can be seen that the polymerization reaction of KL with METAC, increased the nitrogen content of the sample from 0.0% to 5.0%. The increase in nitrogen content, combined with the improved water solubility, were interpreted as an indication that the polymerization reaction was successful. These observations were further confirmed by NMR data in Figure 4-3, which will be discussed later.

Figure 4-1A shows the water solubility and charge density of KL as a function of drying temperature. It can be seen that oven-drying at 55 and 80ºC does not significantly affect KL's water solubility, when comparing to the freeze-dried sample (-55ºC). Yet the KL samples dried at 105 and 130ºC possessed a significantly lower water solubility. All oven-dried samples showed a decrease in charge density as drying temperature increased. Figure 4-1B shows the water solubility and charge density of the KLM samples oven-dried at the various temperatures, 55ºC (KLM-55), 80ºC (KLM-80), 105ºC (KLM-105) and at 130ºC (KLM-130). It can be seen that the water solubility and charge density were both affected by the drying temperature. Overall, it seems that oven-drying at all temperatures results in a stark reduction in both solubility and charge density.

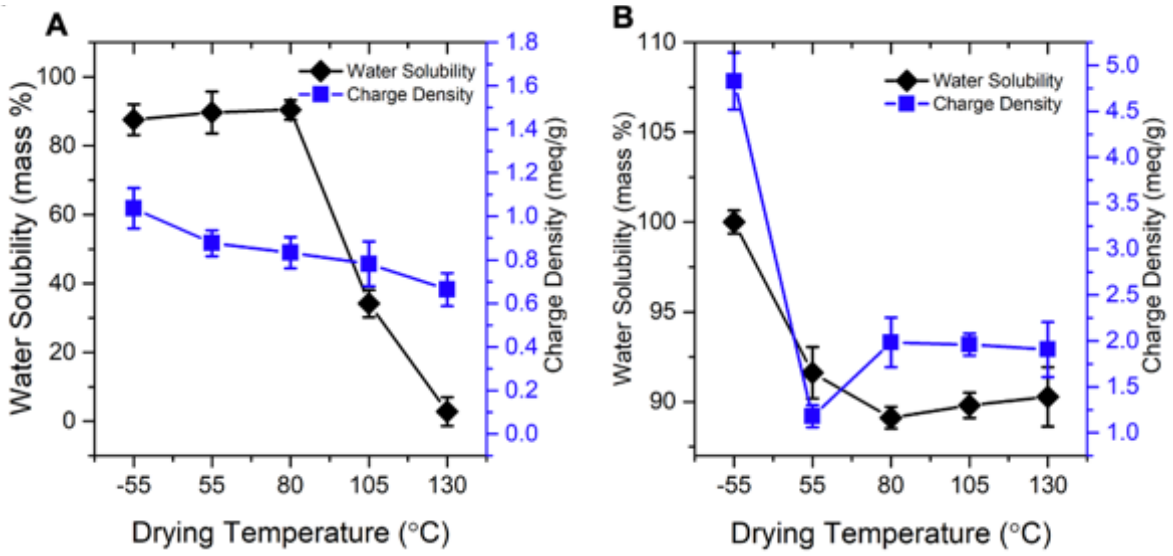

Figure 4-1: Water solubility and charge density for KL (A) and KLM (B), as a function of drying temperature.

4.4.2 ^{1}H NMR analysis

Figure 4-2 shows the ^{1}H NMR of KL-0 and KLM-0. It can be seen that there are five distinct regions. The region between 8 and 10 ppm represents the protons in the unsubstituted phenolic hydroxyl groups [33-35]. The region between 6 and 7.7 ppm represents the protons in the aromatic rings of lignin [33-35]. The region between 4.3 and 5.5 ppm represents the aliphatic protons, specifically the H_{α} & H_{β} protons [33-35]. The methoxy protons are represented by the large broad peak between 3 and 4 ppm, and the aliphatic protons participating in the β-1 linkages of lignin are shown between 0.7 and 2.3 ppm [33-35]. The peak at 2.5 ppm belongs to DMSO-d_6. For the KLM-0 sample, there is an obvious absence of the phenolic -OH group signal (Figure 4-2). Salaghi et al. [20] explained that the absence of this signal was due to the successful participation of the phenolic -OH group of KL in the cationic polymerization reaction [16]. Thus, the absence of signal between 8 and 9 ppm is indicative of successful polymerization [16-18].

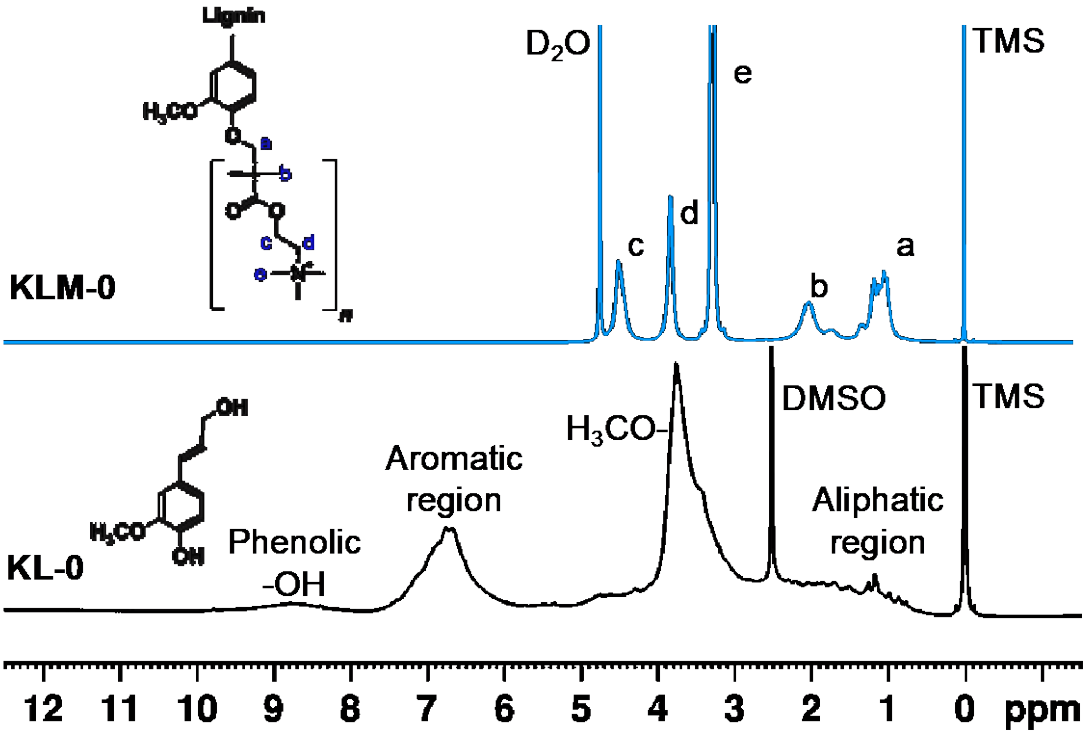

Figure 4-2: ^{1}H NMR spectra of KL-0 (black) and KLM-0 polymer (blue).

The signal (a) at 1.2 ppm was attributed to the methylene protons adjacent to the phenolic oxygen atom of KL. The signal (b) at 2.1 ppm was attributed to the methyl protons adjacent to the -COO group. The signal (c) at 4.6 ppm was attributed to the methylene protons adjacent to the ether linkage of the -COO group. The signal (d) at 4 ppm was attributed to the methylene protons adjacent to the cationic nitrogen atom. The signal (e) at 3.3 ppm was attributed to the cationic methyl protons. These signal assignments were cross-referenced using previous studies published on this polymerization reaction [16, 18].

4.4.3 HSQC NMR analysis

Figure 4-3 shows the HSQC spectra of the aliphatic and oxygenated aliphatic regions of KL-0 (A) and KLM-0 (B). Literature on the linkages identified via HSQC NMR analysis for softwood kraft lignin is well documented. For the HSQC of KL-0, it can be seen that the gamma-carbon, denoted as Cγ in the figure, which is adjacent to the β-O-4 linkages was assigned to the signal appearing

at H_δ/C_δ = 3.6/61 ppm [5]. Another characteristic functional group of KL is the methoxy group, whose signal was attributed to the contour occurring at H_δ/C_δ = 3.2-4/57-60 ppm [5]. Other smaller signals in the aliphatic region were attributed to the protons and carbons involved in the aliphatic chains of KL [5].

For the HSQC of KLM-0, the signal (a) at H_δ/C_δ = 1.2/21 ppm was attributed to the -CH_2- adjacent to the formerly phenolic oxygen atom of KL. The signal (b) at H_δ/C_δ = 2.1/57 ppm was attributed to the methyl groups adjacent to the -COO group [16, 20]. The signal (c) at H_δ/C_δ = 4.6/60 ppm was assigned to the -CH_2-group adjacent to the oxygen atom, participating in the ether linkage of the -COO group [16, 20]. The signal (d) at H_δ/C_δ = 4/64 ppm was attributed to the -CH_2- group attached to the cationic nitrogen atom [16, 20]. The signal (e) at H_δ/C_δ = 3.3/58 ppm was attributed to the methyl groups of the cationic nitrogen atom [16, 20]. Based on these results, it can be concluded that the polymerization reaction was successful in polymerizing chains of METAC to the KL core structure to produce KLM.

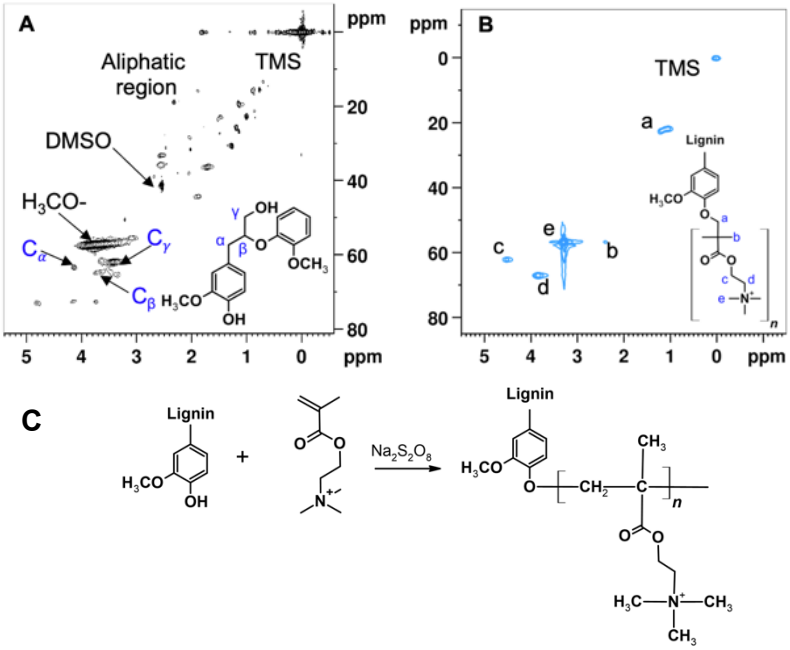

Figure 4-3: HSQC NMR characteristic signals of KL-0 (A) and KLM-0 (B). Reaction scheme (C).

4.4.4 XPS analysis

XPS was used to study the elemental and chemical bonds of the samples as a result of polymerization. Figure 4-4 shows the XPS survey spectra, along with the C1s and O1s scans of KL-0 and KLM-0. Figure 4-4A shows a large sharp peak at 284.5 eV, which was attributed to C1s and another sharp peak at 532 eV, which was attributed to O1s, in both the KL-0 and KLM-0 samples. The smaller peak at 400 eV was attributed to N1s and so confirms that the KLM-0 sample contains nitrogen atoms after the polymerization reaction. By contrast, the N1s peak is absent in the KL-0 sample, as expected. Figures 4-4B and C represent the C1s and O1s spectra fitted for the peaks related to carbon and oxygen structures shown in the figures. Deconvolution of the C1s spectra for KL-0 resulted in two major peaks. These peaks were attributed to C-C/C-H (284.5 eV) and also C-O (286 eV). Meanwhile, for the KLM-0 C1s spectra, three peaks were found. These peaks were attributed to C-C/C-H/C-N+ (284.5 eV); C-O (286 eV) and C=O (288 eV) [36, 37]. The distinct peak at 288 eV can be attributed to the -COO structures that make up the pMETAC structure [36, 37]. The deconvolution of the O1s spectra for KL-0 resulted in three peaks.

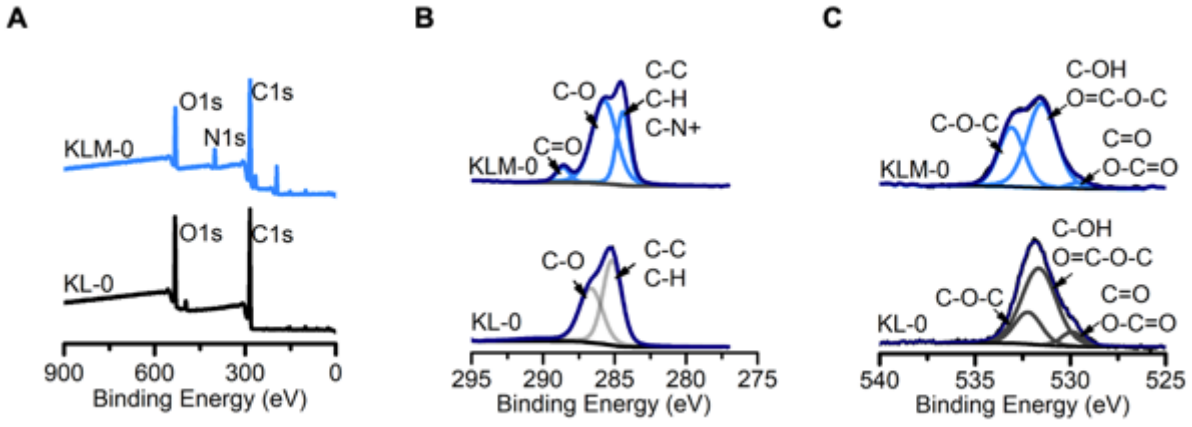

Figure 4-4: XPS spectra for KL-0 and KLM-0 samples. Survey spectra (A), C1s scan (B) and O1s scan (C).

These peaks were attributed to C=O/O-C=O (530 eV), C-OH/O=C-O-C (532 eV) and phenolic C-O-C (533 eV) [8]. For KLM-0, the same set of peaks was found as in KL-0, however, the relative concentration of phenolic C-O-C was more pronounced.

4.4.5 Drying Effect

The effect of drying temperature on the KLM was also investigated by using XPS. Figure 4-5A shows the C1s spectra of KL samples. Notably, KL-130 and KL-105 show a peak for C=O structures, not present in the other lower drying temperatures. The appearance of the C=O peak at higher temperatures is indicative of oxidation reactions, which can cause the cleavage of side chains, producing phenolic aldehydes and acids [38, 39]. This assertion was also further supported by the O1s spectra shown in Figure 4-6A for KL. From this figure, it can be seen that KL-0 did not possess a high relative concentration of C=O structures. Comparatively, the oven-dried samples show a higher relative concentration of C=O structures. This may indicate that some level of oxidation occurs at all the oven-dried temperatures. Further to that, at higher temperatures, the oxidation reaction is known to be accelerated, which can explain why KL-105 and KL-130 show particularly higher concentrations of such structures [38, 39]. Additionally, C-O structures seem prevalent across all temperatures, indicating the presence of ether structures. Figure 4-5B shows the C1s spectra of KLM samples. The overall trend indicates that, as drying temperature increases, the concentration of C-O bonds in the sample increases, except for the KLM-130 sample, where the concentration of C-O bonds is comparable to that of aliphatic bonds.

Figure 4-6 shows the O1s spectra of the KL and KLM samples. The overall trend indicates that as drying temperature increases, the concentration of C=O and O-C=O bonds increase for KLM-55 and KLM-80. This supports the assertion that carboxylic acid production is stimulated during oven-drying, as a result of oxidation.

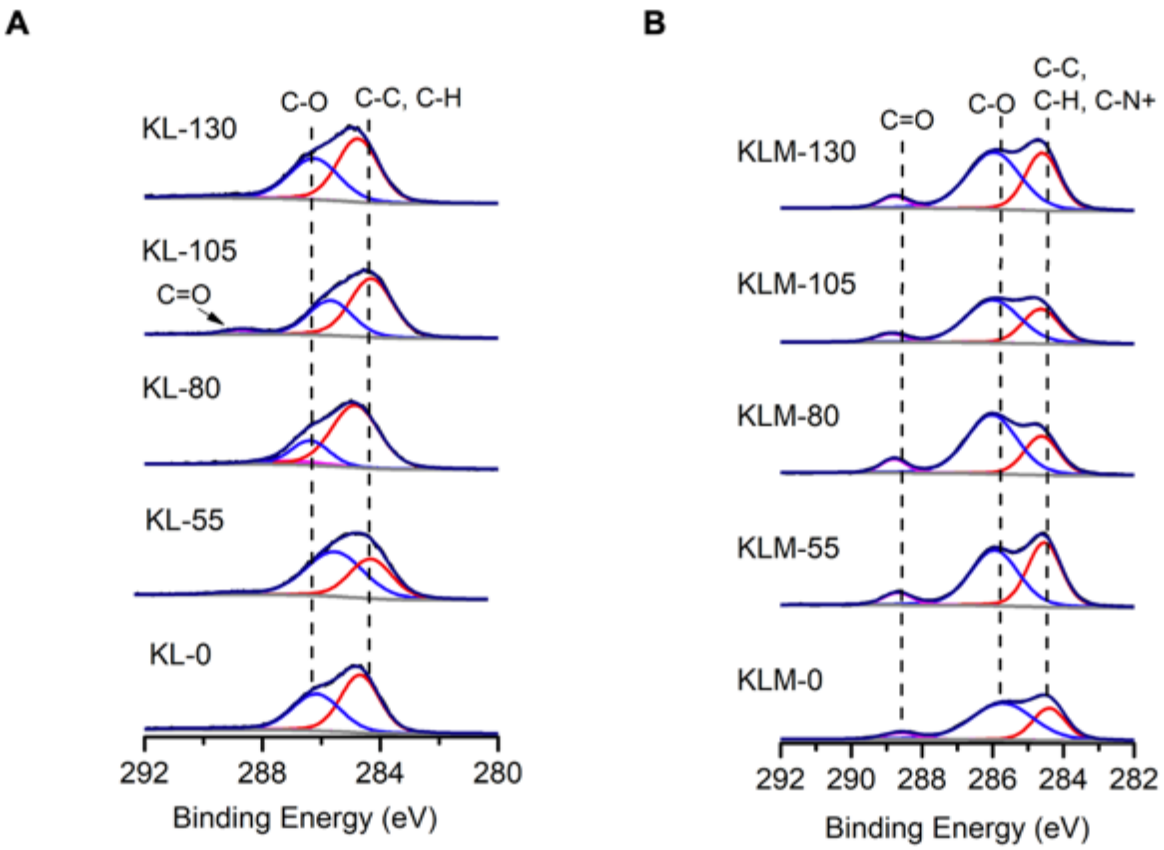

Figure 4-5: XPS binding energy of the KL and KLM samples dried at different temperatures, C1s spectrum of KL-0, KL-55, KL-80, KL-105, KL-130 (A) and C1s spectrum of KLM-0, KLM-55, KLM-80, KLM-105, KLM-130 (B).

This can be seen from the broadening of the binding energy for these samples [38, 39]. However, there is a drop in the concentration of these bonds for KLM-105. Then, there is an increase again for KLM-130, supporting the NMR results, showing the presence of aldehyde structures in the sample (Figure 4-6), which would increase the C=O content. The presence of aldehyde structures could be the result of the hydrolysis of the pMETAC chains [40]. Similarly, an increase in C=O content was observed in the KLM-130 sample ^{1}H NMR depicted in Figure 4-7D. Upon drying at different temperatures, the most significant changes were observed in the β-1 and the Hα aliphatic structures of KL (Figure 4-7A). It seems that after oven-drying, there was a significant reduction in the aliphatic structures of KL.

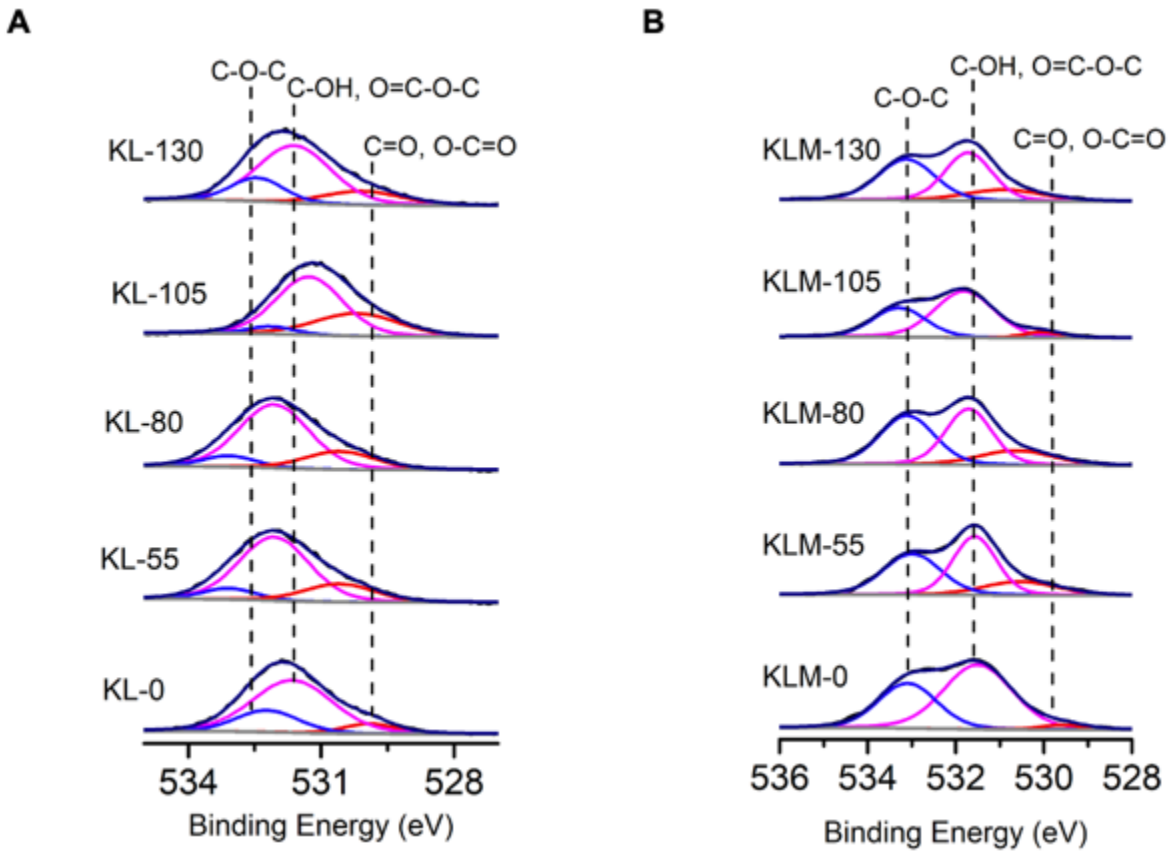

Figure 4-6: XPS binding energy of the KL and KLM samples dried at different temperatures, O1s spectrum of KL-0, KL-55, KL-80, KL-105, KL-130 (A) and O1s spectrum of KLM-0, KLM-55, KLM-80, KLM-105, KLM-130 (B).

It was reported that the aliphatic structural degradation of polyphenolic compounds can occur at temperatures as low as 80ºC [38, 39]. Additionally, another explanation for the observed reduction of aliphatic structures could be attributed to the acceleration of oxidation reactions [38, 39]. Such reactions are known to be accelerated at higher temperatures, i.e., 50ºC [38, 39]. This assertion is supported by the results of the XPS (Figures 4-5 and 4-6) and NMR (Figures 4-7). Furthermore, the appearance of the new signal at 3.2 ppm is indicative of the presence of ether structures [41] within the KL samples after oven-drying. Additionally, Figure 4-7B shows the effect of drying temperature on the chemical structure of KL, by quantification of the proton NMR spectra shown

in Figure 4-7A. Oven-drying as compared to freeze-drying appears to induce chemical structural changes that reduce the concentration of aliphatic structures. Moreover, the oven-dried samples showed the same concentration of the new signal, attributed to ether structures. This seems to imply that the drying of KL has a finite effect on the formation of new structures.

The effect of temperature on the chemical structure of the KLM is also shown in Figure 4-7C and 4-7D. Across all the temperatures, the signals (a) and (b) remain present. KLM-80 showed the same signals that appeared for KLM-55 and also an additional new signal in the proton spectra, that appeared as a 1:3:3:1 quartet centred at 3.6 ppm. Such a signal indicates the presence of a methyl group adjacent to a -CH- group [41]. The position of the signal indicates that it is adjacent to a hydroxyl group, participating in a carboxylic acid functional group [41].

Based on the appearance of these new signals, it seems that drying at 55 and 80ºC results in an increase in carboxylic acid concentration within the sample. This suggests that the pMETAC structures begin to degrade even at lower temperatures, at the c-carbon of the pMETAC structure. This theory was further confirmed by the XPS and NMR results shown in Figures 4-5 and 4-7. Two new signals appeared at 2.7 ppm and 3 ppm in KLM-105 and KLM-130.

These signals can be attributed to the degradation of the pMETAC structure. The signal at 2.7 ppm can be attributed to CH_3-CO-R and the signal at 3 ppm can be attributed to R-N-CH_3 [41].

The oxygenated aliphatic regions of the HSQC NMR spectra of KL and KLM are shown in Figure 4-8. Based on the NMR spectra, Figure 4-8A to 4-8E, no significant changes were seen in KL, as all spectra of KL, dried at various temperatures, other than the appearance of the signal at H_δ/C_δ = 3.2/50ppm, which was attributed to -C-O-C- ether structure formation [41].

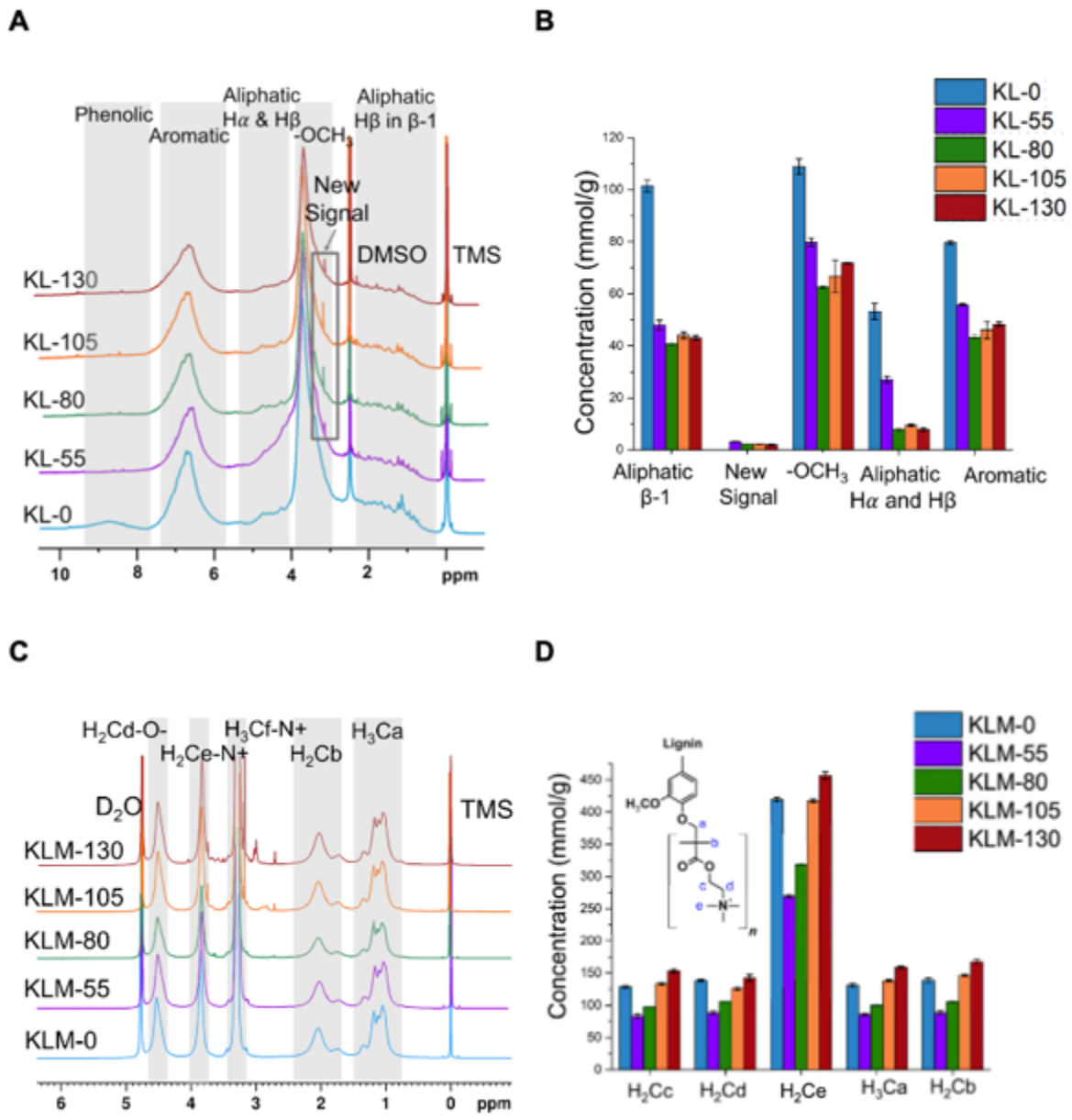

Figure 4-7: ^{1}H NMR spectra of KL dried at different temperatures (A) and concentrations of chemical groups of KL extracted from ^{1}H NMR spectra (B).

However new peaks appeared on the spectra of the oven-dried KLM samples, Figure 4-8I and 4-8J. A new signal at H_{δ}/C_{δ} = 4.4/52 ppm [41] is attributed to a carboxylic acid group. A second new signal appeared in the HSQC of the KLM-55 sample at H_{δ}/C_{δ} = 3.6/58 ppm. This signal was attributed to the second product that may result from a hydrolysis reaction [10]. This would be

quaternary substituted nitrogen, having three methyl groups and an ethyl group attached to the nitrogen atom, as shown in Figure 4-8B. These same signals also appear in KLM-105 and KLM-130. Additionally, KLM-130 showed a signal at H_{δ}/C_{δ} = 3.5/70 ppm, which was attributed to the presence of the resultant aldehyde structure from the hydrolysis of pMETAC groups [41].

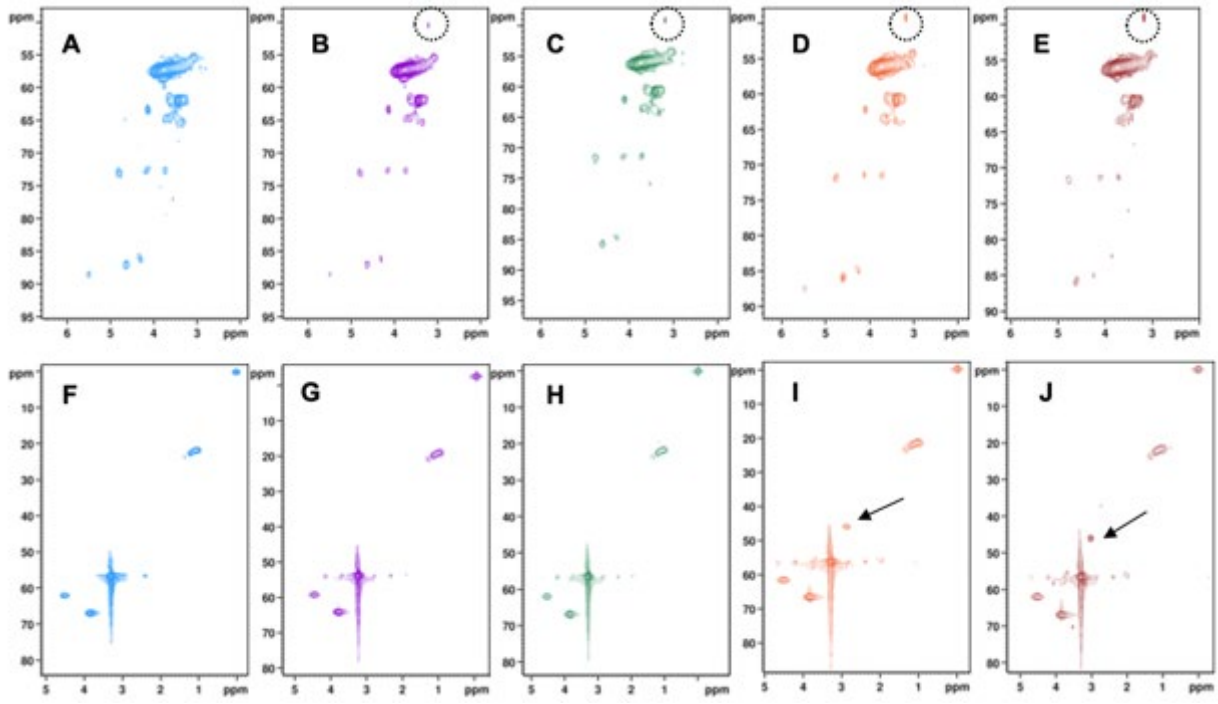

Figure 4-8: HSQC NMR spectra of KL and KLM samples dried at different temperatures, KL-0 (A), KL-55 (B), KL-80 (C), KL-105 (D), KL-130 (E), KLM-0 (F), KLM-55 (G), KLM-80 (H), KLM-105 (I), KLM-130 (J).

4.4.6 KLM molecular weight – GPC

In Figure 4-9, the effect of temperature on the weight-average molecular weight and polydispersity of KL (A) and KLM (C) samples dried for 48 hours, along with molecular weight distribution of KLM samples (B). The PDI of KLM was observed to have a direct relationship with increasing temperature until 80ºC where the PDI seems to plateau. The changes in polydispersity may indicate the existence of multiple reactions occurring during the drying process, causing these observed fluctuations over time; such as hydrolysis of the alkyl chains and also the formation of crosslinked

structures [9, 11]**.** Overall, it can be seen that drying temperatures higher than 55ºC may result in increasing Mw while drying at temperatures beyond 55ºC results in lower Mw of KLM. The reason for this could be more interactions between the pMETAC chains bound to the KL core structure, causing the appearance of larger molecular weight fragments within the sample [42]. This assertion can be supported by the molecular structural changes as confirmed by NMR (Figure 4-8) and XPS (Figures 4-5 and 4-6). These figures show that KLM-55 did not have any increased ether linkages or increased aliphatic concentration, yet it had the greatest Mw. This supports the assertion that chain interactions like chain entanglement interactions, are more prevalent at this drying temperature. As expected, KLM-130 has the narrowest retention time distribution and also the sample eluted fastest from the column at 25 minutes. This is in line with the postulation that the degradation of the KL structure would play more of a role at a drying temperature of 130ºC, as the degradation temperature of KL is known to begin at 120ºC [9, 34]. All other samples exhibited similar trends in terms of breadth of retention, as well as a similar peak retention time of 28 minutes. The observation that KLM-130 had a narrower retention distribution suggests that the sample had a more uniform range of molecular weights as compared to the others [42]. This may be attributed to the fact that the higher drying temperature causes more chemical structural degradation to the KL core structure. Meanwhile, at the lower temperatures, the broader retention time suggests that the sample contained a wider range of molecular weights, as various sizes of molecular chains will elute at different times [42]. The PDI of KL was observed to decrease as the drying temperature increased. Mw also showed an analogous trend.

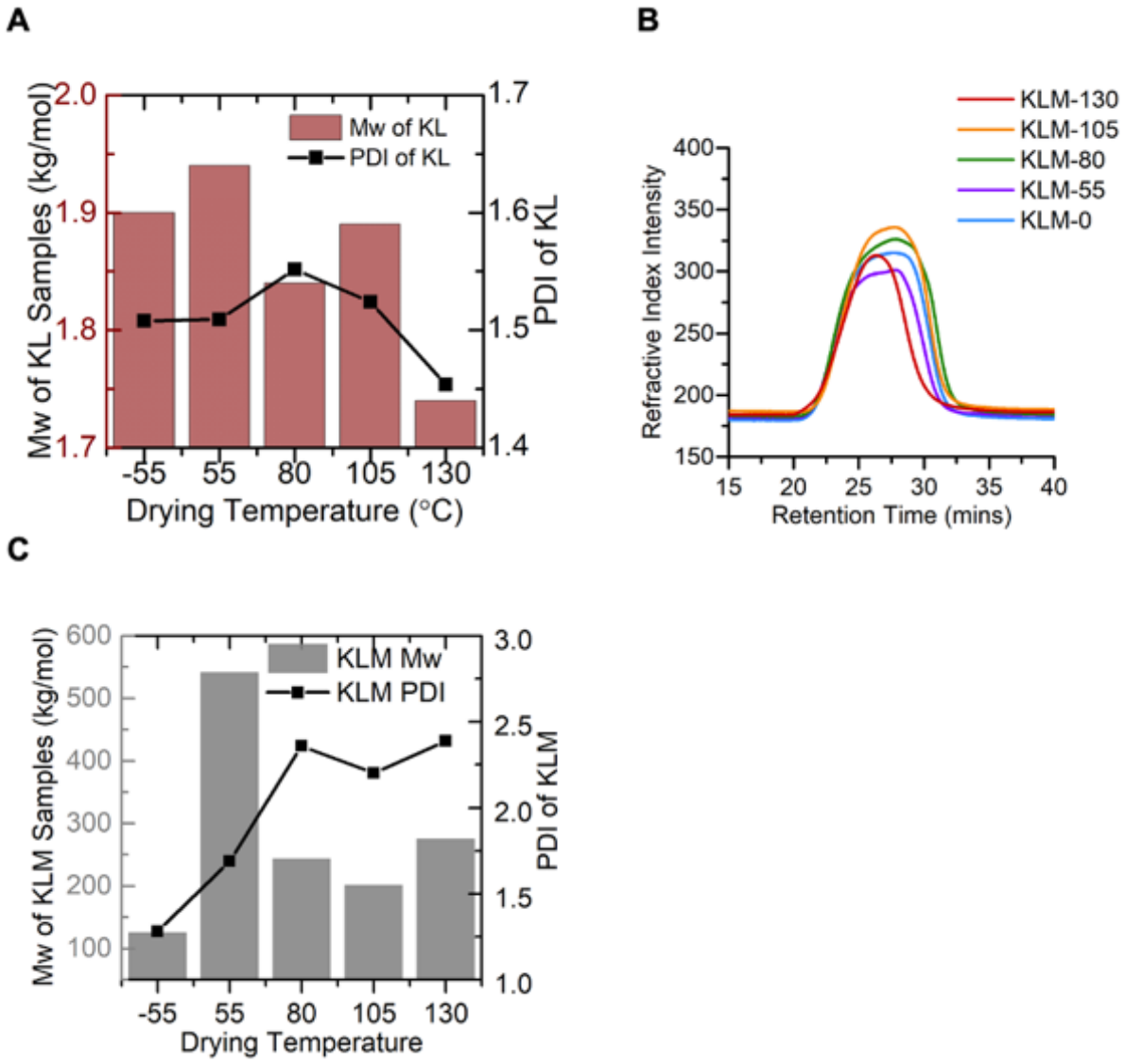

Figure 4-9: Weight-average molecular weight and polydispersity of KL (A) and KLM (C) samples dried for 48 hours, along with molecular weight distribution of KLM samples (B).

4.4.7 Thermal stability analysis

It should be noted that the data in this section for the KL control samples was reported after a smoothing process was applied to the data from thermogravimetric analysis. All of the oven-dried samples showed some amount of noise in their TGA curves, even after repeating the samples. It has been reported that due to reactions within biomass samples during the process of TGA analysis, there can be significant noise in the data [43-46]. However, the literature has shown that this noise

can be reduced in order to derive meaningful information, by applying an appropriate smoothing technique [43-46]. Details on this can be found in appendix A2. Table 4-2 presents the onset degradation temperature, T_o, the 50% degradation, $T_{50\%}$ and the maximum degradation temperature, T_{max} for the KL control samples, which were freeze-dried and oven-dried. It can be seen from these results that low-temperature drying (KL-55 and KL-80) have similar T_o values. Analogously, higher temperature drying (KL-105 and KL-130) share similar T_o values. When examining the $T_{50\%,}$ it can be seen that as oven-drying temperature increases, the resistance to thermal degradation increases up to 105ºC drying temperature. However, $T_{50\%}$ decreases for KL-130. The T_{max} did not exhibit any discernable trend. KL-105 sample showed the highest weight percent remaining at the T_{max}. This result suggests that drying at 105ºC imparts considerable thermal resistance to KL.

Table 4-2: Thermal degradation temperatures and weight percentages for KL control samples and KLM dried for 48 hours.

Sample	**To ,ºC**	**T 50% ,ºC**	**Tmax ,ºC**	**Weight % at Tmax ,ºC**	**Tg,ºC**
KL-0	316	582	372	50	167
KL-55	343	504	504	52	195
KL-80	342	594	610	45	199
KL-105	335	727	433	74	204
KL-130	336	638	635	54	199
KLM-0	270	281	270	61	174

KLM-55	316	315	316	50	163
KLM-80	271	309	315	47	178
KLM-105	270	316	317	49	178
KLM-130	273	290	273	63	172

It can be seen from Table 4-2 that as drying temperature increases, so too does the value of glass transition temperature, T_g KL samples. This trend can be explained by the phenolic -OH groups of KL being free to participate in self-condensation reactions to form ether structures (Figure 4-5A, 4-6A, 4-7A), which results in an increased T_g [47].

The thermal stability of the KLM samples dried at various temperatures was investigated by TGA and DSC. The initial peak in all DTG curves that occurs around 100ºC can be attributed to the removal of adsorbed and bound water [21]. All KLM samples, irrespective of drying conditions, exhibit similar thermal degradation responses. Thermal degradation onset occurred between 270 to 273ºC, with the exception of KLM-55 which was slightly higher at 316ºC. This range was attributed to the thermal degradation of the quaternary ammonium groups in pMETAC [19]. The $T_{50\%}$ fluctuated between 281 to 316ºC with no discernable trend. This range was attributed to the degradation of β-O-4 structure as well as the oxidation of aliphatic hydroxyl groups and also the cleavage of alkyl side chains such as Cβ-Cγ linked to -CH_2OH groups [48, 49]. The T_{max} occurred between 270 to 317ºC for all KLM samples. Beyond the T_{max}, the samples exhibited smaller peaks around 400 and 450ºC, which was attributed to the degradation of aromatic rings, β-β and carbon-carbon structures of KL [21, 50] and the complete breakdown of aromatic linkages and methoxy groups of KL appeared [50].

The T_o, $T_{50\%}$ and T_{max} initially showed an increase for KLM-55, compared to KLM-0. However, the values decreased for the rest of the samples, as drying temperature increased. This improved thermal stability of KLM-55, compared to the other samples, is attributed to increased chain interactions between long aliphatic pMETAC chains on the core structure of KL that will limit molecular mobility of the macromolecular structure, thus, improving thermal stability [51-53]. Additionally, it should be noted that the samples at higher drying temperatures did not exhibit the same trend, as degradation began to play more of a significant role (Figure 4-7). Overall, these results indicate that the temperature of drying has an effect on the thermal degradation of the samples. Specifically, it seems that drying at lower temperatures may cause crosslinking to be the prevalent drying induced reaction, such that it improves the resistance of the KLM polymer to thermal degradation. This was shown in Figures 4-7 and 4-8, by the increased concentration of C-C structures in the KLM-55 sample. However, increasing the drying temperature to 80ºC may allow for hydrolysis reactions to prevail. This was indicated by the two similar peaks, separated by a plateau. Meanwhile drying beyond those temperatures seems to favour degradation reactions during the drying process, as indicated by the reduced TGA temperatures. This is also further supported by the presence of aldehyde structures, as shown in Figures 4-5, 4-6, 4-7 and 4-8.

All the KLM samples had T_g between 172 to 178ºC as can be seen from Table 4-2, with the exception of the KLM-55, having a T_g of 163ºC. This may be indicative of higher chain lengths of pMETAC within the KL structure, resulting in inter-chain interactions, and thus in KLM-55 having a higher Mw (Figure 4-9A). For KLM-80, KLM-105 and KLM-130 samples, the higher T_g values can be attributed to the protons in the carboxylic acid group participating in hydrogen bond interactions with other more electronegative atoms.

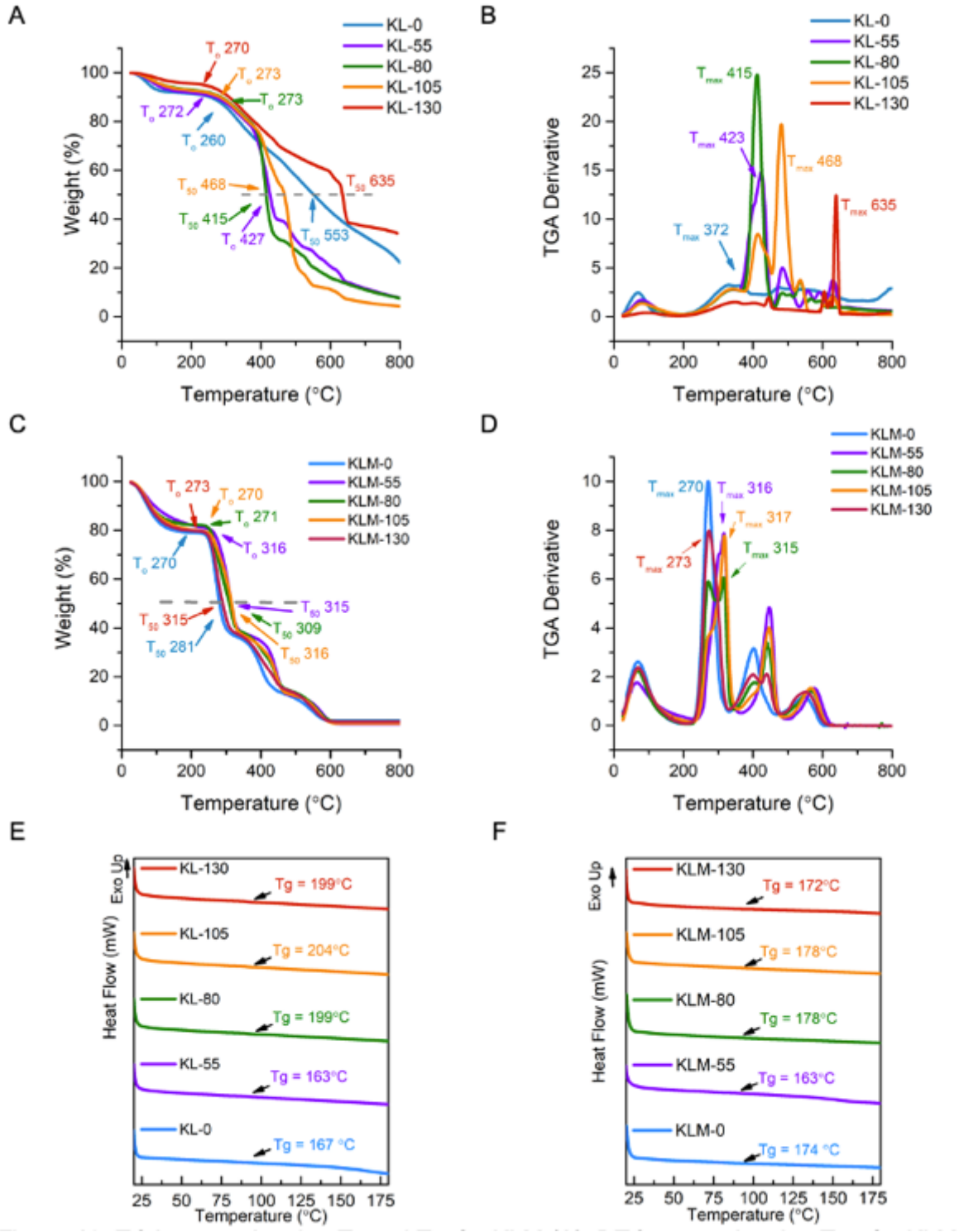

Figure 4-10: TGA curve showing T_o and T_{50} for KLM (A), DTG curve showing T_{max} for KLM (B); analogous curves shown for T_o and T_{50} for KL (C), DTG curve showing T_{max} for KL (D); and DSC curves showing T_g for KL (E) and KLM (F).

The abundance of electronegative atoms, such as oxygen and nitrogen, makes this highly probable to cause structural rearrangement of the polymer chains during heating [51-53]. This is because as the sample is dried some hydrolysis may occur, as seen in the NMR analysis in Figure 4-8. The products of the hydrolysis reactions are highly electronegative and would interact with the polymer chains to cause structural rearrangement [51-53]. Another interesting result was the lower T_g of the KLM-55 sample, whereby this sample exhibited the highest molecular weight (Table 4-2), yet it had the lowest T_g. It is well understood that increasing molecular weight correlates with increasing T_g, as higher molecular weight means a higher number of chains [54-56]. However as discussed in the previous section, this result could be due to more chain interactions between the pMETAC chains bound to the KL core structure. This in turn would cause the appearance of having larger molecular weight fragments within the sample [42]. This can be supported by the molecular structural changes as confirmed by NMR (Figure 4-8) and XPS (Figures 4-5 and 4-6). These figures show that KLM-55 did not have any increased ether linkages or increased aliphatic concentration, yet it had the greatest Mw. This supports the assertion that chain interactions, like chain entanglement, are more prevalent at this drying temperature.

By comparing the results in Table 4-2, it becomes apparent that KLM was less thermally stable than KL, implying that the polymerization of KL with METAC reduced the thermal stability of the product. Further to that, it provides a product that is more uniform in its thermal degradation response, based on the TGA results (Table 4-2). This result makes sense as pMETAC chains are composed of single and double bonds that are known to be much less thermally stable than aromatic rings [48]. Meanwhile, the KL dried under various conditions displayed more variability in its thermal degradation response (Table 4-2). When examining T_{max}, it can be seen that drying KL at 105ºC conferred increased thermal degradation resistance.

Additionally, it can be seen that freeze-drying resulted in comparable T_g in both KL and KLM. However, oven-drying across all temperatures resulted in higher T_g for all the KLM samples than its KL counterpart dried in the same way. The overall conclusion that can be made is that polymerizing pMETAC with KL hampers the thermal degradation resistance that may be innately possessed by KL on its own. It has been reported that the thermal behaviour of the lignin product would depend on the degree to which the phenolic or aliphatic hydroxyl groups are masked with grafted structures [47]. As it pertains to this present work, the pMETAC chains are bound to the phenolic position of lignin, resulting in lesser formation of etherified structures in the KLM samples during drying. However, the KL samples clearly formed more etherified structures during drying, as shown by NMR results (Figure 4-7). The TGA and DSC results suggest that polymerizing METAC and KL would reduce the effect of crosslinking, but drying condition still affects the thermal response of the KLM polymer.

4.4.8 Drying induced events

Based on the results obtained from this work, four main drying induced events are proposed, as is shown in Figure 4-11. For KL, the main drying induced event appears to be condensation reaction, by which hydroxyl groups react with each other during the drying process to form ether structures (Figure 4-11A). At a drying temperature of 55ºC, chain interactions predominate due to electrostatic forces, which was shown by the KLM-55 sample having the highest molecular weight results from GPC (Figure 4-9A). Yet it had the lowest T_g (Table 4-2) and low residual weight percent at T_{max} (Table 4-2). Additionally, at 80ºC, hydrolysis seems to predominate, whereby the cationic structure becomes severed, as was shown from the ^{1}H NMR (Figure 4-7C) and XPS signals (Figures 4-5 and 4-6), resulting in a carboxylic acid structure and a quaternary ammonium group (Figure 4-11B). Finally, at 105 and 130ºC another hydrolysis reaction predominates,

demonstrated by the formation of aldehyde structures detected both by HSQC NMR (Figure 4-8) and XPS signals (Figures 4-5 and 4-6).

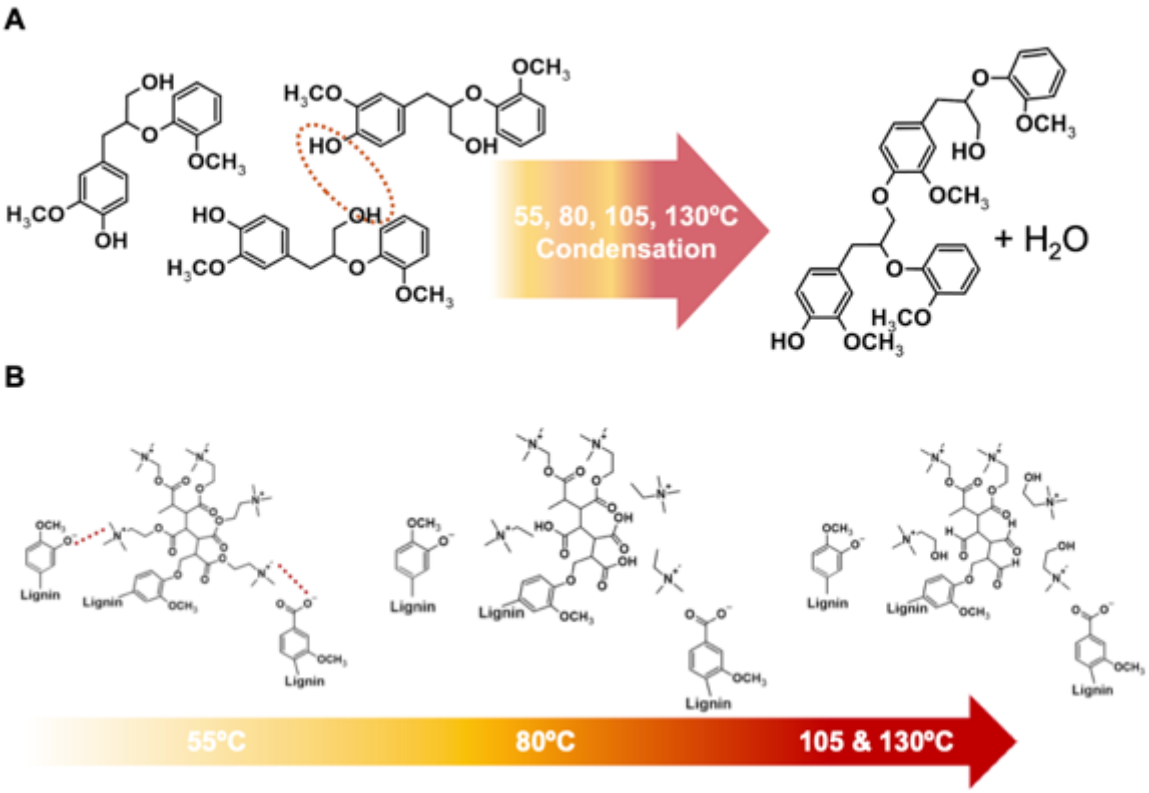

Figure 4-11: Proposed drying induced condensation in KL (A). Proposed drying induced events for KLM (B): electrostatic chain interactions at 55ºC; low-temperature hydrolysis of cationic structures from lignin at 80ºC; and high-temperature hydrolysis of cationic structure.

4.5 Conclusions

It was found that oven-drying at 55 and 80ºC does not significantly affect KL's water solubility, when comparing to the freeze-dried sample. Yet the KL samples dried at 105 and 130ºC possessed a significantly lower water solubility. All oven-dried KL samples showed a decrease in charge density as drying temperature increased. NMR results indicated that, during drying, aliphatic structures of softwood kraft lignin seem prone to self-condensing. As a result, etherified structures were formed in KL samples during drying. This assertion was also supported by the TGA and DSC

results, which indicated that increasing drying temperature to 105ºC yielded KL with robust resistance to thermal degradation. However, upon drying at 130ºC, the degradation of the KL structures was more prevalent as there was a drop in the thermal degradation response of KL as confirmed by the changes in the NMR results.

As for the cationically polymerized KLM polymer, it was found that oven-drying resulted in a significant reduction in water solubility and charge density of KLM samples, when compared to the freeze-dried sample. It was found that low temperature drying at 55ºC results in more chain interactions due to electrostatic interactions amongst the pMETAC chains with the electronegative atoms present in KL. It is theorized that these interactions caused the pMETAC chains to become entangled and form larger chain fragments, causing the M_w values to appear higher. This resulted in larger molecular weight results for the KLM-55 sample. At 80, 105 and 130ºC drying temperatures, it was found that hydrolysis reactions predominated, resulting in lower molecular weight for KLM samples and an increase in C-O structures (as shown in NMR and XPS results). Specifically, at 80ºC, hydrolysis resulted in a quaternary ammonium group and a carboxylic acid group. Meanwhile, at 105 and 130ºC, a quaternary ammonium group and an aldehyde group was detected. Further to this, KLM had lower resistance to thermal degradation than KL control samples which were oven-dried under the same conditions. This finding was expected, as pMETAC chains are mainly aliphatic, and as such, less thermally stable than aromatic rings. Additionally, the pMETAC chains occupy the phenolic position of the KL core structure, effectively preventing self-condensation that is characteristic of KL and contributes to thermal stability of KL [47]. Thus, the KLM polymer was less resistant to thermal degradation, as it did not undergo as much self-condensing as KL does during drying.

This study revealed that there is a complex interplay of chemical and physical phenomena occurring during the drying of KL and KLM. There are key considerations that should be taken into account, such as chain interactions, hydrolysis, and thermal degradation, when selecting the drying conditions.

4.6 References

[1] W. Zhang *et al.*, "Lignin derived carbon materials: current status and future trends," *Carbon Research,* vol. 1, no. 1, p. 14, 2022/07/29 2022, doi: 10.1007/s44246-022-00009-1.

[2] A. Beaucamp *et al.*, "Lignin for energy applications – state of the art, life cycle, technoeconomic analysis and future trends," *Green Chemistry,* 10.1039/D2GC02724K vol. 24, no. 21, pp. 8193-8226, 2022, doi: 10.1039/D2GC02724K.

[3] U. Ejaz and M. Sohail, "Lignin: A Renewable Chemical Feedstock," in *Handbook of Smart Materials, Technologies, and Devices: Applications of Industry 4.0*, C. M. Hussain and P. Di Sia Eds. Cham: Springer International Publishing, 2020, pp. 1-15.

[4] X. Chen, K. Zhang, L.-P. Xiao, R.-C. Sun, and G. Song, "Total utilization of lignin and carbohydrates in Eucalyptus grandis: an integrated biorefinery strategy towards phenolics, levulinic acid, and furfural," *Biotechnology for Biofuels,* vol. 13, no. 1, p. 2, 2020/01/06 2020, doi: 10.1186/s13068-019-1644-z.

[5] C. S. Lancefield, Hans L. J. Wienk, R. Boelens, B. M. Weckhuysen, and P. C. A. Bruijnincx, "Identification of a diagnostic structural motif reveals a new reaction intermediate and condensation pathway in kraft lignin formation," *Chemical Science,* 10.1039/C8SC02000K vol. 9, no. 30, pp. 6348-6360, 2018, doi: 10.1039/C8SC02000K.

[6] W. Mo, K. Chen, X. Yang, F. Kong, J. Liu, and B. Li, "Elucidating the hornification mechanism of cellulosic fibers during the process of thermal drying," *Carbohydrate Polymers,* vol. 289, p. 119434, 2022/08/01/ 2022, doi: https://doi.org/10.1016/j.carbpol.2022.119434.

[7] O. Gordobil, R. Herrera, F. Poohphajai, J. Sandak, and A. Sandak, "Impact of drying process on kraft lignin: lignin-water interaction mechanism study by 2D NIR correlation spectroscopy," *Journal of Materials Research and Technology,* vol. 12, pp. 159-169, 2021/05/01/ 2021, doi: https://doi.org/10.1016/j.jmrt.2021.02.080.

[8] H. Zhang, S. Fu, and Y. Chen, "Basic understanding of the color distinction of lignin and the proper selection of lignin in color-depended utilizations," *International Journal of Biological Macromolecules,* vol. 147, pp. 607-615, 2020/03/15/ 2020, doi: https://doi.org/10.1016/j.ijbiomac.2020.01.105.

[9] C. Cui, H. Sadeghifar, S. Sen, and D. Argyropoulos, "Toward Thermoplastic Lignin Polymers; Part II: Thermal & Polymer Characteristics of Kraft Lignin & Derivatives," *Bioresources,* vol. 8 (1), pp. 864-886, 11/05 2013, doi: 10.15376/biores.8.1.864-886.

[10] Z. Lv *et al.*, "Hydrothermal method-assisted synthesis of self-crosslinked all-lignin-based hydrogels," *International Journal of Biological Macromolecules,* vol. 216, pp. 670-675, 2022/09/01/ 2022, doi: https://doi.org/10.1016/j.ijbiomac.2022.07.003.

[11] L. Duong *et al.*, "Chemical and Rheological Characteristics of Thermally Stable Kraft Lignin Polycondensates Analyzed by Dielectric Properties," *BioResources,* vol. 8, 05/01 2013, doi: 10.15376/biores.8.3.4518-4532.

[12] D. R. Klein, *Organic Chemistry*. Wiley, 2017.

[13] L. Shuai *et al.*, "Formaldehyde stabilization facilitates lignin monomer production during biomass depolymerization," *Science,* vol. 354, no. 6310, pp. 329-333, 2016/10/21 2016, doi: 10.1126/science.aaf7810.

[14] X. Mu, Z. Han, C. Liu, and D. Zhang, "Mechanistic Insights into Formaldehyde-Blocked Lignin Condensation: A DFT Study," *The Journal of Physical Chemistry C,* vol. 123, no. 14, pp. 8640-8648, 2019/04/11 2019, doi: 10.1021/acs.jpcc.9b00247.

[15] K. Shimada, S. Hosoya, and T. Ikeda, "Condensation reactions of softwood and hardwood lignin model compounds under organic acid cooking conditions," *Journal of wood chemistry and technology,* vol. 17, no. 1/2, pp. 57-72, 1997, doi: 10.1080/02773819708003118.

[16] A. Salaghi, J. A. Diaz-Baca, and P. Fatehi, "Enhanced flocculation of aluminum oxide particles by lignin-based flocculants in dual polymer systems," *Journal of Environmental Management,* vol. 328, p. 116999, 2023/02/15/ 2023, doi: https://doi.org/10.1016/j.jenvman.2022.116999.

[17] S. Sabaghi and P. Fatehi, "Phenomenological Changes in Lignin Following Polymerization and Its Effects on Flocculating Clay Particles," *Biomacromolecules,* vol. 20, no. 10, pp. 3940-3951, 2019/10/14 2019, doi: 10.1021/acs.biomac.9b01016.

[18] S. Heydarifard, W. Gao, and P. Fatehi, "Generation of New Cationic Xylan-Based Polymer in Industrially Relevant Process," *Industrial & Engineering Chemistry Research,* vol. 57, no. 38, pp. 12670-12682, 2018/09/26 2018, doi: 10.1021/acs.iecr.8b02589.

[19] S. Wang, F. Kong, W. Gao, and P. Fatehi, "Novel Process for Generating Cationic Lignin Based Flocculant," *Industrial & engineering chemistry research,* vol. 57, no. 19, pp. 6595-6608, 2018, doi: 10.1021/acs.iecr.7b05381.

[20] L. Zhao *et al.*, "Cationic tall oil lignin-starch copolymer as a flocculant for clay suspensions," *Industrial crops and products,* vol. 202, p. 117069, 2023, doi: 10.1016/j.indcrop.2023.117069.

[21] S. Sabaghi, N. Alipoormazandarani, and P. Fatehi, "Production and Application of Triblock Hydrolysis Lignin-Based Anionic Copolymers in Aqueous Systems," *ACS Omega,* vol. 6, no. 9, pp. 6393-6403, 2021/03/09 2021, doi: 10.1021/acsomega.0c06344.

[22] I. M. Garcia, S. B. Rodrigues, G. de Souza Balbinot, F. Visioli, V. C. B. Leitune, and F. M. Collares, "Quaternary ammonium compound as antimicrobial agent in resin-based sealants," *Clinical Oral Investigations,* vol. 24, no. 2, pp. 777-784, 2020/02/01 2020, doi: 10.1007/s00784-019-02971-4.

[23] S. M. North and S. P. Armes, "Synthesis of polyampholytic diblock copolymers via RAFT aqueous solution polymerization," *Polymer Chemistry,* 10.1039/D1PY01020D vol. 12, no. 33, pp. 4846-4855, 2021, doi: 10.1039/D1PY01020D.

[24] S. Sabaghi and P. Fatehi, "Polarity of Cationic Lignin Polymers: Physicochemical Behavior in Aqueous Solutions and Suspensions," *ChemSusChem,* vol. 13, no. 17, pp. 4722-4734, 2020, doi: 10.1002/cssc.202000897.

[25] S. Wang, F. Kong, P. Fatehi, and Q. Hou, "Cationic High Molecular Weight Lignin Polymer: A Flocculant for the Removal of Anionic Azo-Dyes from Simulated Wastewater," *Molecules,* vol. 23, no. 8, p. 2005, 2018. [Online]. Available: https://www.mdpi.com/1420-3049/23/8/2005.

[26] S. Wang, M. K. R. Konduri, Q. Hou, and P. Fatehi, "Cationic xylan-METAC copolymer as a flocculant for clay suspensions," *RSC advances,* vol. 6, no. 46, pp. 4258-4269, 2016, doi: 10.1039/c6ra05223a.

[27] F. Kong, K. Parhiala, S. Wang, and P. Fatehi, "Preparation of cationic softwood kraft lignin and its application in dye removal," vol. 67, p. 345, 2015.

[28] W. Kong, J. Ren, S. Wang, M. Li, and R. Sun, "A promising strategy for preparation of cationic xylan by environment-friendly semi-dry oven process," *Fibers and Polymers,* vol. 15, no. 5, pp. 943-949, 2014/05/01 2014, doi: 10.1007/s12221-014-0943-z.

[29] S. M. Jafari, V. Ghanbari, M. Ganje, and D. Dehnad, "Modeling the Drying Kinetics of Green Bell Pepper in a Heat Pump Assisted Fluidized Bed Dryer," *Journal of Food Quality,* vol. 39, no. 2, pp. 98-108, 2016/04/01 2016, doi: https://doi.org/10.1111/jfq.12180.

[30] D. Dehnad, S. M. Jafari, and M. Afrasiabi, "Influence of drying on functional properties of food biopolymers: From traditional to novel dehydration techniques," *Trends in Food Science & Technology,* vol. 57, pp. 116-131, 2016, doi: 10.1016/j.tifs.2016.09.002.

[31] B. Bhandari, "Handbook of Industrial Drying, Fourth EditionEdited by A. S. Mujumdar: CRC Press: Boca Raton, FL; 2015. ISBN: 978-1-4665-9665-8," *Drying technology,* vol. 33, no. 1, pp. 128-129, 2015, doi: 10.1080/07373937.2014.983704.

[32] M. Konduri and P. Fatehi, "Production of Water-Soluble Hardwood Kraft Lignin via Sulfomethylation Using Formaldehyde and Sodium Sulfite," *ACS Sustainable Chemistry & Engineering,* vol. 3, p. 150508121241009, 05/08 2015, doi: 10.1021/acssuschemeng.5b00098.

[33] K. Bahrpaima and P. Fatehi, "Synthesis and Characterization of Carboxyethylated Lignosulfonate," *ChemSusChem,* https://doi.org/10.1002/cssc.201800994 vol. 11, no. 17, pp. 2967-2980, 2018/09/11 2018, doi: https://doi.org/10.1002/cssc.201800994.

[34] S. Sen, S. Patil, and D. S. Argyropoulos, "Thermal properties of lignin in copolymers, blends, and composites: a review," *Green Chemistry,* 10.1039/C5GC01066G vol. 17, no. 11, pp. 4862-4887, 2015, doi: 10.1039/C5GC01066G.

[35] C. Heitner, D. Dimmel, and J. A. Schmidt, *Lignin and lignans : advances in chemistry*. Boca Raton, FL: Taylor & Francis, 2010.

[36] S. D. K. Seera and C. W. Pester, "Surface-Initiated PET-RAFT via the Z-Group Approach," *ACS Polymers Au,* vol. 3, no. 6, pp. 428-436, 2023/12/13 2023, doi: 10.1021/acspolymersau.3c00028.

[37] D. Son, S. Cho, J. Nam, H. Lee, and M. Kim, "X-ray-Based Spectroscopic Techniques for Characterization of Polymer Nanocomposite Materials at a Molecular Level," *Polymers*, vol. 12, no. 5*,* doi: 10.3390/polym12051053.

[38] A. Antony and M. Farid, "Effect of Temperatures on Polyphenols during Extraction," *Applied Sciences*, vol. 12, no. 4*,* doi: 10.3390/app12042107.

[39] Z. Diaconeasa, "Time-Dependent Degradation of Polyphenols from Thermally-Processed Berries and Their In Vitro Antiproliferative Effects against Melanoma," (in eng), *Molecules,* vol. 23, no. 10, Oct 4 2018, doi: 10.3390/molecules23102534.

[40] Y. Wang, X. Jia, and Y. Zhang, "Study on Hydrolysis Properties and Mechanism of Poly(3-Methacrylamido Propyl Trimethyl Ammonium Chloride) Solution," *Polymers,* vol. 14, no. 14, p. 2811, 2022, doi: 10.3390/polym14142811.

[41] R. M. Silverstein, F. X. Webster, D. J. Kiemle, and D. L. Bryce, *Spectrometric identification of organic compounds*, Eighth edition. ed. Hoboken, New Jersey: Wiley, 2015.

[42] M. M. Phillips, "André M. Striegel, Wallace W. Yau, Joseph J. Kirkland, and Donald D. Bly (Eds.): Modern size-exclusion liquid chromatography. Practice of gel permeation and gel filtration chromatography, 2nd ed," *Analytical and Bioanalytical Chemistry,* vol. 399, no. 4, pp. 1571-1572, 2011/02/01 2011, doi: 10.1007/s00216-010-4482-1.

[43] J. Cai *et al.*, "Processing thermogravimetric analysis data for isoconversional kinetic analysis of lignocellulosic biomass pyrolysis: Case study of corn stalk," *Renewable and Sustainable Energy Reviews,* vol. 82, pp. 2705-2715, 2018/02/01/ 2018, doi: https://doi.org/10.1016/j.rser.2017.09.113.

[44] T. Onsree and N. Tippayawong, "Application of Gaussian Smoothing Technique in Evaluation of Biomass Pyrolysis Kinetics in Macro-TGA," *2017 INTERNATIONAL CONFERENCE ON ALTERNATIVE ENERGY IN DEVELOPING COUNTRIES AND EMERGING ECONOMIES,* vol. 138, pp. 778-783, 2017, doi: 10.1016/j.egypro.2017.10.059.

[45] J. A. Caballero and J. A. Conesa, "Mathematical considerations for nonisothermal kinetics in thermal decomposition," *Journal of Analytical and Applied Pyrolysis,* vol. 73, no. 1, pp. 85-100, 2005/03/01/ 2005, doi: https://doi.org/10.1016/j.jaap.2004.12.003.

[46] H. X. Chen, N. A. Liu, L. F. Shu, and R. W. Zong, "Smoothing and differentiation of thermogravimetric data of biomass materials," *Journal of thermal analysis and calorimetry,* vol. 78, no. 3, pp. 1029-1041, 2004, doi: 10.1007/s10973-005-0468-0.

[47] D. Diment *et al.*, "Study toward a More Reliable Approach to Elucidate the Lignin Structure–Property–Performance Correlation," *Biomacromolecules,* vol. 25, no. 1, pp. 200-212, 2024/01/08 2024, doi: 10.1021/acs.biomac.3c00906.

[48] E. S. Wibowo and B.-D. Park, "Probing the relationship between chemical structure and thermal degradation behavior of acetone fractionated kraft lignin," *Journal of Analytical and Applied Pyrolysis,* vol. 172, p. 106028, 2023/06/01/ 2023, doi: https://doi.org/10.1016/j.jaap.2023.106028.

[49] J. Zhao, W. Xiuwen, J. Hu, Q. Liu, D. Shen, and R. Xiao, "Thermal degradation of softwood lignin and hardwood lignin by TG-FTIR and Py-GC/MS," *Polymer Degradation and Stability,* vol. 108, pp. 133-138, 2014/10/01/ 2014, doi: https://doi.org/10.1016/j.polymdegradstab.2014.06.006.

[50] M. Mennani *et al.*, "Insights on the physico-chemical properties of alkali lignins from different agro-industrial residues and their use in phenol-formaldehyde wood adhesive formulation," *International Journal of Biological Macromolecules,* vol. 221, pp. 149-162, 2022/11/30/ 2022, doi: https://doi.org/10.1016/j.ijbiomac.2022.08.191.

[51] H. Yan, Z. Zhan, H. Wang, J. Cheng, and Z. Fang, "Synthesis, Curing, and Thermal Stability of Low-Temperature-Cured Benzoxazine Resins Based on Natural Renewable Resources," *ACS Applied Polymer Materials,* vol. 3, no. 7, pp. 3392-3401, 2021/07/09 2021, doi: 10.1021/acsapm.1c00361.

[52] T. Periyasamy, S. P. Asrafali, S. Muthusamy, and S.-C. Kim, "Replacing bisphenol-A with bisguaiacol-F to synthesize polybenzoxazines for a pollution-free environment," *New Journal of Chemistry,* 10.1039/C6NJ02242A vol. 40, no. 11, pp. 9313-9319, 2016, doi: 10.1039/C6NJ02242A.

[53] M. Fache, B. Boutevin, and S. Caillol, "Vanillin, a key-intermediate of biobased polymers," *European Polymer Journal,* vol. 68, pp. 488-502, 2015/07/01/ 2015, doi: https://doi.org/10.1016/j.eurpolymj.2015.03.050.

[54] K. J. Bichler, B. Jakobi, and G. J. Schneider, "Dynamical Comparison of Different Polymer Architectures-Bottlebrush vs Linear Polymer," (in eng), *Macromolecules,* vol. 54, no. 4, pp. 1829-1837, Feb 23 2021, doi: 10.1021/acs.macromol.0c02104.

[55] J. E. Pye and C. B. Roth, "Two simultaneous mechanisms causing glass transition temperature reductions in high molecular weight freestanding polymer films as measured by transmission ellipsometry," (in eng), *Phys Rev Lett,* vol. 107, no. 23, p. 235701, Dec 2 2011, doi: 10.1103/PhysRevLett.107.235701.

[56] A. L. Agapov and A. P. Sokolov, "Does the Molecular Weight Dependence of Tg Correlate to Me?," *Macromolecules,* vol. 42, no. 7, pp. 2877-2878, 2009/04/14 2009, doi: 10.1021/ma9002825.

Chapter 5 – Conclusions

In this thesis, the overall objective was to investigate the effect of drying temperature during the drying of kraft lignin and its cationic derivatives. Freeze-drying and oven-drying were used to study the effect of drying on kraft lignin and two different derivatives.

It was discovered that KL experienced condensation during oven-drying, resulting in etherified structures, namely diphenylmethane and phenyldihydrobenzofuran. In particular, the diphenylmethane structure was identified at all oven-drying temperatures, while the phenyldihydrobenzofuran was only present at lower temperatures (80 and 105ºC). At 130ºC, it seems that degradation reactions were more prevalent than condensation reactions. This, combined with the results of M_w and T_g showed that drying KL at 105ºC would yield increased M_w and T_g, likely due to the increase in ether structures.

Additionally, oven-drying at 55 and 80ºC did not significantly affect KL's water solubility when compared to the freeze-dried sample. Yet, the KL samples dried at 105 and 130ºC possessed a significantly lower water solubility. All oven-dried KL samples showed a decrease in charge density as the drying temperature increased. The results indicated that, during drying, aliphatic structures of kraft lignin seem prone to self-condensing. As a result, etherified structures were formed in KL samples during drying. This assertion was also supported by the TGA and DSC results, which indicated that increasing the drying temperature to 105ºC yielded KL with robust resistance to thermal degradation. However, upon drying at 130ºC, the degradation of the KL structures was more prevalent as there was a drop in the thermal degradation response of KL as confirmed by the changes in the NMR results.

For CKL, the results revealed that the cationic products underwent degradation to produce secondary amine structures at 105 and 130ºC. The quaternary substituted nitrogen groups seemed to be prone to degeneration to tertiary nitrogen groups along with the degeneration of those tertiary nitrogen groups to secondary amines. Furthermore, it was found that the CKL samples underwent condensation, was associated with an increase in M_w and T_g. Specifically, it was found that CKL was more susceptible to reductions in -OH groups, which were directly proportional to increasing drying temperature. This was also found to concurrently result in higher molecular weight values as a result of -OH groups condensing during drying. Yet the T_g values were overall lower for cationic lignin than KL due to reduced phenolic content and more branched groups reducing the molecular mobility of the structure in response to heating.

For the cationic polymerized lignin, it was found that oven-drying resulted in a significant reduction in water solubility and charge density of KLM samples, when compared to the freeze-dried sample. It was found that the low-temperature drying at 55ºC results in more chain interactions due to electrostatic interactions amongst the pMETAC chains with the electronegative atoms present in KL. At 80, 105 and 130ºC drying temperatures, it was found that hydrolysis reactions predominated, resulting in lower molecular weight for the samples and an increase in C-O structures. At 80ºC, hydrolysis resulted in a quaternary ammonium group and a carboxylic acid group. Meanwhile, at 105 and 130ºC, a quaternary ammonium group and an aldehyde group was detected. Further to this, the cationic lignin had lower resistance to thermal degradation than KL control samples. Thus, the cationic lignin polymer was less resistant to thermal degradation, as it did not undergo as much self-condensing as KL does during drying. This was due to the phenolic hydroxyl groups being occupied by pMETAC chains, preventing the self-condensation reaction of KL.

Overall, this study revealed that there is a complex interplay of chemical and physical phenomena occurring during the drying of KL and its cationic derivatives. There are key considerations that should be taken into account, such as chain interactions, hydrolysis, thermal degradation, and alkylation when selecting the drying conditions. The results of this work show for the first time that when derivatizing lignin, drying temperature should be carefully selected to conserve the properties of the sample.

Future studies

In this study, the focus was to investigate the drying temperature of cationically derivatized lignin. However, future studies on the effect of drying time and drying rate would be needed to discern more industrially attractive methodology to dry lignin derivatives. As seen from this work, the drying temperature can play an important role in the chemical structural properties of KL and KL derivatives. A comprehensive understanding of how drying time and drying rate affects these materials can lead to optimal production process, ensuring the end-products retain their target properties, while minimizing waste and energy consumption. Furthermore, as the demand for sustainable materials continues, evaluating drying time and drying rate can pave the way for the production of innovative materials that meet the environmental requirements, without compromising on quality or functionality.

Additionally, future studies on drying of other types of lignin derivatives would be beneficial. While this study focused on cationic derivatization, another important grafting strategy is anionic derivatization and polymerization. This can be accomplished through sulfo and carboxy grafting, as well as poly acrylic acid polymerization. These are also promising lignin products that would also require drying studies to ascertain the optimal drying conditions for their productions.

Appendix A1 – Time and temperature effect on CKL

The effect of time and temperature on the water solubility and charge density of CKL samples was investigated. Figure A1-1 shows the solubility (A) and charge density (B) for CKL samples over time. From this figure it can be seen that the water solubility remained constant over time. While the charge density experienced some fluctuation. In particular CKL-105 and CKL-130 experienced the most fluctuation in charge density. However, it can be seen that the cationic charge remained largely intact. These fluctuations may be explained by the findings presented in Chapter 3, regarding the degradation of the quaternary substituted nitrogen groups to tertiary and secondary substituted nitrogen groups.

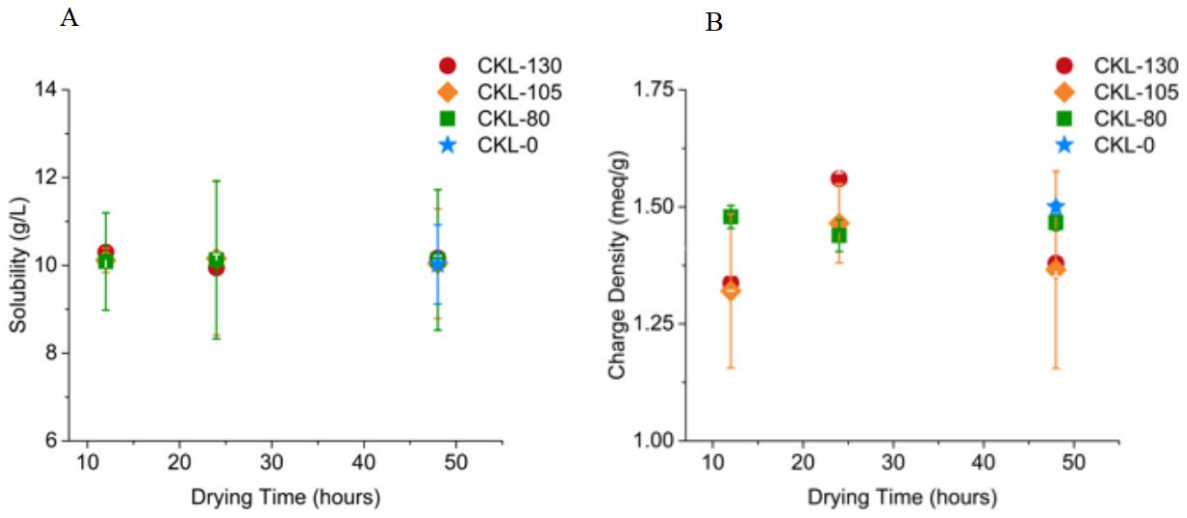

Figure A1-1: Water solubility (A) and charge density (B) for CKL samples dried at -55ºC (CKL-0), 80, 105 and 130ºC for 12, 24 and 48 hours.

The effect of time and temperature was tested on particle size, as measured by differential light scattering (DLS) and molecular weight as measured by gel permeation chromatography (GPC). The results are shown in figure A1-2. The sample CKL-105 dried at 48 hours showed the highest particle size. This may be explained by the chemical structural changes found in Chapter 3. It is

known that increased particle size is correlated with increased molecular weight. In Chapter 3, CKL-105, dried at 48 hours, was shown to have the highest molecular weight. Additionally, the chemical analysis showed that this was a result of condensation reactions occurring during the 105ºC drying process. The molecular weight of the samples did not appear to have a significant time effect, but there was a clear temperature effect. Whereby the CKL-105 samples showed overall the highest molecular weights, followed by the CKL-130 and CKL-80. This finding is also in line with the findings in Chapter 3. CKL-105 having the highest molecular weight indicates that condensation may be the most dominant reaction at this temperature. While for CKL-130, degradation seems to predominate over condensation, as found by the chemical analysis in Chapter 3 and as seen from it having a relatively lower molecular weight trend. CKL-80 showed the lowest molecular weight trend

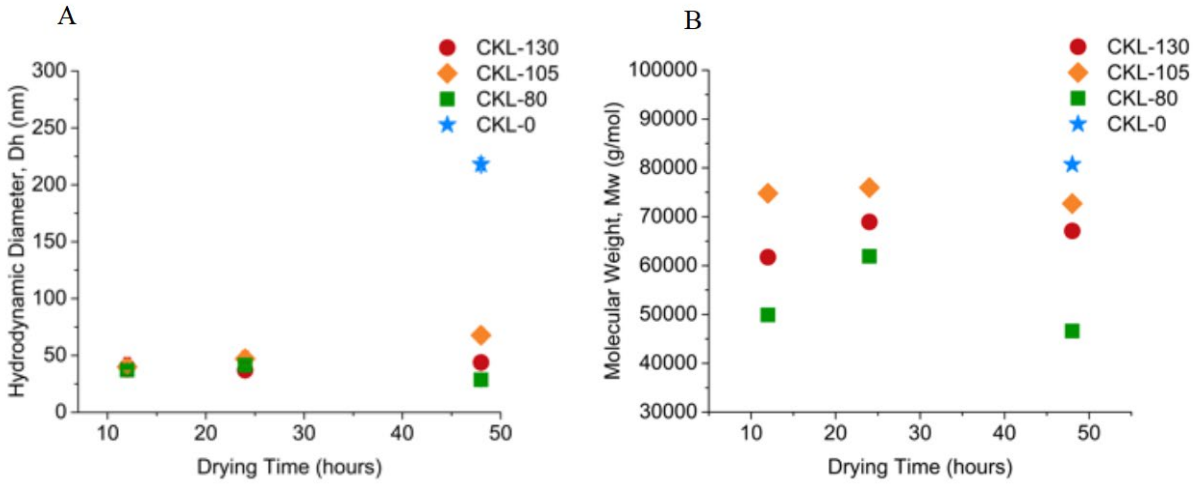

Figure A1-1: Particle size (A) as measured by differential light scattering (DLS) and molecular weight (B) as measured by gel permeation chromatography (GPC) of CKL samples.

Appendix A2 – Smoothing of KL TGA Curves

It was found that the oven-dried samples of the KL control samples resulted in spectral noise in the form of step-like signals in the weight percent curves (figure A2-1) and thus broad step-like signals in the TGA derivatives curves (figure A2-1B). It has been reported that due to reactions within biomass samples during the process of TGA analysis, there can be significant noise in the data [1-4]. In order to derive meaningful information from such curves, smoothing of the data points can be performed by applying an appropriate technique [1-4]. In this work, adjacent-averaging method was applied. Each value of g_i represents the average of the data points of the moving window, of the data set. For the window having a centre of i, the weight of the j^{th} point is given by:

$$w_j = 1 - \left(\frac{j - i}{(N + 1)/2}\right)^2$$

Where N represents the number of data points in the window, in this case, 100. After performing smoothing, it can be seen that the curves became clearer and easier to read the degradation temperatures.

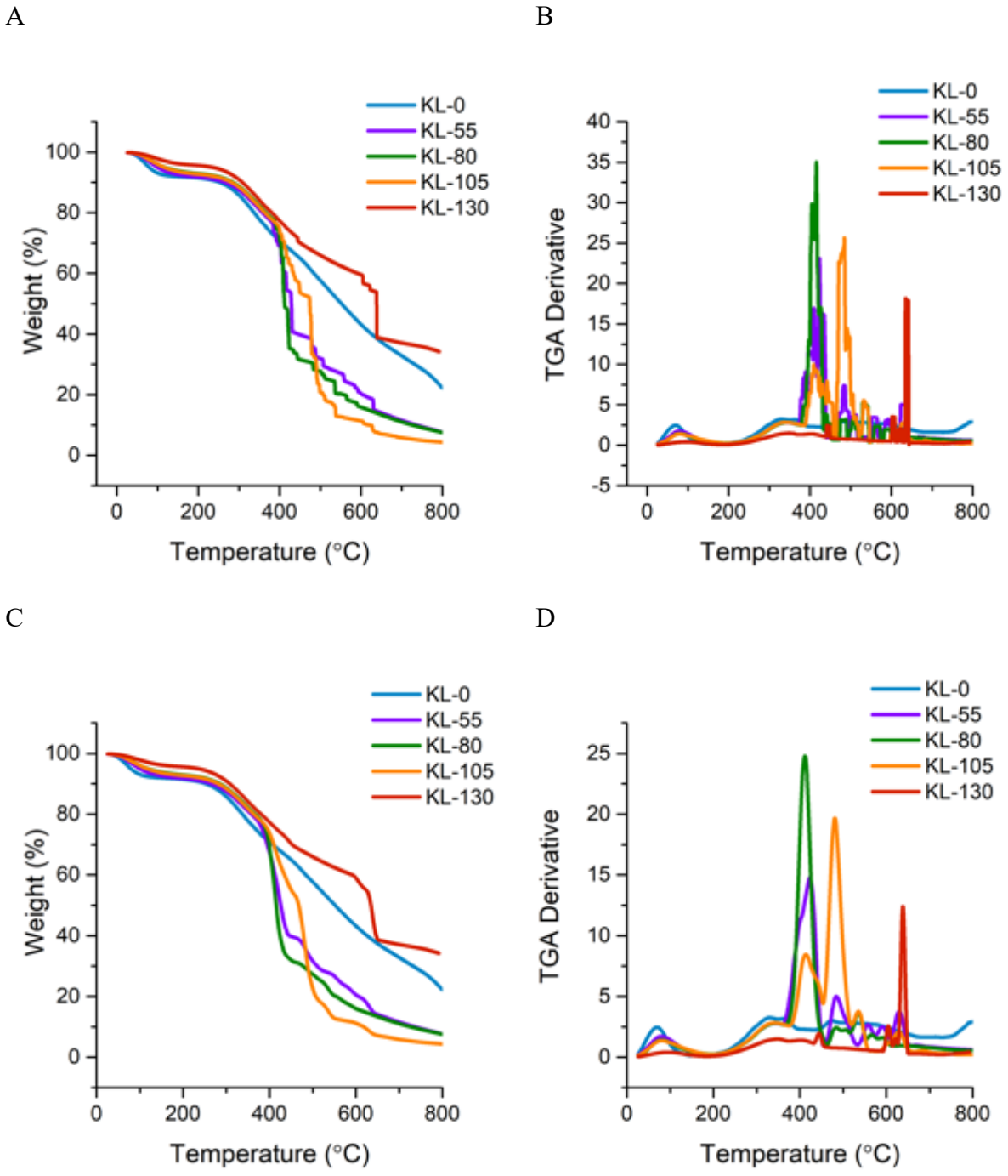

Figure A2-1: As found plots for TGA (A and B) compared to plots after smoothing (C and D).

References

[1] J. Cai *et al.*, "Processing thermogravimetric analysis data for isoconversional kinetic analysis of lignocellulosic biomass pyrolysis: Case study of corn stalk," *Renewable and Sustainable Energy Reviews,* vol. 82, pp. 2705-2715, 2018/02/01/ 2018, doi: https://doi.org/10.1016/j.rser.2017.09.113.

[2] T. Onsree and N. Tippayawong, "Application of Gaussian Smoothing Technique in Evaluation of Biomass Pyrolysis Kinetics in Macro-TGA," *2017 INTERNATIONAL CONFERENCE ON ALTERNATIVE ENERGY IN DEVELOPING COUNTRIES AND EMERGING ECONOMIES,* vol. 138, pp. 778-783, 2017, doi: 10.1016/j.egypro.2017.10.059.

[3] J. A. Caballero and J. A. Conesa, "Mathematical considerations for nonisothermal kinetics in thermal decomposition," *Journal of Analytical and Applied Pyrolysis,* vol. 73, no. 1, pp. 85-100, 2005/03/01/ 2005, doi: https://doi.org/10.1016/j.jaap.2004.12.003.

[4] H. X. Chen, N. A. Liu, L. F. Shu, and R. W. Zong, "Smoothing and differentiation of thermogravimetric data of biomass materials," *Journal of thermal analysis and calorimetry,* vol. 78, no. 3, pp. 1029-1041, 2004, doi: 10.1007/s10973-005-0468-0.